Monash Univeristy

PHS/ASP level 4

Honours Thesis

Cosmological Phase Transition Thermodynamics Using Thermal Effective Field Theories

Author:
William Searle
33653399

Supervisor:
Prof. Csaba Balazs

2023

Abstract

Cosmological phase transitions play an essential part in the contemporary standard model of cosmology. The study of these transitions is motivated by the potential role they play to trigger an inflationary epoch, induce matter-antimatter asymmetry, and contribute to large-scale structure formation. Furthermore, they may be observable by near-future gravitational wave observatories such as LISA. In this thesis, we provide an introduction to the theoretical groundwork needed to understand these transitions, with a focus on deriving the effective potential within an effective field theory approach. Subsequently, we use this framework to determine the thermodynamics of a phase transition within a Standard Model extension, xSM. Our findings demonstrate excellent agreement with other results based upon thermal resummation, whilst providing an analytic and versatile system that can be applied to further models.

Acknowledgements

I would like to express my sincere gratitude to the individuals who have played a role in the successful completion of this thesis. Their guidance, support, and encouragement have been invaluable throughout this year.

First and foremost, I extend my appreciation to my supervisor, Csaba Balazs, for his erudite expertise and infinite patience for my naivete. His insightful feedback and constructive criticism were instrumental in shaping the quality and direction of this research. I am sincerely fortunate to have had the ability to work under his mentorship, and I am truly excited to continue working together.

I am also thankful to the faculty and teachers at both Monash University and the University of Tasmania for their dedication to providing an enriching educational environment. Furthermore, I want to acknowledge the support and camaraderie of my classmates. Our collaborative efforts, discussions, and shared experiences have enriched my learning and made this academic journey all the more memorable. In particular I thank Wilton Deeny, Sam Foster, and Anthony Zulli for their endlessly insightful discussion, as well as Imogen Stephenson and Nikhil Kannachel for their companionship and humour. Lastly, I thank Sophie Young for her friendship during my time at UTas.

Last but certainly not least, I want to express the deepest gratitude to my family for their unwavering support and encouragement. In particular, I dedicate this work to my mother, Elizabeth, whose love and belief in my abilities have been my constant source of motivation.

To everyone mentioned above and to those who have supported me in various ways, your contributions have been instrumental in the successful completion of this thesis.

Contents

1 Introduction

The Standard Model (SM) of particle physics is the most successful scientific theory of all time, providing physical predictions to an unmatched level of accuracy compared to any other known scientific theory. Despite this, it can be defined by what it fails to predict and the vacancies it leaves in our knowledge of the universe around us. Famously, the SM provides no account of gravity, nor the bulk of the universe's constituents in the form of dark matter. But beyond this, there are the further issues of neutrino oscillation, the number of free parameters, and the hierarchy problem to name a few. This motivates the quest of much of modern theoretical physics: to probe what lies beyond the Standard Model (BSM). Grand unification [1], supersymmetry [1], and string theory [2] have all emerged from this mission. However, in our journey to explore these theories we are limited by the technology of our time. To go beyond the SM requires high energy experiments, and the energy level of say, grand unification, would require an astronomic leap in our current engineering capacity.

Cosmological phase transitions provide as with a way around this technological hurdle. These transitions emerge from the spontaneous breaking of symmetries of the SM Lagrangian, and hence naturally provide us with a glimpse into BSM physics. Better still, these phase transitions are predicted to generate gravitational wave radiation [3], which leaves their signature upon the universe's cosmic past. These waves are predicted to be observable by future detectors [4, 5], so the development of observatories such as LISA [6] motivates their study.

But beyond being natural probes for BSM physics, cosmological phase transitions also serve to address many of the open problems in cosmology. An inflationary period during the grand unification epoch has been long proposed as a solution to several cosmological problems, such as the horizon and flatness issues [7]. One suggested mechanism for this inflationary period is that it was instigated by a scalar field formed during a grand unification phase transition [8]. There is also the problem of the non-homogeneity in the large-scale structure of the universe, such as galaxy clusters. This was likely to have been seeded by some primordial gravitational perturbation [9]. One origin for this perturbation is via topological defects appearing during phase transitions, such as cosmic strings [10] or textures [11]. These give rise to localised regions of energy density, and hence positive gravitational pull [12, 13]. Lastly, the origin of baryonic matter asymmetry in our universe (that is, why we have more matter than antimatter) is likely tied to a cosmological phase transition. A baryon generating process is required to satisfy the Sahkarov conditions [14], which are found to be satisfied by the electroweak phase transition [15], making the process of electroweak baryogenesis and the electroweak phase transition of principal importance within this field.

To understand the gravitational waves produced during phase transitions, it is imperative that we have a comprehensive and accurate understanding of their thermodynamics. The evolution and thermodynamics of a phase transition is captured by the effective potential. The most common method to determine this potential is by means of a loop expansion and daisy ressummation [16]. An alternative procedure is via constructing a high temperature effective field theory [17, 18]. Despite this framework emerging over 40 years ago, it has seen limited use within the literature, perhaps due to the complexity of its construction. Fortunately, with the advent of packages such as DRalgo [19] this approach has become markedly more accessible. This effective field theory approach suffers from less theoretical uncertainty arising from perturbative effects [20], and furthermore enables easier integration into lattice simulations to circumvent the Linde problem [21]. The objective of our work will be to explore the use of this effective field theory framework for determining thermodynamics of cosmological phase transitions.

This thesis serves two purposes. The first will be establishing the theory that underpins cosmological phase transitions. We do not attempt to provide a thorough survey of the landscape, but rather we establish this theory with the particular focus on determining the effective potential. We do not shy away from

mathematical rigour, providing as much detail as necessary for a comprehensive discussion. With this in mind, in places we have relegated calculations to the appendix, should they detract from the narrative. We expound both approaches to the effective potential here, being the resummation of thermal masses and the effective field theory approach, elucidating the differences and short comings of each. This provides a basis for the second purpose of this thesis, to investigate the use of the effective field theory approach for determining thermodynamics. We engage in this task to lay a foundation on which further work on using these methods can sit.

The structure of the remainder of thesis is as follows. Section 2 begins with a pedagogical introduction to cosmological phase transitions, and serves to contextualise the rest of this thesis as well as to clarify any relevant terminology. In Section 3 we introduce path integrals, which provide the language the theoretical background of this thesis is formulated in. In Section 4 we derive the effective action as the generating functional of 1PI Feynman diagrams, and use it to derive the conventional 4d approach to the effective potential at finite temperature. Section 5 provides a formal introduction to finite temperature field theory, and develops the framework of dimensionally reduced effective field theories. Then begin our two results sections. Section 6 serves as a proving grounds to substantiate effective field theories in which we approach and elucidate their challenges in the context of the Abelian Higgs model. In Section 7 we derive various thermodynamics for a first-order phase transition in the scalar singlet extension of the SM. Finally, we conclude our thesis in Section 8.

We invoke natural units $c = \hbar = k_B = 1$ within this thesis, where c is the speed of light, $\hbar$ is the reduced Planck's constant, and k_B is the Boltzmann constant. Lastly a note on denoting agency: henceforth the pronoun *I* is used to designate original work, whereas *we* appears in derivations of known or established results.

2 Prelude: Cosmological Phase Transitions

We begin with the question: "*What is a cosmological phase transition?*" The answer is that it is a type of symmetry breaking phase transition (PT) in which invariances of the standard model are spontaneously broken, leading to the formation of new states of matter. This symmetry breaking is initiated by scalar fields. That is, suppose a scalar field ϕ transforms under some representation of a symmetry group $\mathcal{G}$ of our Lagrangian. Further suppose $\mathcal{G}$ is a Lie group with generators $\mathcal{R}_a$, such that elements near the identity are of the form $\exp(i\alpha_a\mathcal{R}_a)$[1]. This symmetry is upheld provided the vacuum state of ϕ, $\langle\phi\rangle$, is zero. Suppose then that ϕ instead obeys a potential with a non-zero vacuum expectation value (VEV): $\langle\phi\rangle = \eta \neq 0$. This picks out a particular configuration for ϕ, breaking the gauge symmetry and sparking the PT. Now, if there exists a subset of generators $\mathcal{R}_b$ that leave this vacuum state $\langle\phi\rangle = \eta$ invariant, then they define the symmetry group $\mathcal{H}$ of this new phase. Lastly, we define the vacuum manifold $\mathcal{M}$ as the space of degenerate points ϕ_i such that $\langle\phi_i\rangle = \eta$, where $\mathcal{M} \simeq \mathcal{G}/\mathcal{H}$ [13, 22, 23].

An example of such a PT which we refer to throughout this work is the electroweak symmetry breaking (EWSB) phase transition [24]. This is mitigated by the Higgs mechanism, in which the complex doublet Higgs field Φ — which transforms under the fundamental representation of electroweak gauge group $SU(2)_L \times U(1)_Y$ — takes on the non-zero VEV $\Phi \propto (0,\ v)^T$. This vacuum state is invariant under a transformation obtained by mixing the neutral generators for $SU(2)_L$ and $U(1)_Y$, leading to the subgroup $U(1)_{EM}$. This group corresponds to the familiar quantum electrodynamic interaction, and we thus describe the electroweak phase transition (EWPT) by $SU(2)_L \times U(1)_Y \to U(1)_{EM}$ where $\mathcal{M} \simeq S^3$.

The idea is that these PTs are defined by the symmetries of the Standard Model and hence allow us to the probe physics beyond by studying them. These transitions are (perhaps incorrectly) said to occur

[1] Formally, $\mathcal{R}_a$ form the basis of the ϕ-representation of $\mathfrak{g}$, the Lie algebra of $\mathcal{G}$.

'spontaneously'. In finite temperature quantum field theory, we find the VEV is zero at high temperatures, and it is only once the system cools does the VEV become non-zero. We can thus find a well defined temperature point (the critical temperature, T_c) beyond which we expect this transition to occur. However, if there is a potential barrier separating the vanishing VEV and the non-zero VEV, then the PT must occur through quantum tunnelling or thermal fluctuations which transition the field into the new VEV. It is in this sense that the transition is spontaneous.

These first-order phase transitions (FOPTs) proceed through bubble nucleation, in which bubbles of the new phase form in the plasma of the old phase. Provided these have a sufficiently large radius to not immediately collapse, they then expand at a speed close to the speed of light (although this expansion is combated by frictional forces arising across the bubble wall) to engulf the entire cosmos. This allows us to define two different temperature milestones, the nucleation temperature T_n and the percolation temperature T_p. T_n is defined as the point where approximately one bubble is nucleated per Hubble horizon, which captures the relationship between the decay rate Γ and the expanding universe [25, 26]. T_p is the point where the nucleated bubbles percolate - i.e., where the is a connected cluster of bubbles that spans the universe [27]. These milestones, $\{T_c, T_n, T_P\}$, can all be used as a benchmark temperature to evaluate thermodynamics.

Above we mentioned the decay rate of the false vacuum, Γ. By far the most common approach to evaluate this is Coleman's bounce formalism [28, 29], as well as the finite temperature modification courtesy of Linde [30, 31]. In this formalism the decay rate is of the form e^{-S_E}, where S_E is an $O(n)$ symmetric 'bounce' action. The field, $\phi(\tau)$, is assumed to start at the false vacuum for $\tau \to -\infty$, before reaching and 'bouncing' off the true vacuum at $\tau = 0$, then returning to the false vacuum at $\tau \to \infty$. The field configuration is solved by a semi-classical analogy of a ball rolling in the upturned potential $V' = -V$, which begins at the true vacuum, then rolls down the potential and stops at the false vacuum due to some frictional force.

We observe FOPTs using gravitational waves. These are generated by the collisions of nucleated bubbles as they expand. This generates waves from three sources: disturbances from the collisions themselves [32, 33], sound waves within the plasma after the collisions [34], and magnetohydrodynamic turbulence within the plasma due to the collisions [35]. These contributions combine linearly, with sound waves providing the dominant contribution. These produce waves that depend strongly on the transition thermodynamics, namely the latent heat, α, and the linearised bounce action, β. In this thesis we attempt to determine these. They also have dependence on the energy fraction κ of the latent heat that goes into producing each source, as well as the bubble wall velocity v_w. These are hydrodynamical in nature, and are beyond the scope of this work.

3 Functional Integrals in Quantum and Statistical Mechanics

Quantum field theory is often taught using one of two equivalent formalisms: the second quantisation approach, or the path integral approach. The former owes its development to Paul Dirac, whilst the latter is attributed to Richard Feynman. In the second quantisation approach, one quantises fields as operators satisfying commutation relations — akin to how one quantises a classical system by promoting dynamical variables to operators in conventional quantum mechanics. These operators are then used to construct physical states in, say, a scattering process. In the path integral approach the principle quantity is no longer the fields themselves, but is instead the action. Amplitudes are considered by integrating over all possible paths a system can take, each weighted by an associated action. Both methods have seen extensive use in the study of QFT. However, it is the path integral approach (or more generally the method of functional integrals) that we employ to develop the framework that follows. As such, we now establish the necessary prerequisites.

3.1 Feynman's Path Integral

Feynman devised his path integral using intuition from the double split experiment. In this experiment, the amplitude for the propagation from source to detector comes from the contributions of both slits. If a second screen is added, the contribution comes from summing over the possible paths between both screens. Continuing in this fashion, if an infinite number of screens with an infinite number of slits are added, the amplitude is then the sum of all possible paths between the source and detector. This is the principle of the path integral, which we will now derive in the context of non-relativistic quantum mechanics, following chapter 14 of [36].

Consider a particle within a one-dimensional potential, with the associated Hamiltonian:

$$\hat{H} = \frac{\hat{p}^2}{2m} + V(\hat{x}, t). \tag{3.1.1}$$

We consider the state $|i\rangle$ localised at a position x_i at some time t_i, and we project onto another state $\langle f|$ localised at position x_f at time t_f. If the Hamiltonian is time-independent we have

$$\langle f|i\rangle = \langle x_f|e^{-i(t_f - t_i)\hat{H}}|x_i\rangle. \tag{3.1.2}$$

Alternatively, if the Hamiltonian carries time dependence we consider discretising the path from x_i to x_f into N steps, separated by a time interval δt over which $\hat{H}$ is constant. This obtains:

$$\langle f|i\rangle = \langle x_f|e^{i\hat{H}(t_f)\delta t} \dots e^{i\hat{H}(t_{i+1})\delta t} e^{i\hat{H}(t_i)\delta t}|x_i\rangle. \tag{3.1.3}$$

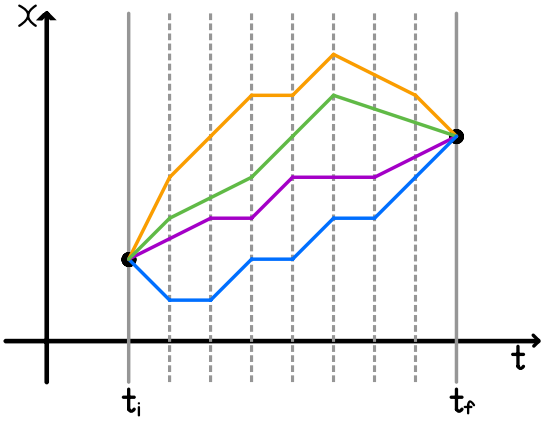

Figure 1: A representation of summing over all paths in Feynman's approach.

Then, we use the completeness of our position basis to insert a set of position eigenstates between each $e^{i\hat{H}\delta t}$. Conceptually, this has the effective of splitting our path into N discrete sections, where we integrate over the possible values of each intermediate point between x_i and x_f, equivalent to integration over all possible paths (see Figure 1):

$$\langle f|i\rangle = \int dx_n \dots dx_1 \langle x_f|e^{i\hat{H}(t_f)\delta t}|x_n\rangle\langle x_n| \dots |x_1\rangle\langle x_1|e^{i\hat{H}(t_i)\delta t}|x_i\rangle. \tag{3.1.4}$$

To evaluate each matrix element in this expression, we insert a set of momentum states:

$$\begin{aligned}
\langle x_{j+1}|e^{-i\hat{H}(t_j)\delta t}|x_j\rangle &= \int \frac{dp}{2\pi}\langle x_{j+1}|p\rangle\langle p| \exp\left[-i\left(\frac{\hat{p}^2}{2m} + V(\hat{x}, t)\right)\delta t\right]|x_j\rangle \\
&= e^{-iV(x_j,t_j)\delta t}\int \frac{dp}{2\pi}\exp\left[-i\frac{p^2}{2m}\delta t + ip(x_{j+1} - x_j)\right] \\
&= Ne^{-iV(x_j,t_j)}\exp\left[-i\frac{m}{2}\delta t\frac{(x_{j+1} - x_j)^2}{(\delta t)^2}\right] \\
&= Ne^{iL(x_j,\,\dot{x}_j)\delta t}.
\end{aligned} \tag{3.1.5}$$

Where the normalisation factor N scales with δt^{-1} and is thus formally infinite in the continuum limit, however, this does not appear in calculations of observable quantities. Inserting these into our amplitude, we have

$$\langle f|i\rangle = N\int dx_n \dots dx_1 \prod_{j=0}^{N} e^{iL(x_j,\dot{x}_j)\delta t}. \tag{3.1.6}$$

We take the continuum limit as $\delta t \to 0$ to obtain:

$$\langle f|i\rangle = N \int_{x(t_i)}^{x(t_f)} \mathcal{D}x(t) e^{iS[x]}, \tag{3.1.7}$$

where the integration measure $\mathcal{D}x(t)$ is defined as in (3.1.6). This is Feynman's path integral for the probability amplitude. It represents summing over all paths connecting the initial and final states, weighted by the action of each. Importantly, the objects in this equation are not operators, but classical variables.

3.2 Functional Representation of the Partition Function

We divert now from discussing quantum mechanics to demonstrate the use of functional methods in statistical mechanics, which will expose a connection between quantum and statistical physics that serves as the foundation of thermal field theory. We use the conventions of [37].

To begin, consider the partition function of a quantum system expressed in the canonical formalism:

$$Z(\beta) = \mathrm{Tr}(e^{-\beta \hat{H}}) = \int dx \langle x|e^{-\beta \hat{H}}|x\rangle, \tag{3.2.1}$$

where we have taken our trace in the position basis. We then evaluate this matrix element using the trick above. That is, we split $e^{-\beta \hat{H}}$ into the product of N parts $e^{-\epsilon \hat{H}}$ where $\epsilon = \beta/N$ and N will be taken to infinity. The derivation then proceeds as in Section 4.1. We insert a set of position eigenstates, before evaluating each matrix element via a set of momentum eigenstates. In essence, the algebra results in replacing every instance of $i\delta t$ in the previous section with ϵ. Thus, we skip to the final result:

$$Z(\beta) = N \int_{x(\beta)=x(0)} \mathcal{D}x(\tau) \exp\left[-\int_0^\beta d\tau \left(\frac{m}{2}\left(\frac{dx(\tau)}{d\tau}\right)^2 + V(x(\tau))\right)\right]. \tag{3.2.2}$$

A strikingly similar formula, with some caveats. Previously, we imposed the boundary conditions that our paths start and end at $x(t_i)$ and $x(t_f)$ respectively. This time, in computing the trace our start and end states are the same, so this requirement manifests as the periodicity (or anti-periodicity for fermions) requirement $x(0) = x(\beta)$. Secondly, our continuous variable previously was t, whereas we now employ the continuous variable τ. These are related, however the latter lacks the same physical interpretation of time and instead arises naturally as a parameterisation of the continuum limit.

The similarities between the partition function above and the path integral for $\langle f|i\rangle$ are notable. To demonstrate the connection between them, we employ the *imaginary-time formalism* [38]. We begin with the argument of Feynman's path integral: $\exp i\int dtL$, where

$$L = \frac{m}{2}\left(\frac{dx(t)}{dt}\right)^2 - V(x,t). \tag{3.2.3}$$

We then Wick rotate to imaginary time via $\tau = -it$, and introduce the Euclidean action

$$L_E(\tau) = -L(\tau = it) = \frac{m}{2}\left(\frac{dx(\tau)}{d\tau}\right)^2 + V(x,\tau). \tag{3.2.4}$$

Finally, we restrict the τ variable to the domain $(0,\beta)$ and impose corresponding periodicity requirements on $x(\tau)$. Following this procedure, we can derive the partition function from Feynman's path integral as

$$\exp\left[i\int dtL\right] \to \exp\left[-\int_0^\beta d\tau L_E\right]. \tag{3.2.5}$$

The periodicity of τ then quantises the states $x(\tau)$ of such systems, just as the boundary conditions of an infinite well quantises the corresponding energy levels. This leads to a Fourier decomposition of the form:

$$x(\tau) = T \sum_{n=-\infty}^{\infty} x_n e^{i\omega_n \tau}. \tag{3.2.6}$$

The corresponding amplitudes x_n are known as *Matsubara modes*, whilst the frequencies ω_n are known as *Matsubara frequencies*. These will have a profound impact when it comes to discussing finite temperature QFT. Indeed, we will see that the imaginary time formalism reduces a relativistic finite temperature theory in $d+1$ dimensions to a Euclidean field theory in d dimensions comprising of infinitely many particles, each represented by a Matsubara mode.

3.3 Path Integrals in Field Theory

We now extend these ideas to field theory. We detail path integrals in zero temperature QFT, whilst their finite temperature counterparts are derived formally in Section 5. Once again we are following Schwarz [36].

The derivation of the path integral in QFT is similar to the procedure for quantum mechanics, whilst the differences that occur are typical of those seen in generalisations to field theory. For instance, instead of position and momentum eigenstates, $|x\rangle$ and $|p\rangle$, we use eigenstates of the field and conjugate momentum operators:

$$\hat{\phi}(\mathbf{x})|\Phi\rangle = \Phi(\mathbf{x})|\Phi\rangle \text{ and } \hat{\pi}(\mathbf{x})|\Pi\rangle = \Pi(\mathbf{x})|\Pi\rangle. \tag{3.3.1}$$

Furthermore, the action becomes the spacetime integral over a Lagrangian density, $\mathcal{L}$, with the conjugate Hamiltonian density $\mathcal{H}$. We refer the reader to [36] for the full derivation, and quote the final result for the vacuum to vacuum amplitude:

$$\langle 0; t_f | 0; t_i \rangle = N \int \mathcal{D}\Phi(\mathbf{x}, t)\ e^{iS[\Phi]}, \tag{3.3.2}$$

where $S = \int d^4x \mathcal{L}$. The time integral is taken from t_i to t_f, however in S matrix elements this extends to $\pm\infty$ such that all of spacetime is integrated over. Again we take the opportunity to reiterate that the object in this expression, Φ, is a classical field and not an operator.

Now, thus far we are yet to provide any demonstration of the utility of the path integral. It is time to change this by introducing the time-ordered product in the path integral formulation. To derive this, we momentarily revert back to our quantum mechanical formulation comfortable in the knowledge the principle generalises immediately to the continuum case. Consider the expression for $\langle f|i\rangle$, and suppose we insert some x_k into our integral, giving us the object: $\int \mathcal{D}x(t)\ e^{iS[x]}\ x_k$. To determine the effect of this, we consider our expansion in terms of position eigenstates:

$$\begin{aligned}
\int \mathcal{D}x(t) e^{iS[x]} x_k &= \int dx_n \dots dx_1 \langle x_f | e^{i\hat{H}(t_f)\delta t} | x_n \rangle \langle x_n | \dots | x_k \rangle \langle x_k | \dots | x_1 \rangle \langle x_1 | e^{i\hat{H}(t_i)\delta t} | x_i \rangle x_k \\
&= \int dx_n \dots dx_1 \langle x_f | e^{i\hat{H}(t_f)\delta t} | x_n \rangle \langle x_n | \dots | x_k \rangle \hat{x}_k \langle x_k | \dots | x_1 \rangle \langle x_1 | e^{i\hat{H}(t_i)\delta t} | x_i \rangle \\
&= \langle f | \hat{x_k} | i \rangle.
\end{aligned} \tag{3.3.3}$$

Thus, we have inserted the operator $\hat{x}_k$ into our matrix element. This result generalises to QFT as:

$$N \int \mathcal{D}\Phi(\mathbf{x}, t)\ e^{iS[\Phi]} \Phi(x_k) = \langle 0 | \hat{\phi}(x_k) | 0 \rangle. \tag{3.3.4}$$

Furthermore, suppose we insert both $\Phi(x_{k_1})$ and $\Phi(x_{k_2})$. Then, we are able to freely move these fields through our eigenstates until they align with their corresponding matrix element, at which point we exchange the

field for the corresponding operator. This grants us time-ordering as the matrix elements within our path integral are themselves time-ordered. Hence, if we generalise to n fields we have:

$$\langle 0|T\hat{\phi}(x_1)\dots\hat{\phi}(x_n)|0\rangle = N\int \mathcal{D}\Phi(\mathbf{x},t)\; e^{iS[\Phi]}\Phi(x_1)\dots\Phi(x_n). \tag{3.3.5}$$

And in the interacting case, we normalise such that $\langle\Omega|\Omega\rangle = 1$, giving us the expression

$$\langle\Omega|T\hat{\phi}(x_1)\dots\hat{\phi}(x_n)|\Omega\rangle = \frac{\int \mathcal{D}\Phi(\mathbf{x},t)\; e^{iS[\Phi]}\Phi(x_1)\dots\Phi(x_n)}{\int \mathcal{D}\Phi(\mathbf{x},t)\; e^{iS[\Phi]}}, \tag{3.3.6}$$

where the formally infinite normalisation N has cancelled.

4 The Effective Action

Here we establish a framework for calculating effective potentials for cosmological phase transitions dynamics. We develop formal foundations for the effective action as a generating functional, building on the path integral methods established in the previous section. We then derive the effective potential from this action for the case of translational invariance. With this, we determine the effective potential to one-loop order for scalar ϕ^4 theory, including both zero and finite temperature contributions. We discuss the role of gauge theories as well as a general form for the effective action in the Standard Model, before concluding with a discussion of the limitations of this approach.

4.1 Generating Functionals

We begin by introducing generating functionals, with much of this discussion borrowing from P&S [39]. Recall from Section 2.3 we expressed the general n-point correlation function as:

$$\langle\Omega|T\hat{\phi}(x_1)\dots\hat{\phi}(x_n)|\Omega\rangle = \frac{\int \mathcal{D}\Phi(\mathbf{x},t)\; e^{iS[\Phi]}\Phi(x_1)\dots\Phi(x_n)}{\int \mathcal{D}\Phi(\mathbf{x},t)\; e^{iS[\Phi]}}. \tag{4.1.1}$$

These can be evaluated on their own, however, taking influence from statistical mechanics, we now introduce a means of determining these by introducing the source term $J(x)$. We couple this source to our scalar field $\phi(x)$ and consider the *generating functional*, $Z[J]$, defined as

$$Z[J] = \int \mathcal{D}\phi \exp\left\{i\int d^4x\,(\mathcal{L} + J(x)\phi(x))\right\}. \tag{4.1.2}$$

Suppose we now vary this with respect to some particular $J(y)$. We have:

$$\begin{aligned}\frac{\delta Z[J]}{\delta J(y)} &= \frac{\delta}{\delta J(y)}\int \mathcal{D}\phi \exp\left\{i\int d^4x\,(\mathcal{L} + J(x)\phi(x))\right\} \\ &= i\int \mathcal{D}\phi \exp\left\{i\int d^4x\,(\mathcal{L} + J(x)\phi(x))\right\}\frac{\delta}{\delta J(y)}\int d^4x\,(\mathcal{L} + J(x)\phi(x)) \\ &= i\int \mathcal{D}\phi \exp\left\{i\int d^4x\,(\mathcal{L} + J(x)\phi(x))\right\}\phi(y).\end{aligned} \tag{4.1.3}$$

We multiply by $-i$ and set $J = 0$, before dividing by the normalisation $Z[0]$. This gives:

$$\frac{-i}{Z[0]}\frac{\delta Z[J]}{\delta J(y)}\bigg|_{J=0} = \frac{\int \mathcal{D}\phi e^{iS[\phi]}\phi(y)}{\int \mathcal{D}\phi e^{iS[\phi]}} = \langle\Omega|\hat{\phi}(y)|\Omega\rangle. \tag{4.1.4}$$

This equation has the immediate generalisation to the n-point correlation function:

$$\frac{(-i)^n}{Z[0]}\frac{\delta Z[J]}{\delta J(x_1)\dots J(x_n)}\bigg|_{J=0} = \langle\Omega|T\hat{\phi}(x_1)\dots\hat{\phi}(x_n)|\Omega\rangle. \tag{4.1.5}$$

Thus, in order to determine any n-point correlation function, we simply need to determine $Z[J]$ and take n functional derivatives. It follows $Z[J]$ is the generating functional of correlation functions.

The analogy here is to statistical mechanics, in which we can determine any thermodynamic quantity of a given system by determining the partition function. Continuing this analogy, we are familiar with the concept of free energy which can be derived from the partition function. In particular, if Z is our partition function, then we have both the Helmholtz free energy, F, which is related to Z via

$$Z = e^{-\beta F}, \tag{4.1.6}$$

and the Gibbs free energy, G, which is the Legendre transformation of F. Significantly, the minimum of G defines the ground state of the system. This property will prove to be very in the following section. We now introduce analogs of F and G in quantum field theory.

First, we introduce the functional $W[J]$ as an analog to F defined according to

$$Z[J] = e^{iW[J]}. \tag{4.1.7}$$

Then, we introduce the analog of G, Γ, which will be related to $W[J]$ via a Legendre transformation in the conjugate variables $J(x)$ and $\delta W[J]/\delta J$:

$$\Gamma = W[J] - \int d^4y J(y)\frac{\delta W[J]}{\delta J(y)}. \tag{4.1.8}$$

In performing the Legendre transformation, we have shifted the dependence on J to a dependence on the new quantity $\delta W/\delta J$, which we see is given by:

$$\begin{aligned}\frac{\delta W[J]}{\delta J(x)} &= \frac{\delta}{\delta J(x)}(-i\ln(Z)) \\ &= \frac{-i}{Z[J]}\frac{\delta Z}{\delta J(x)} \\ &= \langle\Omega|\phi(x)|\Omega\rangle_J,\end{aligned} \tag{4.1.9}$$

where we have applied equation (4.1.5), however we note that unlike the definition in (4.1.5), we have not set $J = 0$. Hence, we include the subscript J as this is the vacuum expectation value of the field in the presence of a background source J. Upon setting $J = 0$, it yields the true vacuum expectation value. We call this quantity the *classical field*, ϕ_{cl}. Correspondingly, $\Gamma \equiv \Gamma[\phi_{\text{cl}}]$.

Now, as Z is a generating functional, so are W and Γ. Without justification, these correspond to generating functionals for connected and 1PI correlation functions respectively. Hence, written as a perturbative expansion in J and ϕ_{cl}, we have [40]:

$$Z[J] = \sum_{n=0}^{\infty}\frac{(i)^n}{n!}\int dx_1\dots dx_n\; G_n(x_1,\dots,x_n)J(x_1)\dots J(x_n) \tag{4.1.10}$$

$$iW[J] = \sum_{n=0}^{\infty}\frac{(i)^n}{n!}\int dx_1\dots dx_n\; G_n^{\text{C}}(x_1,\dots,x_n)J(x_1)\dots J(x_n) \tag{4.1.11}$$

$$\Gamma[\phi_{\text{cl}}] = \sum_{n=0}^{\infty}\frac{1}{n!}\int dx_1\dots dx_n\; G_n^{\text{1PI}}(x_1,\dots,x_n)\phi_{\text{cl}}(x_1)\dots\phi_{\text{cl}}(x_n) \tag{4.1.12}$$

where we have denoted the correlators as Green's functions:

$$G_n(x_1,\dots,x_n) \equiv \langle\Omega|T\hat{\phi}(x_1)\dots\hat{\phi}(x_n)|\Omega\rangle. \tag{4.1.13}$$

4.2 The Effective Potential

Recall Γ was introduced as the analog to the Gibbs free energy. Hence, we expect this equation to define the vacuum state of our theory. We demonstrate this by varying Γ with respect to the classical field ϕ_{cl}:

$$\begin{aligned}\frac{\delta\Gamma[\phi_{\text{cl}}(x)]}{\delta\phi_{\text{cl}}(x)} &= \frac{\delta W[J]}{\delta\phi_{\text{cl}}(x)} - \frac{\delta}{\delta\phi_{\text{cl}}(x)}\int d^4y J(y)\phi_{\text{cl}}(y)\\ &= \int d^4y \frac{\delta W[J]}{\delta J(y)}\frac{\delta J(y)}{\delta\phi_{\text{cl}}(x)} - \int d^4y \frac{\delta J(y)}{\delta\phi_{\text{cl}}(x)} - J(x)\\ &= -J(x).\end{aligned} \tag{4.2.1}$$

Hence, the vacuum of our theory is defined according to

$$\left.\frac{\delta\Gamma[\phi_{\text{cl}}(x)]}{\delta\phi_{\text{cl}}(x)}\right|_{J=0} = 0. \tag{4.2.2}$$

We call the quantity Γ the *effective action*. Given Γ includes all quantum corrections, it is taken to define the *true* vacuum state of our theory. To elaborate, at tree-level the vacuum state of our theory is defined as the state which minimises the potential as it appears in the Lagrangian. However, this tree-level potential can be modified by the inclusion of, say, loop corrections and so on. These radiative corrections can then shift the location of the vacuum state. The beauty of the effective action is that it always defines the true vacuum state of the theory (up to a given order in the perturbative expansion (4.1.12)).

Now, the classical field ϕ_{cl} depends on J and is thus implicitly spacetime dependent, $\phi_{\text{cl}} \equiv \phi_{\text{cl}}(x)$. However, we now consider a spacetime independent theory. In this case, it follows the classical field is now a constant independent of x, which we will simply refer to as ϕ: $\phi_{\text{cl}}(x) \to \phi$. We are then lead to disregard an overall factor of spacetime volume and define the *effective potential*, V_{eff}, according to

$$\Gamma[\phi] = -\int d^4x\ V_{\text{eff}}(\phi). \tag{4.2.3}$$

The effective potential then defines the vacuum of our theory according to:

$$\left.\frac{\partial V_{\text{eff}}}{\partial\phi}\right|_{\phi=v} = 0, \tag{4.2.4}$$

where symmetry breaking is signalled by a non-zero VEV $v \neq 0$.

Evaluating the effective potential is typically done in one of two methods. The first is by shifting the field [41]. The second method makes use of a loop expansion, which we employ. The details of this derivation are mathematically involved, and are thus relegated to Appendix A. To quote the result:

$$V_{\text{eff}}(\phi) = -\sum_{n=0}^{\infty}\frac{\phi^n}{n!}\tilde{G}_n^{\text{1PI}}(p_i = 0). \tag{4.2.5}$$

That is, we expand in terms of the momentum space 1PI Green's functions $\tilde{G}_n^{\text{1PI}}$ of zero external momenta. For example, to zeroth order in this expansion we obtain the tree-level potential. To first order we must sum over all one-loop 1PI Feynman diagrams, and so on. Hence, we obtain an expression of the effective potential of the form:

$$V_{\text{eff}} = V_0 + V_1 + \dots. \tag{4.2.6}$$

4.3 The One Loop Effective Potential for Phi Fourth Theory

The purpose of this section is to derive the one-loop effective potential for ϕ^4 theory, and is drawn from [40]. We include in this calculation both zero-temperature and finite-temperature corrections. Whilst the reader may be familiar with the Feynman rules for such a theory, they can be found in Appendix B at both zero and finite temperature.

Consider the following Lagrangian:

$$\mathcal{L} = \frac{1}{2}(\partial\phi)^2 - \frac{1}{2}m^2\phi^2 - \frac{\lambda}{4!}\phi^4. \tag{4.3.1}$$

We have the following expression for the effective potential:

$$V_{\text{eff}}(\phi) = V_0(\phi) + V_1(\phi) + V_T(\phi), \tag{4.3.2}$$

where $V_0(\phi)$ is the tree-level potential which can immediately be read off the Lagrangian as:

$$V_0(\phi) = \frac{1}{2}m^2\phi^2 + \frac{\lambda}{4!}\phi^4. \tag{4.3.3}$$

V_1 and V_T refer to the one-loop corrections at zero and finite temperature respectively. To calculate the one-loop correction we sum over all 'sun' diagrams of the form of Figure 2. Using the zero-temperature Feynman rules from Appendix B as well as an additional symmetry factor of $1/2n$ to account for the symmetry in both reflections and rotations $\mathbb{Z}_n$, this corresponds to:

$$V_1(\phi) = i\sum_{n=1}^{\infty}\int\frac{d^4p}{(2\pi)^4}\frac{1}{2n}\left[\frac{i}{p^2-m^2+i\epsilon}\right]^n\left[\frac{-i\lambda}{2}\right]^n\phi^{2n}. \tag{4.3.4}$$

Note the factor of i is to ensure this agrees with the definition of the generating functional. This series converges to the Taylor expansion of a logarithm, thus[2]:

$$V_1(\phi) = -\frac{i}{2}\int\frac{d^4p}{(2\pi)^4}\log\left(1-\frac{1}{2}\frac{\lambda\phi^2}{p^2-m^2+i\epsilon}\right). \tag{4.3.5}$$

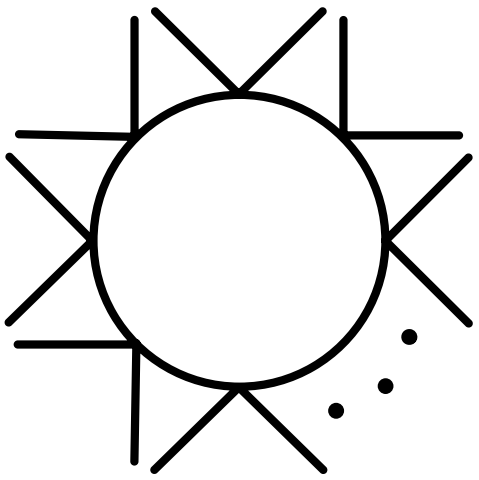

Figure 2: General form of the n-point one-loop diagrams contributing to the one-loop effective potential.

This integral seems intimidating, however we can simplify by first introducing a Wick rotation (at which point the $i\epsilon$ becomes redundant). Then, we can write the expression in terms of the field-dependent mass and disregard any field-independent terms, giving:

$$V_1(\phi) = \frac{1}{2}\int\frac{d^4p}{(2\pi)^4}\log\left(p^2+m^2(\phi)\right), \tag{4.3.6}$$

where:

$$m^2(\phi) = \frac{d^2V_0}{d\phi^2} = m^2 + \frac{1}{2}\lambda\phi^2. \tag{4.3.7}$$

This integral is ultraviolet divergent and thus requires regularisation. To do so, we employ dimensional regularisation in the modified minimal subtraction ($\overline{\text{MS}}$) scheme [42, 43]. This is done in Appendix C, in which we obtain:

$$V_1(\phi) = \frac{m^4}{64\pi^2}\left(\log\left(\frac{m^2}{\overline{\mu}^2}\right) - \frac{3}{2}\right). \tag{4.3.8}$$

[2] That is, $\log(1-x) = -\Sigma_{n=1}^{\infty}\, x^n/n$.

To obtain V_T, we repeat this process using the rules of finite temperature field theory, which gives

$$V_T(\phi) = \frac{T}{2} \sum_{n=-\infty}^{\infty} \int \frac{d^3p}{(2\pi)^3} \log(\omega_n^2 + \omega^2), \tag{4.3.9}$$

in which the temporal component has been discretised into a sum over Matsubara modes defined by $\omega_n = 2n\pi\beta^{-1}$, whilst the remainder is a conventional Euclidean integral in three dimensions. Evaluating this sum (see the technique in Appendix E) obtains:

$$V_T(\phi) = \int \frac{d^3p}{(2\pi)^3} \left[\frac{\omega}{2} + \frac{1}{\beta} \log(1 - e^{-\beta\omega}) \right]. \tag{4.3.10}$$

That is, the potential splits into temperature independent and dependent component. The temperature dependent part of our potential can be written as follows:

$$\frac{1}{\beta} \int \frac{d^3p}{(2\pi)^3} \log(1 - e^{-\beta\omega}) = \frac{1}{2\pi^2\beta^4} J_B[m^2(\phi)\beta^2], \tag{4.3.11}$$

where J_B is the thermal bosonic function, defined as:

$$J_B[z] = \int_0^\infty dx\ x^2 \log[1 - e^{-\sqrt{x^2+z^2}}]. \tag{4.3.12}$$

This gives us the temperature-dependent one-loop correction to our effective potential. The full one-loop effective potential becomes:

$$V_{\text{eff}}(\phi) = \frac{1}{2}m^2\phi^2 + \frac{\lambda}{4!}\phi^4 + \frac{m^4}{64\pi^2}\left(\log\left(\frac{m(\phi)^2}{\overline{\mu}^2} \right) - \frac{3}{2} \right) + \frac{1}{2\pi^2\beta^4} J_B[m^2(\phi)\beta^2]. \tag{4.3.13}$$

4.4 Gauge Theories and the Standard Model

Throughout this section we have used ϕ^4 theory as a computational tool, due to its simplicity. However, the scenario is complicated once we consider both fermionic and gauge fields. The former requires the introduction of Grassmann numbers in to treat their anti-commuting nature, which we do not provide here. On the other hand, we turn now to discussing gauge fields.

In Appendix D we discuss generating functionals for Yangs-Mills gauge theories. We show that gauge invariance introduces divergences in our Gaussian integrals, as a consequence of integrating over infinitely many gauge-equivalent (and hence redundant) field configurations. That is, the path integral formulation provides no mechanism for selecting out physically unique solutions. We enforce such a mechanism by hand by introducing a gauging fixing term to the potential, which is associated by non-physical *ghost* particles. For example, a pure $SU(N)$ gauge theory has the gauge-fixed Lagrangian:

$$\mathcal{L} = -\frac{1}{4}(F^a_{\mu\nu})^2 - \frac{(\partial^\mu A^a_\mu)^2}{2\xi} + \bar{c}^a \left(-\partial^2\delta^{ac} - g\partial^\mu f^{abc} A^b_\mu \right) c^c, \tag{4.4.1}$$

where ξ specifies the gauge and c corresponds to the N ghost fields. This are known as the generalised R_ξ gauge.

Despite the manifest dependence in the Lagrangian, ξ does not appear in physical observables. This is provided the caveat that calculations are performed with a consistent choice of ξ. However, the case is complicated when we consider symmetry breaking. Even at tree-level the parameter ξ appears in the potential, such that the effective potential is a manifestly gauge dependent quantity. However, this does not

mean that we should disregard the theory entirely. The effective potential itself isn't physically observable, but rather *differences* in the potential are. We circumvent the gauge dependence of the potential by ensuring that the minimum of the potential are gauge independent.

This may seem paradoxical, so we illustrate the point further. Suppose $V(\phi, \xi)$ is a gauge dependent effective potential with minima $\bar{\phi}(\xi)$, which, as expected, is gauge dependent. Suppose we want to enforce that the minimum of V at $\phi = \bar{\phi}$ is gauge independent[3]:

$$\left.\frac{\partial V}{\partial \xi}\right|_{\phi=\bar{\phi}} = 0. \tag{4.4.2}$$

This can be achieved if there exists some function $C(\phi, \xi)$ such that:

$$\left(\xi \frac{\partial}{\partial \xi} + C(\phi, \xi)\frac{\partial}{\partial \phi}\right) V = 0. \tag{4.4.3}$$

Then, evaluating this expression at $\phi = \bar{\phi}$, we have:

$$\xi \left.\frac{\partial V}{\partial \xi}\right|_{\phi=\bar{\phi}} + C(\bar{\phi}, \xi)\left.\frac{\partial V}{\partial \phi}\right|_{\phi=\bar{\phi}} = \xi \left.\frac{\partial V}{\partial \xi}\right|_{\phi=\bar{\phi}} = 0, \tag{4.4.4}$$

where the first equality is from the definition of $\bar{\phi}$. Hence, (4.4.3) ensures the minimum is gauge independent. The existence of such a $C(\phi, \xi)$ is proven by the Nielsen Identities [44], which are a consequence of the Ward-Takahashi identities, however a detailed derivation extends beyond the scope of this discussion. It is sufficient for our purposes to have the core message: a ξ-dependent physical observable is permissible, provided any change in the gauge parameter is associated with a compensating change in the minima $\bar{\phi}$[4]. A further example can be seen in the Nielsen identity for the mass $m^2(\phi, \xi)$, which has the associated Nielsen identity [45]:

$$\left(\xi \frac{\partial}{\partial \xi} + C(\phi, \xi)\frac{\partial}{\partial \phi}\right) m^2 = 0 \text{ if } \frac{\partial V}{\partial \phi} = 0. \tag{4.4.5}$$

This can likewise be shown to imply the mass is gauge-invariant:

$$\frac{dm^2}{d\xi} = \frac{\partial m^2}{\partial \bar{\phi}}\frac{d\bar{\phi}}{d\xi} + \frac{\partial m^2}{\partial \xi} = 0. \tag{4.4.6}$$

To demonstrate the explicit ξ dependence at one loop, we provide the general result for the effective potential in a theory involving scalars, fermions, and gauge bosons. For the zero temperature contribution, we have [46]:

$$\begin{aligned} V_1(\phi) = &\sum_i \frac{n_i}{4(4\pi)^2} m_i^4(\phi, \xi)\left[\ln\left(\frac{m_i^2(\phi, \xi)}{\mu^2}\right) - \frac{3}{2}\right] + \sum_a \frac{n_a}{4(4\pi)^2} m_a^4(\phi, \xi)\left[\ln\left(\frac{m_i^2(\phi)}{\mu^2}\right) - \frac{5}{6}\right] \\ &- \sum_a \frac{1}{4(4\pi)^2}(\xi m_a^2(\phi, \xi))^2\left[\ln\left(\frac{\xi m_i^2(\phi)}{\mu^2}\right) - \frac{3}{2}\right] - \sum_I \frac{n_I}{4(4\pi)^2} m_I^4(\phi, \xi)\left[\ln\left(\frac{m_I^2(\phi, \xi)}{\mu^2}\right) - \frac{3}{2}\right], \end{aligned} \tag{4.4.7}$$

where i, a, and I represent the scalar, massive gauge boson, and fermion sums, with respective degrees of freedom $n_i = 1$, $n_a = 3$, and $n_I = 2$. Likewise, the temperature dependent one loop correction is given

[3] Note my distinction between the *minima* $\bar{\phi}$, and the *minimum* $V(\bar{\phi})$.

[4] Since $\bar{\phi}$ depends on ξ, another way of phrasing this is that both the implicit $\bar{\phi}$ and explicit V dependencies on ξ cancel each other.

by[46]:

$$V_T(\phi) = \frac{T^4}{2\pi^2}\left[\sum_i n_i J_B\left(\frac{m_i^2(\phi,\xi)}{T^2}\right) + \sum_a n_a J_B\left(\frac{m_a^2(\phi,\xi)}{T^2}\right) - \frac{1}{3}\sum_a n_a J_B\left(\frac{\xi m_a^2(\phi,\xi)}{T^2}\right) + \sum_I n_I J_F\left(\frac{m_I^2(\phi,\xi)}{T^2}\right)\right], \tag{4.4.8}$$

where J_B and J_F are the thermal bosonic and fermionic functions. These two expressions can be used to calculate corrections to the effective potential at one-loop for the Standard Model. In this case, we sum over the Higgs field, W and Z bosons (as well as any associated Goldstone bosons), and the only fermion contribution with a non-negligible mass to be summed over is the top quark [40].

4.5 Thermal Functions and the Infrared Problem

We have established a means of determining the effective potential for a thermal theory containing any arbitrary number of scalars, gauge fields, and fermions in any R_ξ gauge. We now briefly remark on some of the conceptual and practical issues faced by this approach.

The one-loop corrections at zero-temperature involve simple logarithms of the fields. However, the finite-temperature contributions involve bosonic and fermionic thermal functions. These have no closed form in the sense they cannot be expressed in terms of elementary functions [37] and must be approached numerically. There are ways of overcoming this hurdle however. We notice these functions have as their arguments the ratio m/T, and hence admit both high temperature ($m/T \ll 1$) and low temperature ($m/T \gg 1$) limits.

For the low temperature case, we use the convergent sum representation of these integrals in terms modified Bessel functions. In the bosonic case for $z = m/T \gg 1$, this corresponds to:

$$J_B[z] = \int_0^\infty dx\; x^2 \log[1 - e^{-\sqrt{x^2+z^2}}] = -z^2 \sum_{n=1}^\infty \frac{K_2(nz)}{n^2}, \tag{4.5.1}$$

in which $K_2(nz) > K_2((n+1)z)$ for $z \gg 1$, a result that follows immediately from the integral expression of $K_2(nz)$:

$$K_2(nz) = \int_0^\infty dt \cosh(2t) e^{-nz\cosh(t)}, \tag{4.5.2}$$

such that our integrand is suppressed by the factor $e^{-z\cosh(t)} \ll 1$ and this summation converges. Alternatively, we can Taylor expand our logarithm to leading order for small $e^{-\sqrt{x^2+z^2}}$ which gives [37]:

$$\int_0^\infty dx\; x^2 \log[1-e^{-\sqrt{x^2+z^2}}] = -\int_0^\infty dx\; x^2 e^{-\sqrt{x^2+z^2}} + O(e^{-2z}) = -\sqrt{2}\Gamma\left(\frac{3}{2}\right) z^{\frac{3}{2}} e^{-z}\left[1 + O\left(\frac{1}{z}\right) + O(e^{-z})\right]. \tag{4.5.3}$$

As for the high temperature limit $z = m/T \ll 1$, we quote the following result derived by Jackiw [47]:

$$\frac{T^4}{2\pi^2}\int_0^\infty dx\; x^2 \log[1 - e^{-\sqrt{x^2+z^2}}] = -\frac{\pi^2 T^4}{90} + \frac{m^2 T^2}{24} - \frac{m^3 T}{12\pi} - \frac{m^4}{2(4\pi)^2}\left[\ln\left(\frac{m e^{\gamma_E}}{4\pi T}\right) - \frac{3}{4}\right] + \frac{m^6 \zeta(3)}{3(4\pi)^4 T^2} + O\left(\frac{m^8}{T^4}\right). \tag{4.5.4}$$

These expansions allow one to circumvent the problem of a non-elementary potential, and place the finite temperature effective potential the form of a polynomial in T, making it much simpler to perform calculations with. Inconveniently, these expansions are valid in opposite regimes. This can be resolved by patching the

two pieces smoothly together at a value of $z = m/T$ where their first derivatives match at the transition point [48]. This has been shown to provide a good approximation for the full integral across the entire temperature range.

Whilst being non-elementary, the integral appearing in thermal corrections is a function of a single variable, with a single output. As such, an alternative approach that is employed in the cosmological phase transition packages *CosmoTransitions* [49] and *PhaseTracer* [50], is to simply tabulate the values of these functions. Regardless of the approach used, the complexity of the thermal potential requires careful treatment in order to extract workable physical quantities.

Aside from this quantitative issue, there are problems with the validity of the perturbative expansion at finite temperature. The phenomena of symmetry restoration states that a possibly broken symmetry at tree-level theory can be restored by finite temperature corrections [51]. E.g., the tree-level Higgs potential is broken for a negative squared mass, yet this symmetry is restored if we push finite-temperature corrections to a high enough temperature. However, the work of [52] is based off the observation that a symmetry broken at one order of perturbation theory should remain broken at all orders, an idea which conflicts with the notion of symmetry restoration unless perturbation theory breaks down at high temperatures. The reason for this breakdown of perturbation theory at high temperature comes from infrared bosonic modes, which we demonstrate now. This method is attributed to Weinberg [52], and we will follow the application of the method to ϕ^4 from [53] and [54]. Consider again our conventional ϕ^4 theory of mass m and quartic coupling λ. We consider a single loop diagram with superficial divergence D, such as Figure 3 with $D = 2$. Upon rescaling all internal momenta and energy by T, the amplitude associated with this diagram goes like $T^D I(m/T)$, which, provided there are no infrared divergences when $m/T \to 0$, goes like T^D for large T.

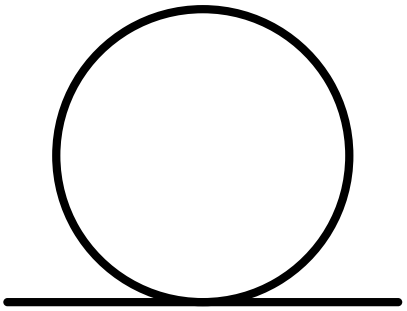

Figure 3: Feynman diagram with superficial degree of divergence $D = 2$.

If $D \leq 0$, then infrared divergences invalidate this argument, however, this only occurs in the infrared $n = 0$ mode from our loop integral — from which the only temperature dependence comes from the T in front of the integral (see Appendix B). Conversely, due to the $\omega_0 = 0$ term the loop integral also goes like T. Thus, a quadratically divergent loop contributes T^2, with every other loop giving a factor of T.

Thus, in a high temperature theory, the largest graphs at any order in the loop expansion are those that provide a maximum number of quadratically divergent loops. These correspond to the 'daisy' diagrams, as seen in Figure 4. Introducing a mass scale $\mathcal{M}$, the amplitude of an n-loop daisy diagram goes like:

$$\lambda^2 \frac{T^3}{\mathcal{M}} \left(\frac{\lambda T^2}{\mathcal{M}^2} \right)^{n-1}, \tag{4.5.5}$$

and hence the expansion parameter has gained a temperature enhancement $\lambda \to \lambda T^2/\mathcal{M}^2$. As claimed, at high temperatures $T \gg \mathcal{M}$, these finite temperature effects can compensate for the smallness of $\lambda \ll 1$ leading to a breakdown of perturbation theory.

The solution is to resum these daisy diagrams introducing an effective mass M containing a finite temperature mass counter-term to absolve these effects, restoring the validity of perturbation theory. We define the effective mass in terms of the full propagator, which is expanded in terms of 1PI insertions as in Figure 5. If we define Π to be the self-energy we have:

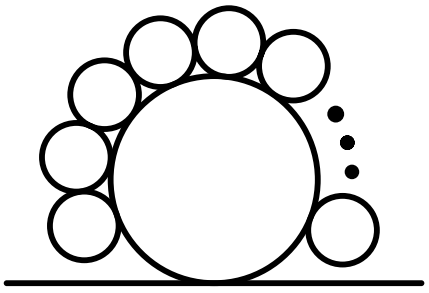

Figure 4: n-point daisy diagram that requires resummation. The additional daisy loops arise strictly from $n = 0$ modes.

$$\frac{1}{p^2 + M^2} = \frac{1}{p^2 + m^2} \sum_{n=0}^{\infty} \frac{(-\Pi)^n}{(p^2 + m^2)^n} = \frac{1}{p^2 + m^2 + \Pi}, \tag{4.5.6}$$

such that $M^2 = m^2 + \Pi$. We estimate Π by taking only the contribution from the lowest term given in Figure 3 to obtain:

$$\Pi \approx \frac{\lambda T}{2} \sum_{n=0}^{\infty} \int \frac{d^3p}{(2\pi)^3} \frac{1}{p^2 + m^2 + \omega_n^2}. \tag{4.5.7}$$

In a high temperature limit, this integral evaluates to $\Pi = \lambda T^2/24$, such that the effective mass becomes temperature dependent:

$$M^2 = m^2 + \frac{\lambda T^2}{24} = m^2 + m_D^2, \tag{4.5.8}$$

where we call the finite temperature corrected mass, m_D, the thermal or Debye mass. The potential with Debye mass is given by:

$$V_{\text{eff}}(\phi, T) = \left(m^2 + \frac{\lambda T^2}{12} \right) \frac{\phi^2}{2} + \frac{\lambda \phi^4}{4}. \tag{4.5.9}$$

This can be thought of as taking only the leading contribution from the high temperature effective potential [54]. There are different methods to performing daisy resummation, with two popular methods being the Parwani procedure [55] and the Arnold and Espinosa procedure [56]. The former corresponds to replacing the boson masses in the potential (including thermal functions) with their thermally corrected counterparts: $m^2 \to m^2_{\text{eff}}(T)$. The latter procedure involves first taking the high temperature expansion of the thermal functions in the effective potential (c.f. (4.5.4)), then replacing any masses with their thermal counterparts. The approach we have employed here is thus the Parwani method at leading order, however up to one loop they are equivalent.

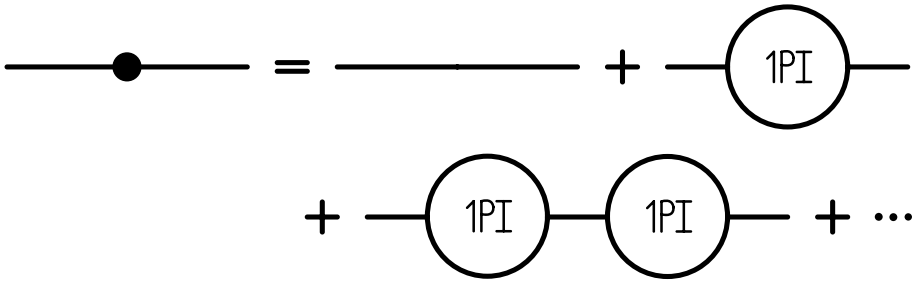

Figure 5: Expansion of the full 2-point correlator as a geometric series in terms of 1PI insertions to the free 2-point correlator.

Now, an alternative method for dealing with the problematic $n = 0$ infrared modes is to construct an effective field theory for the $n = 0$ via the integrating out the non-zero modes. Given the imaginary time formalism trades time evolution for temperature dependence, the resulting effective field theory is three dimensional. This framework will be developed in the forthcoming section.

5 Finite Temperature Effective Field Theories

We have thus far circumvented a formal treatment of thermal field theory, which we now provide. To understand the construction of a finite temperature effective field theory, we first require some understanding of finite temperature QFT. In this section, we will first establish the basics of thermal field theory in the imaginary time formalism, detailing the path integral representation of the partition function following [57]. We then calculate the partition function and free energy for a real scalar field theory, and demonstrate that the free energy corresponds precisely to the one-loop correction of our effective potential. We conclude with a discussion of finite temperature effective field theories.

5.1 An Introduction to Finite Temperature Field Theory

In 3.2 we discussed the derivation of a path integral representation of the partition function in quantum statistical mechanics. We now generalise this discussion to continuous systems. For the field case, our path integral is represented by:

$$Z = \sum_a \int d\phi_a \langle \phi_a | e^{-\beta \mathcal{H}} | \phi_a \rangle, \tag{5.1.1}$$

where $|\phi_a\rangle$ are eigenstates of our field operator:

$$\hat{\phi}(\mathbf{x}, 0)|\phi\rangle = \phi(\mathbf{x})|\phi\rangle, \tag{5.1.2}$$

and the trace is then taken over all such orthogonal states:

$$\langle \phi_a | \phi_b \rangle = \prod_x \delta(\phi_a(x) - \phi_b(x)). \tag{5.1.3}$$

There likewise exist similar states for the momentum field operator, $|\pi_a\rangle$. We can derive the path integral representation of Z following the derivation of 4.1. However, we offer an alternative derivation that takes full advantage of the imaginary time formalism by using a Wick rotation. We consider the vacuum to vacuum amplitude (3.3.2) from zero temperature QFT:

$$\langle 0|0\rangle = N \int \mathcal{D}\phi e^{iS[\phi]}. \tag{5.1.4}$$

Consider the action:

$$iS[\phi] = i \int d^4x \left[(\partial\phi)^2 + V(\phi) \right] = i \int dt d^3\mathbf{x} \left[\left(\frac{d\phi}{dt} \right)^2 - (\nabla\phi)^2 - V(\phi) \right]. \tag{5.1.5}$$

Performing a Wick rotation $t = -i\tau$, we obtain:

$$iS[\phi] = i \int d(-i\tau) d^3\mathbf{x} \left[\left(i\frac{d\phi}{d\tau} \right)^2 - (\nabla\phi)^2 - V(\phi) \right] = - \int d\tau d^3\mathbf{x} \left[\left(\frac{d\phi}{d\tau} \right)^2 + (\nabla\phi)^2 + V(\phi) \right]. \tag{5.1.6}$$

We then enforce periodic boundary conditions in the new compact τ direction, ensuring $\phi(\tau = 0) = \phi(\tau = \beta)$. If we compare this result to, say, (3.2.2), we find that what we have obtained above is precisely the partition function, now generalised to a continuous system. That is, in the imaginary time formalism, the quantum average of the vacuum, $\langle 0|0\rangle$, is equivalent to the thermal average of the partition function, Z. If we restore the factor of $1/2$ in front of our kinetic term and write the potential as $V(\phi) = m^2\phi^2/2 + U(\phi)$, we obtain:

$$Z = \int_{\phi(0,\mathbf{x}) = \phi(\beta,\mathbf{x})} \mathcal{D}\phi \exp \left[- \int_0^\beta d\tau \int d\mathbf{x} \left(\frac{1}{2} \left(\frac{d\phi}{d\tau} \right)^2 + \frac{1}{2}(\nabla\phi)^2 + \frac{m^2}{2}\phi^2 + U(\phi) \right) \right]. \tag{5.1.7}$$

Which generalises to any arbitrary field theory as:

$$Z = \int_{\phi_i(0,\mathbf{x})=\pm\phi_i(\beta,\mathbf{x})} \mathcal{D}\phi_i \exp\left[-\int_0^\beta d\tau \int d\mathbf{x}\ \mathcal{L}_\mathrm{E}\right], \tag{5.1.8}$$

for any number of fields ϕ_i. Note that Fermionic fields satisfy anti-periodic boundary conditions. This result can also be derived taking (5.1.1) as a starting point and expanding conventionally. As mentioned in 3.2, the periodicity constraints on the compact τ direction result in only discrete particle modes being allowed. Hence, in the imaginary time formalism each particle present in the zero temperature theory gets broken into a tower of infinitely many particles in the thermal theory.

5.2 Thermodynamics of Scalar Field Theory

Consider for now a non-interacting real scalar field theory, such that $U(\phi) = 0$ in (5.1.7). The partition function becomes:

$$\begin{aligned} Z &= \int_{\phi(0,\mathbf{x})=\phi(\beta,\mathbf{x})} \mathcal{D}\phi \exp\left[-\int_0^\beta d\tau \int d\mathbf{x} \left(\frac{1}{2}\left(\frac{d\phi}{d\tau}\right)^2 + \frac{1}{2}(\nabla\phi)^2 + \frac{m^2}{2}\phi^2\right)\right] \\ &= \int_{\phi(0,\mathbf{x})=\phi(\beta,\mathbf{x})} \mathcal{D}\phi \exp\left[-\int_0^\beta d\tau \int d\mathbf{x} \left(-\frac{1}{2}\phi\frac{d^2\phi}{d\tau^2} - \frac{1}{2}\phi\nabla^2\phi + \frac{m^2}{2}\phi^2\right)\right]. \end{aligned} \tag{5.2.1}$$

Where we have integrated by parts. We can enforce periodicity constraints on ϕ by expanding in terms of Fourier modes:

$$\phi(\tau,\mathbf{x}) = \sqrt{\beta}\sum_n \phi_n(\mathbf{x}) e^{i\omega_n\tau}, \tag{5.2.2}$$

where $\omega_n = 2\pi nT$. The factor of $\sqrt{\beta}$ is a matter of normalisation convention — akin to analogous factors of spacetime volume that typically associate momentum-space Fourier expansions. We then expand each ϕ in our potential using n and m as indices. Acting out our τ second derivative, we can integrate over τ using the orthogonality condition:

$$\int_0^\beta d\tau\ \exp\left[i\tau(\omega_n + \omega_m)\right] = \beta\delta_{n,-m}. \tag{5.2.3}$$

We also note that ϕ being real requires $\phi_{-n} = \phi_n^*$, hence, we obtain:

$$\begin{aligned} Z &= \int \mathcal{D}\phi \exp\left[-\frac{\beta^2}{2}\sum_n \phi_n^*\left(\nabla^2 + m^2 + (2\pi nT)^2\right)\phi_n\right] \\ &= \prod_n \int \mathcal{D}\phi \exp\left[-\frac{1}{2}\int d^3x d^3y\ \phi_n^*(x) K_n(x,y)\phi_n(y)\right], \end{aligned} \tag{5.2.4}$$

where we have written the partition function as a Gaussian integral involving the quadratic form determined by the Kernel:

$$K_n(x,y) = \beta^2(-\nabla_x^2 + m_n^2)\delta(x-y), \tag{5.2.5}$$

for Matsubara modes with masses $m_n^2 = m^2 + (2\pi nT)^2$. This Gaussian integral then admits the formal solution:

$$Z = \prod_n (\det K_n)^{-1/2}, \tag{5.2.6}$$

where we have neglected arbitrary normalisations. To evaluate this determinant, we can expand the 3d field $\phi(\mathbf{x})$ in momentum space. That is, we write the expansion as:

$$\phi(\tau,\mathbf{x}) = \sqrt{\frac{\beta}{V}}\sum_n\sum_{\mathbf{p}} e^{i(\mathbf{p}\cdot\mathbf{x}+\omega_n\tau)}\phi_n(\mathbf{p}). \tag{5.2.7}$$

Proceeding as we did above, the action becomes:

$$S = -\frac{\beta^2}{2} \sum_n \sum_{\mathbf{p}} (\omega_n^2 + \omega^2) \phi_n^*(\mathbf{p}) \phi_n(\mathbf{p}), \tag{5.2.8}$$

where $\omega^2 = \mathbf{p}^2 + m^2$. Hence, we find the dynamical variable is $A_n(\mathbf{p}) = |\phi_n(\mathbf{p})|$, not ϕ_n — an expected result as the phase of the modes is arbitrary. We change variables in our partition function to an integral over A_n, such that it becomes a product of Gaussian integrals:

$$Z = \prod_n \prod_{\mathbf{p}} \int dA_n \exp\left[-\frac{1}{2} \beta^2 (\omega_n^2 + \omega^2) A_n^2 \right]. \tag{5.2.9}$$

Performing each Gaussian integral, we find the following equivalent representation of the partition function:

$$Z = \prod_n \prod_{\mathbf{p}} \left[\beta^2 (\omega_n^2 + \omega^2) \right]^{-1/2}. \tag{5.2.10}$$

This representation also follows from writing the Kernel $K_n(x, y)$ in momentum space[5]. With this, we can derive any number of thermodynamic quantities for our field theory, such as the pressure or entropy. Arguably the most important of these is the free energy, which requires the logarithm or our partition function:

$$\ln(Z) = \ln\left(\prod_n \prod_{\mathbf{p}} \left[\beta^2 (\omega_n^2 + \omega^2) \right]^{-1/2} \right) = -\frac{1}{2} \sum_n \sum_{\mathbf{p}} \ln\left(\beta^2 (\omega_n^2 + \omega^2) \right). \tag{5.2.11}$$

Evaluation of this expression is somewhat involved. We refer the reader to Appendix E for details, in which we derive the following expression:

$$\ln(Z) = V \int \frac{d^3 p}{(2\pi)^3} \left[-\frac{\beta\omega}{2} - \ln(1 - e^{-\beta\omega}) \right]. \tag{5.2.12}$$

The free energy per volume is then defined as:

$$F = -\frac{T}{V} \ln(Z) = \int \frac{d^3 p}{(2\pi)^3} \left[\frac{\omega}{2} + \frac{1}{\beta} \ln(1 - e^{-\beta\omega}) \right]. \tag{5.2.13}$$

We immediately recognise this as the one-loop potential (4.3.10), here derived formally within the context of finite temperature field theory. The correspondence between the one-loop effective potential and the zeroth-order (non-interacting!) free energy exposes a contradiction within the use of the effective potential in the previous section. We see there that the leading order effective potential is temperature independent. However, upon a rigorous finite temperature treatment of the free energy we see that what was previously considered a perturbative effect, arises instead as the leading order contribution. Furthermore, in our formal framework we haven't considered interactions at all (recall we set $U(\phi) = 0$), whereas in the effective potential derivation these temperature effects only come from one-loop diagrams generated by a quartic ϕ^4 interaction. This is a consequence of the effective potential framework not treating both zero temperature and finite temperature effects on an equal footing, treating the latter as a perturbative afterthought.

[5] That is, $-\nabla^2 + m_n^2$ has eigenvalue $\omega_n^2 + \omega^2$ for $\omega^2 = m^2 + \mathbf{p}^2$. The determinant is then the product over $\mathbf{p}$ of all such eigenvalues.

5.3 Dimensionally Reduced Effective Field Theories

We have now discussed the prerequisite theory to explore finite temperature effective field theory, following the methodology developed in [58, 59, 60]. This is motivated by a simple observation. Consider the thermal masses of the 3d Matsubara modes ϕ_n:

$$m_n^2 = m^2 + (2\pi n T)^2. \tag{5.3.1}$$

Note for fermionic masses the anti-periodicity requires the thermal contribution to be $[(2n+1)\pi T]^2$. Suppose we are then dealing with sufficiently high enough temperatures such that $2\pi T \gg m$. This admits a hierarchy of energy scales that separates the zero mode m_0^2 (which we recall causes the infrared issues at high temperature) and the non-zero thermal modes $m_{n\neq 0}^2$. It follows then that we can integrate out these high temperature modes to create an effective field theory for the infrared mode. Upon integrating out these modes, the resulting Lagrangian is three dimensional and fully bosonic. This procedure is often called dimensional reduction, but due to the confusion nature of this name (c.f. the similar dimensional regularisation approach to renormalisation), we'll aim to refer to it as the effective field theory technique instead[6].

We 'integrate out' all extra fields by positing a simpler 3d Lagrangian for the effective theory, then solve for the constants in this Lagrangian by matching Green's functions. In this section, we will detail the methodology involved in constructing the effective field theory.

To begin, consider an arbitrary gauge theory defined by the Lagrangian:

$$\mathcal{L} = \frac{1}{4}F_{\mu\nu}F^{\mu\nu} + (D_\mu\phi)^\dagger(D_\mu\phi) + V(\phi) + g_Y\bar{\psi}\phi\psi + \delta\mathcal{L}, \tag{5.3.2}$$

for gauge fields A_μ, scalar fields ϕ, and fermion fields ψ. For the sake of power counting we assume $\lambda \sim g^2$ and $g_Y \sim g$. The theory is renormalisable with all counterterms being contained in δL, such that ϕ is allowed a quartic interaction:

$$V(\phi) = m_s^2\phi^\dagger\phi + \lambda(\phi^\dagger\phi)^2. \tag{5.3.3}$$

Now, consider the 1-loop Debye mass contributions of the zero boson modes ϕ_0 due to the modes $\phi_{n\neq 0}$ and ψ_n. These have the form:

$$m_i^2(T) = m_i^2 + \alpha_i T^2. \tag{5.3.4}$$

For example, in the scalar ϕ^4 theory of 4.5, we saw that the Debye mass from the non-zero modes corresponds to $\alpha_i \propto \lambda \sim g^2$. It can be shown that the spatial components of the gauge fields gain no corrections, $m_i, \alpha_i = 0$, the temporal components gain purely Debye corrections, $m_i = 0$, $\alpha_i \neq 0$, whilst the scalar fields have both $m_i, \alpha_i \neq 0$. These masses can be separated depending on their scales.

All fermionic modes and non-zero bosonic modes scale with πT, and are called hard modes. All temporal gauge modes scale with gT and are called soft. Finally, scalar fields are either soft when m_i^2 is different from $-\alpha_i T^2$, or ultrasoft when $m_i^2 \approx -\alpha_i T^2$ (such as near a phase transition where $m_i^2(T) \approx 0$). These ultrasoft masses scale with g^2T. In the example from 4.5, the scalar mass is ultrasoft, as expected. This establishes a hierarchy in the effective field theory. Firstly, we can integrate out all hard modes, yielding a theory valid for scales up to gT. We can then further integrate all temporal gauge fields to yield the ultrasoft theory, which is valid for up to energy scales up to g^2T. Because spatial gauge fields are ultrasoft they will remain in the theory at all levels of integration.

[6] More confusing nomenclature is no doubt inbound for readers unfamiliar with effective field theories, as use of *effective* in *effective potential* and in *effective field theories* are not equivalent terminologies.

If we construct a Lagrangian for the soft scale for the theory described by (5.3.2), we include the following terms:

$$\mathcal{L} = \frac{1}{4}F_{ij}F_{ij} + (D_i\phi)^\dagger(D_i\phi) + V_3(\phi, A_0) + \frac{1}{2}(D_iA_0)^2 + \delta\mathcal{L}, \tag{5.3.5}$$

where the potential is now:

$$V_3(\phi, A_0) = m^2\phi^\dagger\phi + \lambda_3(\phi^\dagger\phi)^2 + h_3\phi^\dagger\phi A_0^2 + \frac{1}{2}m_D^2A_0^2 + \frac{1}{4}\lambda_A A_0^4. \tag{5.3.6}$$

Hence, we see all fermionic fields have been integrated out, and the scalar fields contained here are only those corresponding to the zero infrared modes of the full theory. Likewise, a Lagrangian at the ultrasoft scale has the following form:

$$\mathcal{L} = \frac{1}{4}F_{ij}F_{ij} + (D_i\phi)^\dagger(D_i\phi) + V_3(\phi), \tag{5.3.7}$$

where

$$V_3(\phi) = m_3^2\phi^\dagger\phi + \lambda_3(\phi^\dagger\phi)^2. \tag{5.3.8}$$

Thus, at the ultrasoft scale only the spatial gauge fields and infrared scalar fields remain within the theory. As mentioned, because fermion modes always have temperature dependent masses (recall $m_f^2 = m^2 + [(2n+1)\pi T]^2$), they are always integrated away at the hard scale. Thus, these effective field theories are purely bosonic.

The problem facing the construction of the effective field theory now lies in the evaluation of the 3d parameters, such as m_3 and λ_3. Once we obtain these, the effective theory is fully determined. This is done via matching Green's functions. That is, we first compute n-point 1PI Matsubara Green's functions in both the full and effective theory (using full finite temperature Feynman rules in the former, and 3d Euclidean rules in the latter). Then, we fix the values of the 3d parameters such that these Green's functions agree.

This involves determination of the 2, 3, and 4 point functions (to a given loop order set by accuracy constraints on the Green's functions, e.g. $\Delta G/G \sim O(g^4)$) for a theory involving any number of gauge, scalar, and fermion fields. Naturally, the evaluation of these diagrams in the Euclidean theory incorporates no temperature dependence. Hence, all temperature dependence in the effective theory is contained within the effective 3d parameters themselves and arises from the matching prescription. That is, unlike in the 4d approach in which temperature dependence arises as a perturbative effect, this framework incorporates finite temperature at all orders. The full theory is computed rigorously using finite temperature field theory, then the effective theory is matched to absorb the temperature dependence.

Thus far we have covered a sufficient amount of theory to provide an example calculation of the dimensional reduction procedure. However, as one may imagine, the evaluation and matching of the required Green's functions is a tedious and cumbersome procedure. For this reason, we omit any details on their calculation. It is also this reason that we suspect this framework has been unappreciated in the literature on cosmological phase transitions. Fortunately, advancements have been made in automating this process, such as the dimensional reduction algorithm DRalgo [19] built within Mathematica. This motivates implementation of these potentials into withstanding framework for the study of cosmological phase transitions.

5.4 Finite Temperature Effective Potentials

We can see from (5.3.8) that the potential at the ultrasoft level is remarkably simple. If we enforce $\mathbb{Z}_2$ on our scalar fields (as was done in the above example), then post-symmetry breaking we are left with a theory that involves only quadratic mass terms as well as quartic interactions. Minimisation of this potential then involves solving a system of cubic equations — a problem with an analytical solution. However, in the 4d

theory radiative corrections become important as they generate potential barriers for first-order transitions. One might naturally wonder then if it is possible to derive radiative corrections in the 3d theory.

This is a thorny topic. DRalgo provides expressions for the potential at NLO and NNLO, allowing one to find the 3d effective potential as a perturbative expansion. For example, scalar terms in the NLO potential have the form $V_{\text{NLO}} \supset -\mu_i(\phi)^{3/2}/12\pi$, where the elements μ_i are eigenvalues of the tree-level mass matrix. We can derive this by summing over all one loop Feynman diagrams in the Euclidean effective theory. The process is completely analogous to the derivation in 4.3, such that after summing over all one loop diagrams we obtain:

$$V_{\text{eff, 1}} = \frac{1}{2}\left(\frac{e^{\gamma_E}\Lambda^2}{4\pi}\right)^{\frac{3-d}{2}} \int \frac{d^dp}{(2\pi)^d} \log(p^2+\mu^2). \tag{5.4.1}$$

We have written our renormalisation parameter Λ using the $\overline{\text{MS}}$ scheme. Differentiating with respect to the mass μ^2 we obtain

$$V_{\text{eff, 1}} = \int d\mu^2 \, \frac{1}{2}\left(\frac{e^{\gamma_E}\Lambda^2}{4\pi}\right)^{\frac{3-d}{2}} \int \frac{d^dp}{(2\pi)^d} \frac{1}{p^2+\mu^2}. \tag{5.4.2}$$

This can then be evaluated using an application of (C.3):

$$\begin{aligned} V_{\text{eff, 1}} &= \left(\frac{e^{\gamma_E}\Lambda^2}{4\pi}\right)^{\frac{3-d}{2}} \int d\mu^2 \, \frac{1}{2}\frac{1}{(4\pi)^{d/2}}(\mu^2)^{\frac{d}{2}-1}\Gamma(1-d/2) \\ &= \left(\frac{e^{\gamma_E}\Lambda^2}{4\pi}\right)^{\frac{3-d}{2}} \frac{1}{d}\frac{1}{(4\pi)^{d/2}}(\mu^2)^{\frac{d}{2}}\Gamma(1-d/2) \end{aligned} \tag{5.4.3}$$

We then take the limit as $d \to 3$, such that $\Gamma(1-d/2) = \Gamma(-1/2) = -2\sqrt{\pi}$, giving:

$$V_{\text{eff, 1}} = -\frac{1}{3}\frac{2\sqrt{\pi}}{(4\pi)^{3/2}}(\mu^2)^{3/2} = -\frac{(\mu^2)^{3/2}}{12\pi}, \tag{5.4.4}$$

As required. The reader should note that in the context of the 3d effective potentials, the terms 1-loop and next-to-lowest order (NLO), as well as 2-loop and next-to-next-to-lowest order (NNLO), will be used interchangeably.

At this point we note that the use of the effective potential in the effective theory is dubious. For instance, the effective potential is obtained by treating all interactions as weakly coupled and therefore perturbative. However, in the 3d theory the temperature dependent interaction terms, such as $\lambda_3(T)$, are neither dimensionless nor small at high temperature. Hence, assuming the convergence of any perturbative expansion is problematic. Nevertheless, we regard these terms as still possessing a qualitative description of what the radiative corrections may look like at high temperature. We will explore alternative constructions for perturbative corrections in the next section.

6 Abelian Higgs at Finite Temperature

Having developed the framework surrounding the effective field theory approach, we now use this section to provide its practical use in the context of the Abelian Higgs model. I will first introduce the model as well as a description of both the expected zero temperature symmetry breaking and thermal history. I then proceed to demonstrate the effective field theory description of this model obtained from DRalgo, showing that it successfully reproduces the expected thermal history at leading order. I will conclude on a discussion of the key points and issues that arise in this framework, with a particular focus on those not present in the old 4d approach.

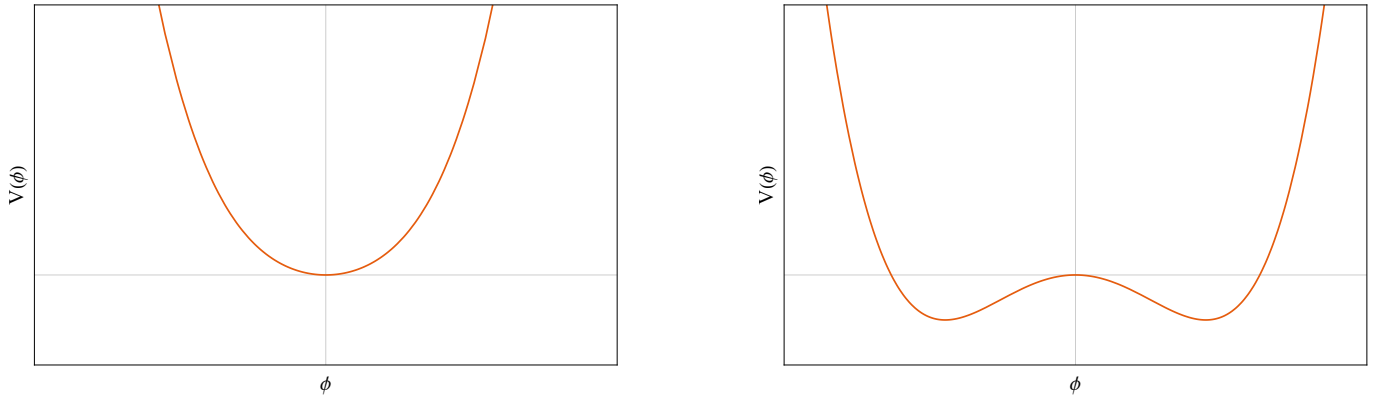

(a) (b)

Figure 6: Qualitative behaviour of the Abelian Higgs potential for $m^2 > 0$ (a.) and $m^2 < 0$ (b.).

6.1 Model

The Abelian Higgs contains a $U(1)$ gauge group with gauge field A_μ, which couples to a complex scalar field ϕ [24, 61]. The Lagrangian is thus:

$$\mathcal{L} = -\frac{1}{4}F_{\mu\nu}F^{\mu\nu} + |D_\mu\phi|^2 - V(\phi), \tag{6.1.1}$$

where $V(\phi)$ is a Higgs-like potential

$$V(\phi) = m^2|\phi|^2 + \lambda(|\phi|^2)^2. \tag{6.1.2}$$

This is the simplest potential that is both gauge invariant and renormalisable. The scalar field has gauge charge g, such that $D_\mu = \partial_\mu - igA_\mu$. This leaves three parameters that fully determine the theory: g, m, and λ. Now, if $m^2 > 0$ is positive then $V(\phi)$ resembles a parabola with a symmetric minima at the origin (see Figure 6a). However, if $m^2 < 0$ then we have a Mexican-hat potential (see Figure 6b) in which the stable vacuum state satisfies:

$$|\phi| = \sqrt{-\frac{m^2}{2\lambda}} = \frac{v}{\sqrt{2}}. \tag{6.1.3}$$

The vacuum state is thus any configuration $\phi_m = ve^{i\theta}/\sqrt{2}$, with the phase θ breaking the $U(1)$ gauge invariance of the model. We then expand about this minima in the polar basis according to:

$$\phi = \frac{1}{\sqrt{2}}e^{i\frac{\chi}{v}}(v + h). \tag{6.1.4}$$

Such that post symmetry-breaking our Lagrangian becomes:

$$\mathcal{L} \supset -\frac{1}{4}F_{\mu\nu}F^{\mu\nu} + \frac{g^2v^2}{2}A_\mu A^\mu + \frac{1}{2}\left(\partial_\mu h\partial^\mu h + 2m^2h^2\right). \tag{6.1.5}$$

We omit any terms involving the Goldstone boson χ, as these can be disregarded by working in the unitary gauge. We thus recognise the physical masses:

$$m_A^2 = g^2v^2 \quad \text{and} \quad m_h^2 = 2m^2. \tag{6.1.6}$$

These definitions, as well as the definition of v, allow us to recast m and g in terms of the physically observable m_h and m_A as follows:

$$m^2 = \frac{m_h^2}{2} \quad \text{and} \quad g^2 = \frac{2\lambda m_A^2}{m_h^2}. \tag{6.1.7}$$

Another popular choice is to parameterise in terms of the zero-temperature Higgs VEV itself, however I have opted for masses. In setting the values of m_h and m_A, we must ensure $m^2 < 0$ to realise a non-zero VEV and $m_A \sim m_h$ such that $\lambda \sim g^2$, otherwise we are free to set them as we please. I chose $m_h = 125.35$ GeV and $m_A = 91.19$ GeV. Then, I set $\lambda = 0.12959$ such that $v = 246.22$ GeV.

Now, at finite temperature symmetry is restored by a thermal Debye mass proportional to T^2: $m^2_{\text{eff}} = -m^2 + \alpha T^2$. That is, we have a symmetric quadratic potential whilst the effective squared mass is positive $m^2_{\text{eff}} > 0$ (Figure 6a). As temperature decreases, we hit a pseudo-critical temperature, T_c, at which point the effective mass vanishes. Below T_c, we cool into the regime where $m^2_{\text{eff}} < 0$, leading to the formation of the broken phase (Figure 6b). At leading order there is no potential barrier separating the true and false vacuum states, such that the transitions proceeds via a smooth crossover. That is, the minima defining the new phase smoothly descends from the symmetric phase $\phi = 0$ before reaching the tree-level vacuum at $T = 0$. There is no sharply defined transition point, so this cannot be considered a genuine phase transition. Alternatively, additional radiative corrections generate a potential barrier between the false and true minimum [51, 62], such that the phase transition is first order and proceeds via bubble nucleation.

An important feature of this framework, which we will see is not shared by the effective field theory approach, is that the zero-temperature limit yields the tree-level potential and VEV. This is a consequence of treating finite temperature effects as an additional correction to the base tree-level potential. In this sense, the labels of 'finite temperature' and 'zero temperature' are truly applicable. In the effective field theory framework, these become less appropriate.

6.2 Dimensional Reduction

We now investigate the Abelian Higgs model at finite temperature. This was achieved by using the potential at the ultrasoft scale obtained from DRalgo, in which the Lagrangian is of the following form:

$$\mathcal{L}_3 = -\frac{1}{4}F_{ij}F^{ij} + |D_i\phi_3|^2 + \frac{m_3^2}{2}\phi_3^2 + \frac{\lambda_3}{4}\phi_3^4. \tag{6.2.1}$$

I will relegate the details of the 3d parameters to Appendix F, however, each constant is shown to have the following form:

$$g_3^2 = \xi T; \quad \lambda_3 = \beta T; \quad m_3^2 = -m^2 + \alpha T^2. \tag{6.2.2}$$

Where ξ, α, and β are functions of the various 4d Lagrangian parameters. It should be noted that the soft scale (prior to integration of the temporal $U(1)$ fields), these parameters scale as $g_3^2 \sim g^2T + g^4T$, $\lambda \sim g^2T + g^4T$, and $m_3 \sim g^2T^2$. At the ultrasoft scale g^2 remains unchanged, whilst λ_3 gains corrections of the order $\sim g^3T + g^5T + g^7T$, and m_3^2 of the order $\sim g^3T^2 + g^5T^2$. The 3d field above is related to the 4d field by:

$$\phi_4^2 = T\phi_3^2. \tag{6.2.3}$$

At first glance, this potential resembles that obtained in the 4d approach via thermal resummation, and indeed, the parameter α is the same in both approaches (to leading order). The difference however is that in this framework, not only does the mass obtain corrections from the hard modes, but so do the other couplings. The powers of temperature that appear in these additional couplings mean that they vanish at $T = 0$, such that this theory does not have a well-defined zero temperature limit.

Setting the constants according to (6.1.7), the potential above is plotted to investigate the behaviour as temperature evolves, done so in Figure 7. This shows the potential at $2T_c$, T_c, and $0.5T_c$, where T_c is the value such that $m_3^2(T_c) = 0$ to leading order: $T_c = 312.18$ GeV. The potential is plotted as a function of $\phi_4/\sqrt{T}$, ranging ϕ_4 from 0 GeV to 400 GeV (the scale set naturally by $v \sim 246.22$ GeV in the 4d framework).

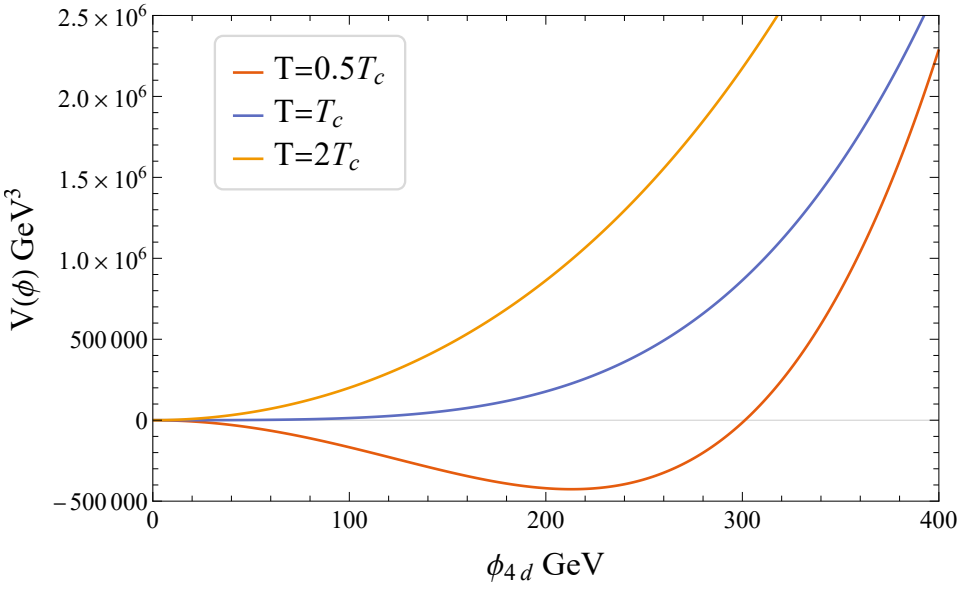

Figure 7: The Abelian Higgs model at finite temperature. The potential has been plotted for the temperatures $T = 0.5T_c$, $T = T_c$, and $T = 2T_c$.

The effective model captures the correct thermal structure of the Abelian Higgs model. There is symmetry restoration above T_c and a smooth cross-over to the broken phase below T_c — precisely what is expected from the 4d resummation approach. However, unlike the 4d approach, there is not well defined minima as $T \to 0$. I.e., the location of the minima and the corresponding value of the potential are given by:

$$\phi_{\text{min}} = \sqrt{-\frac{m_3^2}{\lambda_3}}; \quad V(\phi_{\text{min}}) = -\frac{m_3^4}{4\lambda_3}. \tag{6.2.4}$$

As $m_3^2 \to -m^2$ and $\lambda_3 \to 0$, these diverge to ∞ and $-\infty$ respectively. This non-physical behaviour is indicative of the assumed hierarchy of scales in the EFT. That is, we assume the separation of scales $\pi T > gT > g^2T$, and furthermore that there is a separation between thermal modes and the $n = 0$ mode. Consequently this is an inherently high temperature theory. For low temperatures, such as $T < m/2\pi$, we expect the EFT to begin breaking down — which is observed in these results. For determining thermodynamics this is not problematic, as in the region of a phase transition we have $T \sim m$ and the theory is reliable. However, this theory cannot be used to trace the location of the minima at low temperatures. Given knowing the $T = 0$ location of the minima is significant in the context of vacuum stability [63], a way of integrating this framework with one suitable as $T \sim 0$ is needed.

6.3 Beyond Leading Order Corrections

We can investigate the effect of beyond leading order contributions to the effective potential, which to one-loop have the following form:

$$V_{\text{NLO}} = -\frac{(m_V^2)^{3/2}}{6\pi} - \frac{(m_{S,1}^2)^{3/2}}{12\pi} - \frac{(m_{S,2}^2)^{3/2}}{12\pi}, \tag{6.3.1}$$

where we have the field-dependent mass states:

$$\begin{aligned} m_V^2 &= g_3^2\phi_3^2, \\ m_{S,1}^2 &= m_s^3 + \lambda_3\phi_3^2, \\ m_{S,2}^2 &= m_s^3 + 3\lambda_3\phi_3^2. \end{aligned} \tag{6.3.2}$$

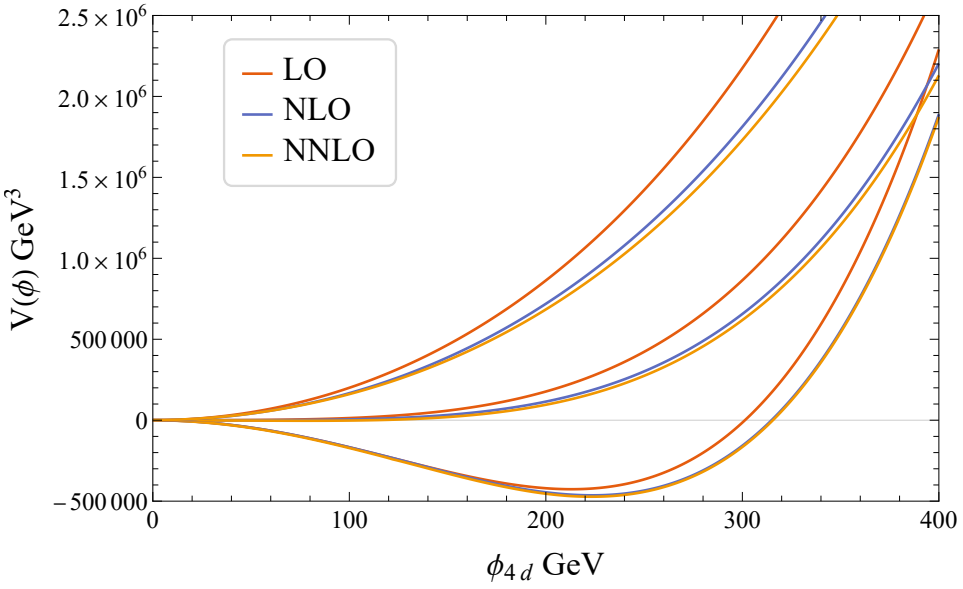

Figure 8: Beyond leading order corrections for the finite temperature Abelian Higgs model. The potential has been plotted for the temperatures (c.f. Figure 7) $T = 0.5T_c$, $T = T_c$, and $T = 2T_c$ for LO, NLO, and NNLO contributions to the effective potential.

The two-loop potential can likewise be expressed as a function of these mass states. For the sake of brevity, I omit the expression. However, note two important features. The first are terms of the order ϕ^{-n} for integers n. The second are terms depending on the 3d renormalisation parameter μ_3, which have the form:

$$H_i(\phi) = \frac{1}{2} + \log\left(\frac{\mu_3}{a_i m_V + b_i m_{S,1} + c_i m_{S,2}}\right). \tag{6.3.3}$$

Here μ_3 is the 2-loop renormalisation scale in the effective theory and a_i, b_i, and c_i are integer coefficients. In the effective approach, there are two renormalisation parameters, μ and μ_3, which must be handled independently. The latter has been set to $\mu \sim T$, whilst I will discuss the former shortly.

6.3.1 NLO and NNLO Corrections

In Figure 8 are plots of the potential with both the 1-loop (NLO) and 2-loop (NNLO) corrections. Note the 2-loop correction has renormalisation group dependence in the form of the parameter μ_3, which has been set to $\mu_3 = \pi T$. Also, the beyond leading order corrections have been normalised to zero by plotting $V_3(\phi_3, T) - V_3(0, T)$[7].

These corrections provide only small contributions to the potential. Above T_c the effect of these contributions is not of qualitative significance provided the potential still has a minimum at $\phi = 0$ and V is well behaved. Below the critical temperature these corrections become significant as as they modify the location of both the minima ϕ_m and $V(\phi_m)$ which are physically observable.

However, the location of the minima is only slightly modified by these corrections. Indeed, I verify this by numerically solving for the location of the minima at $T = 0.5Tc$, with the results provided in Table 1. We see that each order in the perturbation theory adds only a small change to the minima, with the difference between NLO and LO only being roughly 5%, whilst the difference between NNLO and NLO is even lower at roughly 0.004%. These results are sensitive to the location within the (m_h, m_A, λ) parameter

[7]Beyond leading order, $V_3(0, T)$ is non-zero and large for high T. We impose normalisation such that $V_3(0, T) = 0\ \forall T$.

space, however for reasonable choices (masses as the EWSB scale and small coupling $\lambda < 1$) the differences between minima is always at the percent level. Given that both the issues discussed in the next section arise at NNLO, this is a promising indication that studies involving these potentials can be terminated at NLO or even LO (additionally this is exciting as the long expressions for the NNLO potentials are challenging to implement).

Order	ϕ_m (GeV)	$V(\phi_m)$ (GeV^3)
LO	17.0539	-426277
NLO	17.9037	-463928
NNLO	17.9029	-470970

Table 1: Comparison of the minima for various orders of perturbation theory evaluated at $T = 0.5T_c$. Given here are the values for the 3d field, $\phi_{3d} = \phi_{4d}/\sqrt{T}$.

An important observation of these corrections is that they do not provide a potential barrier between the true and false minima. At both 1-loop and 2-loop order the transition proceeds via a smooth crossover, in contrast to the 4d framework wherein these corrections are known to generate a radiative barrier (see Section 6.1). This demonstrates an inconsistency between the two approaches, however I argue the effective field theory approach should be regarded as more consistent, given it preserves the order of the transition in each level of perturbation theory. The order of a PT drastically changes the way it physically manifests, and it is incongruous to suggest it should be altered by perturbative corrections.

Finally, thus far I have employed a naive implementation of the effective potential and renormalisation scale dependence. A full treatment would utilise renormalisation group improvement of the effective potential. This has been shown to improve convergence of radiative corrections [58], however, since I have already demonstrated fast convergence at NLO, slight improvements are not of interest in this study. Furthermore, a full application of RG improvement is beyond the scope of this work.

6.3.2 Divergences at NNLO

Having shown the effectiveness of beyond leading order contributions to the effective potential, I demonstrate now two issues that arise in the 2-loop potential. The first are divergences in the potential, and the second is the additional scale dependence in the form of the 3d parameter μ_3, which is addressed in Section 6.3.3.

The NNLO potential contains terms of the form (6.3.3). The numerator of this log term is a function of the field-dependent mass eigenstates. Particular combinations of these eigenstates can yield functions which vanish for some real ϕ, causing the logarithms to diverge. I demonstrate this manifestly in this model by plotting just the NNLO contribution[8], seen in Figure 9. We see that there is both a discontinuity and sharp divergence in the potential, as predicted.

These divergences are not singularities in the same sense as an infrared or ultraviolet divergence, but they are genuine infinities arising from dividing by zero and thus cannot be renormalised away by conventional techniques. Hence, there is not one well defined prescription for regularising these singularities. One solution I explored is to identify which denominators go to zero, and then match the parameter μ_3 to these combinations. This removes the contribution and hence the singularities. However this is not a good idea on a two-fold front.

The first reason is that matching μ_3 like this means it depends on m_3, which itself is μ_3 dependent (I elaborate on this in the next section). The second reason is it is possible to have multiple divergent terms,

[8]That is, we plot V_{NNLO} opposed to $V_{\text{LO}} + V_{\text{NLO}} + V_{\text{NNLO}}$.

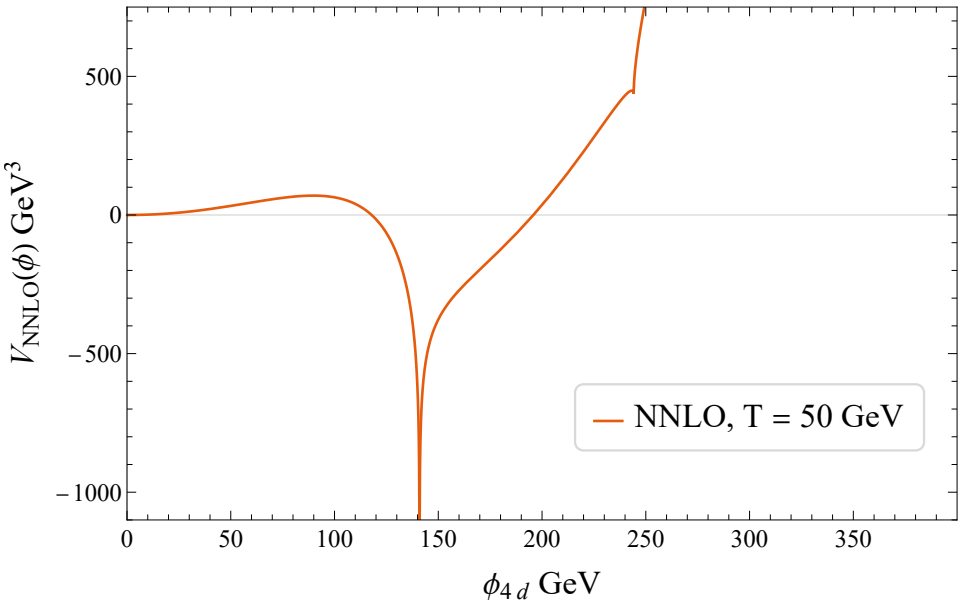

Figure 9: Plot of the 2-loop correction to the potential at $T = 250$ GeV (corresponding to $T \sim 0.16T_c$). This demonstrates the singularity in the potential at this order in perturbation theory.

and naturally we cannot match μ_3 to deal with all of them. These terms must simply be keep in mind when performing studies in this framework, particularly as they may be problematic in numerical calculations.

Another more pressing matter is a singularity at $\phi = 0$ at NNLO. This arises as the potential contains terms proportional to ϕ^{-n}, which have their origin due to terms like:

$$\frac{m_i^2(\phi_3)}{m_j^2(\phi_3)}. \tag{6.3.4}$$

I.e., ratios of our mass eigenstates which arise from scalar-scalar-vector diagrams at 2-loop [58]. Now, recall $m_V^2 \propto \phi_3^2$, whilst $m_{S,i}^2 \propto a + b_i\phi_3^2$. Hence, ratios of two scalar or vector mass eigenstates are finite, but ratios mixing scalar and vector mass eigenstates diverge. If m_S^2 appears in the denominator we have divergences like Figure 9, however when m_V^2 appears in the denominator there is the more problematic $\phi = 0$ divergence.

The potential always has a symmetric minimum located at the origin: $V(0,T) = 0$, becoming a global minimum at high temperatures. The potential being undefined at this location is then extremely problematic and an indication of the theory being unreliable. I have circumvented this by avoiding the point $\phi = 0$ in my study, and instead worked in the limiting case near the origin, taking $\phi = 10^{-4}$. However, this is a deeply troubling issue that should be addressed in further work.

6.3.3 Renormalisation Scale Dependence

Thus far I have mentioned the renormalisation scale μ_3 that manifests directly in the 2-loop potential. This term also manifests in beyond leading order corrections to the scalar mass. So far, I have set $\mu_3 \sim \pi T$ and omitted the beyond leading order mass corrections. I now include these mass corrections, and investigate the effect of changing μ_3. Firstly, I provide a brief discussion on the scale dependence of this framework.

The first renormalisation parameter, μ, is the 4d renormalisation scale. This arises in the matching of the

3d and 4d scales, and thus manifests in all 3d parameters in the form of two constants:

$$L_b = \ln\left(\frac{\mu^2}{T^2}\right) + 2\gamma_E - 2\ln(4\pi), \quad L_f = L_b + 4\ln(2). \tag{6.3.5}$$

Naturally a suitable choice for this parameter is $\mu \sim T$, effectively eradicating the temperature dependence of these constants and ensuring we don't have large logarithms at high temperature. For this reason we set $\mu = T$. However, the prescription offered by the authors of DRalgo is to range μ from $0.5\pi T$ to $2\pi T$, whilst keeping the parameter μ_3 constant [19].

This parameter μ_3 comes from both the matching procedure which introduces logarithms of the form $\log(\mu_3/\mu)$ in NLO corrections to our 3d masses, as well as in the evaluation of two-loop diagrams in the effective potential, introducing manifest dependence in the form of terms like (6.3.3). The fact m_3 depends on μ_3 is itself alarming, since the critical temperature is defined by when the value m_3^2 becomes negative, which is hence directly affected by the choice of μ_3.

Setting $\mu_3 \sim \pi T$ was a simple choice, and I now investigate more suitable values. For now, disregard the fact that running $\mu_3 \sim m_3$ results in an implicit equation for μ_3. Then, one choice mentioned above was to consider setting μ_3 to remove logarithms that diverge in field space. I disregarded this as it cannot deal with cases that have multiple divergences. Another possibility explored in this work was to set μ_3 to minimise the NNLO contributions to the potential. That is, I extract the coefficient of each $H_i(\phi)$, find the largest, and set μ_3 to remove it. E.g., suppose the largest coefficient responds to;

$$H(\phi) = \frac{1}{2} + \log\left(\frac{\mu_3}{2m_v + m_{S,1}}\right). \tag{6.3.6}$$

Then, we can set μ_3 as:

$$\mu_3 = e^{-1/2}(2m_V + m_{S,1}). \tag{6.3.7}$$

This removes the largest contribution and also serves to suppress other similar terms, such as those like $2m_V + m_{S,2}$. However, the issue with such an approach is that minimising the potential itself is not advisable given it isn't directly physically observable. A more suitable candidate would be the derivative, $dV/d\phi$, which directly affects observable states. Indeed $dV/d\phi$ satisfies a RG equation involving the parameter μ_3 which can thus be used to investigate improvements of the potential via setting μ_3 accordingly. Such methods are beyond our scope but will be explored in future work.

Alternatively, I investigated the dependence on the potential with variation of μ_3, as opposed to the alternative of fixing μ_3 and varying μ. In Table 2, I have calculated $\phi_m(0.5T_c)$ for various choices of μ_3. Both the LO and NLO calculations are sensitive to changes in μ_3, a consequence of the susceptibility of m_3 to changes in this scale. That said, the variation is small enough to be treated as a theoretical uncertainty. At NNLO (where the potential obtains additional μ_3 dependence from regularisation of 2-loop integrals) the dependence on μ_3 is reduced. This is unsurprising, as the exact effective potential is invariant to changes to μ_3, so increasing orders of the expansion should be expected to decrease this dependence.

Order	$2\pi T$	$0.5\pi T$	gT	g^2T	g_3^2
LO	16.9976	17.1100	17.2265	17.3061	17.3062
NLO	17.8476	17.9597	18.0757	18.1549	18.1557
NNLO	17.9053	17.9003	17.8939	17.8885	17.8957

Table 2: Evaluation of $\phi_m(0.5T_c)$ for various choices of μ_3.

Given the results of this table, I will set $\mu_3 \sim \pi T$ when determining thermodynamics in the effective field theory approach. The reader may be concerned about the non-physical scale dependence present in

these results, but I offer some words of comfort by saying that whilst this is bad, it could be much worse. Perturbative calculations in cosmological phase transitions are arbitrary. In the 4d approach, arbitrary choices such as renormalisation scheme, resummation scheme, and gauge dependence all effect physical observables, to the extent that a model can exhibit a FOPT in some regimes, and not exhibit one in another [64]. The 3d approach is promising in decreasing this uncertainty [20], but it still remains a problematic aspect of phase transition calculations.

6.3.4 Comparison to the x-Expansion

The use of the effective potential in the 3d theory clearly provides workable results. However, perturbative studies in the effective 3d framework suffer from some self consistency issues. As mentioned in 5.4, the NLO contributions to the 3d effective potential are derived as an expansion in the couplings λ_3 and g_3. Not only are these large at high temperatures, but are not dimensionless like their 4d counterparts[9]. A solution to these issues come in the form of implementing an x-expansion [65, 66, 67, 58].

In this approach, we reorganise the effective potential into a perturbative expansion in the parameter x which is both dimensionless and consequently temperature independent, furthermore, this parameter is small for theories which have radiatively generated barriers [65]. This provides a means of restoring the perturbative expansion at high temperatures, and indeed the effects of issues such as the infrared Linde problem are suppressed in this framework [65]. Formally the effective potential is not written in terms of loops, but instead in terms of powers of $x^{1/2}$:

$$V_{\text{eff},\,x} = V_{\text{LO},\,x} + x\; V_{\text{NLO},\,x} + x^{3/2}\; V_{\text{NNLO},\,x} + \dots \tag{6.3.8}$$

I now construct this expansion for the Abelian Higgs model. Consider the dimensionless potential $V_x = V_3/g_3^6$, given by:

$$V_x = \frac{1}{2}\frac{m_3^2}{g_3^4}\left(\frac{\phi_3}{g_3}\right)^2 + \frac{1}{4}\frac{\lambda_3}{g_3^2}\left(\frac{\phi_3}{g_3}\right)^4 = \frac{y}{2}\varphi^2 + \frac{x}{4}\varphi^4, \tag{6.3.9}$$

where I introduce the dimensionless $y = m_3^2/g_3^4$, $x = \lambda_3/g_3^2$, and $\varphi = \phi_3/g_3$. For my choice of parameters, $x \sim O(1)$. All temperature evolution of this model is contained within the 'mass term' y. Both x or y can be treated as an expansion parameter, but the temperature independence of the former makes it the most suitable candidate. As $x \sim y^{-1}$ in the region of T_c, all terms in this expression are of the same order near a PT.

In the same way, I investigate the effect of radiative corrections to this model. To begin, consider the gauge boson and scalar 1-loop contributions. For the gauge boson term:

$$\begin{aligned}(m_V^2)^{3/2} = \left[g_3^2\phi_3^2\right]^{3/2} &\to \frac{1}{g_3^6}\left[g_3^2\phi_3^2\right]^{3/2} \\ &= \left[\left(\frac{\phi_3}{g_3}\right)^2\right]^{3/2} \\ &= \left[\varphi^2\right]^{3/2} \\ &= \varphi^3,\end{aligned} \tag{6.3.10}$$

Hence, the gauge boson loop arises as a *leading order* effect within the x expansion. I.e., the leading order potential is given by:

$$V_{\text{LO},\,x} = \frac{y}{2}\varphi^2 + \frac{x}{4}\varphi^4 - \frac{1}{6\pi}\varphi^3. \tag{6.3.11}$$

[9] Recall $[\phi_2] = 1/2$, such that we require $[\lambda_3] = 1$, and $[g_3] = 1/2$ to make $[V_3] = 3$. This can also be read off from their temperature dependence as $[T] = 1$.

Recall that this gauge boson term is responsible for radiatively generated potential barriers in the loop expansion. Within this context, such barriers are present at leading order and hence the transition is first order at all orders of perturbation theory. Likewise, for the scalar 1-loop contributions:

$$\begin{aligned}(m_{S,i}^2)^{3/2} = \left[m_s^3 + \alpha_i \lambda_3 \phi_3^2\right]^{3/2} &\to \frac{1}{g_3^6}\left[m_s^3 + \alpha_i \lambda_3 \phi_3^2\right]^{3/2} \\ &= \left[\frac{m_s^2}{g_3^6} + \alpha_i \frac{\lambda_3}{g_3^2}\left(\frac{\phi_3}{g_3}\right)^2\right]^{3/2} \\ &= \left[y + \alpha_i x \phi^2\right]^{3/2} \\ &\sim O(x^{3/2}),\end{aligned} \tag{6.3.12}$$

where $\alpha_i = 1,\ 3$. Thus, these contributions arise as a NNLO perturbative effect. By omitting these terms I can performing a leading order calculation in the x-expansion, with a potential given by (6.3.11). I will calculate the location of ϕ_m and compare to the LO calculation of the conventional loop expansion.

Solving $dV_x/d\varphi = 0$ gives:

$$\varphi_m = 0, \frac{1 \pm \sqrt{1 - 16\pi^2 xy}}{4\pi x}. \tag{6.3.13}$$

The positive root solution corresponds to the location of the minima. Multiplying this by g_3 and showing explicit temperature dependence, we obtain:

$$\phi_m(T) = g_3(T)\left(\frac{1 + \sqrt{1 - 16\pi^2 xy(T)}}{4\pi x}\right). \tag{6.3.14}$$

Evaluating this at $0.5T_c$ yields $\phi_m(0.5T_c) = 17.0494$ GeV. This result is clearly in good agreement with the leading order prediction from the conventional loop expansion. To proceed beyond leading order we seek Feynman diagrams that scale as $O(x)$. Such terms arise from diagrams involving the gauge boson propagator, as the simplest pure scalar diagrams arise beyond NLO at $O(x^{3/2})$. We can determine which terms to include by applying a power-counting in x to the 2-loop effective potential. However, a full computation of beyond leading order effects is beyond the scope of this thesis and is left as an exciting prospect for future work.

Whilst appearing to sit on firmer ground than the conventional loop expansion, an objective for further work is to test whether perturbative calculations converge faster in this framework. Indeed, whilst the ratio x is small for our choice of parameters, the assumption that $\lambda \sim g^2$ in this model obviously restricts how small this parameter can be. For fast convergence we need $\lambda \ll g^2$, which violates the hierarchy of scales in constructing the effective field theory. The conventional loop expansion however has been demonstrated above to converge rapidly, with NLO and beyond yielding only small corrections.

6.4 Final Remarks

To summarise this section I have demonstrated the following:

- The effective field theory framework provides a simple implementation of temperature dependence in quantum field theories.
- Beyond leading order corrections converge at finite temperature and provide small corrections to the potential.
- The NNLO potential features both explicit RG dependence and divergences, suggesting it should not be implemented until these issues are resolved.

- Scalar mass terms introduce scale dependence, however it is small. The NNLO corrections further minimise this dependence.
- For theories with radiatively generated potential barriers, we can reorganise our perturbative expansion to increase the accuracy of analytical solutions.

7 Thermodynamics of the Real Scalar Singlet Extension

The previous section established a landscape for using the effective field theory framework. This section will now apply this framework to the calculation some basic thermodynamic properties using the effective field theory approach, and comparing to equivalent results from the 4d framework. As demonstrated in the previous section, the effect of beyond leading order corrections are non-negligible, but small. Hence, I perform these calculations at leading order. This has the advantage of allowing me to derive these results analytically. I consider extensions of the Standard Model via the inclusion of additional scalar fields that allow for a FOPT, starting first with an additional real scalar field (xSM), but proceeding to discuss further extensions.

7.1 Model

Consider the $\mathbb{Z}_2$ xSM model. That is, the Standard Model with the inclusion of an additional real scalar field S which couples to the Higgs field, on which we impose symmetry under $S \to -S$. We can describe this model by the potential:

$$V_0(H,S) = \mu_h^2 H^\dagger H + \lambda_h (H^\dagger H)^2 + \frac{\lambda_{hs}}{2}(H^\dagger H)S^2 + \frac{\mu_s^2}{2}S^2 + \frac{\lambda_s}{4}S^4. \tag{7.1.1}$$

The parameters μ_h and λ_h are related to the physical Higgs mass, m_h, and VEV, v_h, according to:

$$m_h^2 = 2\mu_h^2 \quad \text{and} \quad v_h^2 = -\frac{\mu_h^2}{\lambda_h}. \tag{7.1.2}$$

The $SU(2)$ and $U(1)$ gauge couplings of H are fixed via the physical masses of the massive W and Z bosons post-symmetry breaking:

$$g_2 = \frac{2m_W}{v_h} \quad \text{and} \quad g_1 = \sqrt{\left(\frac{2m_Z}{v_h}\right)^2 - \left(\frac{2m_W}{v_h}\right)^2} \tag{7.1.3}$$

We also use the physical scalar mass:

$$m_s^2 = \mu_s^2 + \frac{\lambda_{hs} v_h^2}{2}, \tag{7.1.4}$$

opposed to μ_s^2. This leaves three free variables: the scalar mass, m_s, the Higgs-scalar portal coupling, λ_{hs}, and the scalar self coupling, λ_s.

Upon symmetry breaking we expand our fields in the unitary gauge as $H = (0,\ v_h + h)^T/\sqrt{2}$ and $S = v_s + s$[10]. Solving our symmetry breaking conditions $\partial V/\partial\phi_i = 0$ for $\phi_i = h, s$ yields 9 total solutions, with one being origin. If we enforce an EWSB minima in the Higgs direction, 2 of these solutions describe the Higgs minima along the h axis. We then further enforce $\mu_s < 0$ giving 2 degenerate minima along the s direction. The final four solutions then describe the potential barrier that separates these h and s minima, which is generated by the portal coupling λ_{hs}.

The phase structure of this model is then varied. We can have a smooth crossover into either the s and h direction, yielding no observable gravitational waves. In the more interesting case, we initially have a

[10] Alternatively, we may opt for $S = (v_s + s)/\sqrt{2}$, which changes the factors of 1/2 in our Lagrangian.

smooth crossover in one direction before having a FOPT as the vacuum transitions into a global minimum in the other. To ensure we break the $SU(2) \times U(1)$ symmetry, we fix the free parameters of our system such that the crossover occurs first in the s direction, with the FOPT transitioning into the h direction. I discuss the necessary conditions for this in the next section.

7.2 Dimensional Reduction

In the finite temperature effective field theory, the potential takes the following form:

$$V_3 = \frac{m_{h,3}^2}{2} h_3^2 + \frac{m_{s,3}^2}{2} s_3^2 + \frac{\lambda_{hs,3}}{4} h_3^2 s_3^2 + \frac{\lambda_{h,3}}{4} h_3^4 + \frac{\lambda_{s,3}}{4} s_3^4. \tag{7.2.1}$$

These parameters have the following temperature and renormalisation dependence (see Appendix F for details):

$$m_{h,3}^2 = -m_h^2 + \alpha_h(\mu_3) T^2;\ m_{s,3} = -m_s^2 + \alpha_s(\mu_3) T^2;\ \lambda_{hs,3} = \chi T;\ \lambda_{h,3} = \xi_h T;\ \lambda_{s,3} = \xi_s T. \tag{7.2.2}$$

The location of the minima in both the Higgs and scalar directions is then defined by:

$$h_m = \sqrt{-\frac{m_{h,3}^2}{\lambda_{h,3}}} \quad \text{and} \quad s_m = \sqrt{-\frac{m_{s,3}^2}{\lambda_{s_3}}}, \tag{7.2.3}$$

where the corresponding value of the potential at each minimum is:

$$V(h_m) = -\frac{m_{h,3}^4}{4\lambda_{h,3}} \quad \text{and} \quad V(s_m) = -\frac{m_{s,3}^4}{4\lambda_{s,3}}. \tag{7.2.4}$$

From these, the condition for the Higgs minima to be the global minimum is:

$$\frac{m_h^4}{\lambda_h} > \frac{m_s^4}{\lambda_s}. \tag{7.2.5}$$

Likewise, for the scalar direction to break first it requires the temperature value at which $m_{s,3}^2 = 0$ is greater than the value at which $m_{h,3}^2 = 0$, giving the condition:

$$\frac{m_s^2}{\alpha_s} > \frac{m_h^2}{\alpha_h}. \tag{7.2.6}$$

This limits the parameter space for our model. To proceed further, I selected the benchmark point (λ_s, m_s, λ_{hs}) = (0.1, 100 GeV, 0.5), which satisfies the above restraints. I then visualised the behaviour of this model by creating a contour plot of the potential, as seen in Figure 10. This shows the point where the potential is symmetric, the formation of the scalar VEV, the critical point where a transition first becomes possible, and the broken Higgs state. In Figure 11, I have constructed a phase tracing diagram showing the evolution of the minimum as the system cools.

7.3 Phase Transition Dynamics

At leading order, we can use the above finite temperature model to derive analytical solutions for the various thermodynamic properties associated with our phase transition. These include the critical temperature, T_c, the transition order parameter ϕ_c/T_c, and the latent heat released, L. Now, the phase transition does not immediately proceed at $T = T_c$ and hence evaluation of the latent heat at T_c is not entirely representative of the physical scenario. Regardless, it still provides a meaningful measure of the transition strength. Regarding the free parameters of our theory, λ_s, λ_{hs}, and m_s, we must ensure λ_s is small such that the scalar self-interaction is weakly coupled. With this in mind I set $\lambda_s = 0.1$ as this parameter introduces no qualitative changes in our thermodynamics. As for m_s and λ_{hs} I perform the analysis over points in the parameter space where a FOPT is permitted. Finally, these parameters are manifestly dependent on μ_3, which is accounted for by varying across $\mu_3 \in \{0.5\pi T, 2\pi T\}$.

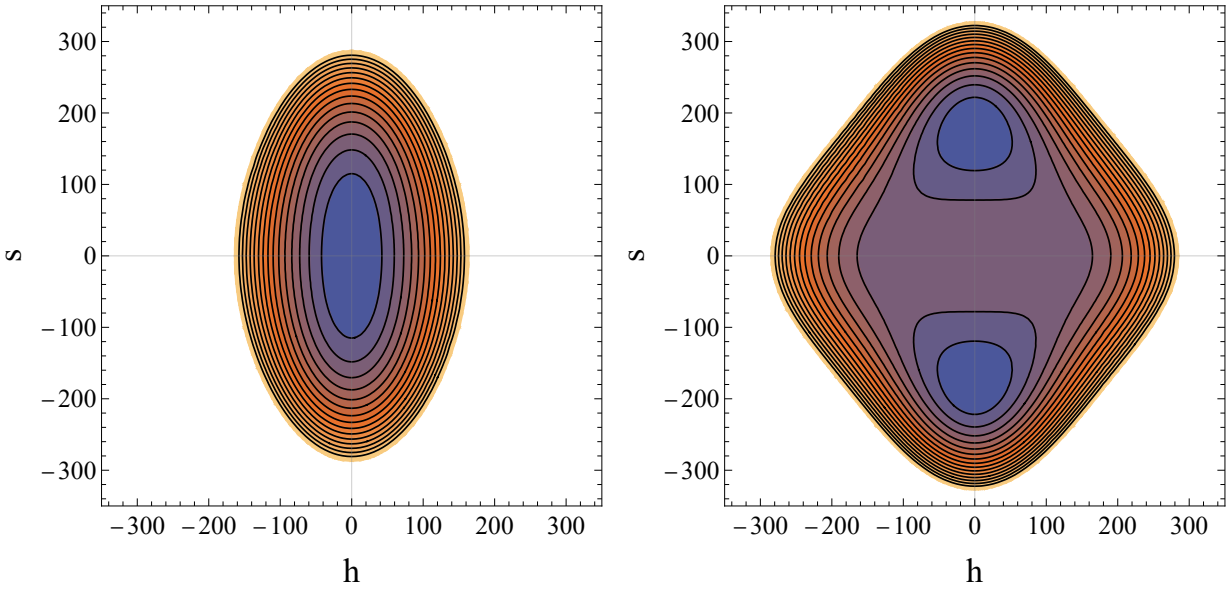

(a) $T = 250$ GeV.

(b) $T = 125$ GeV.

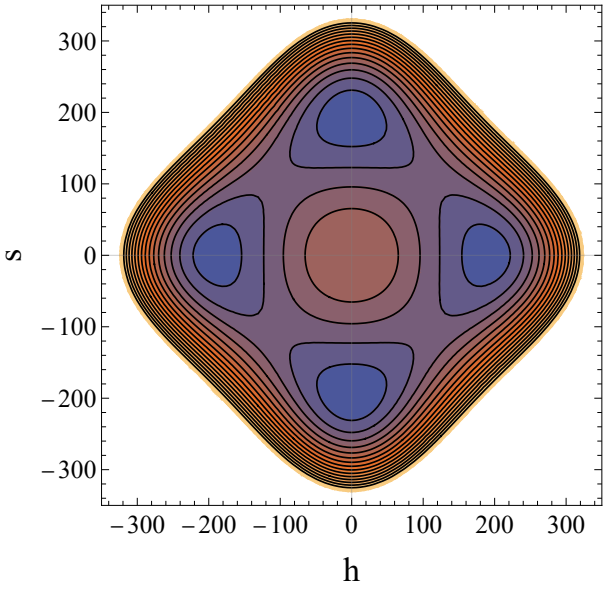

(c) $T = T_c = 95$ GeV.

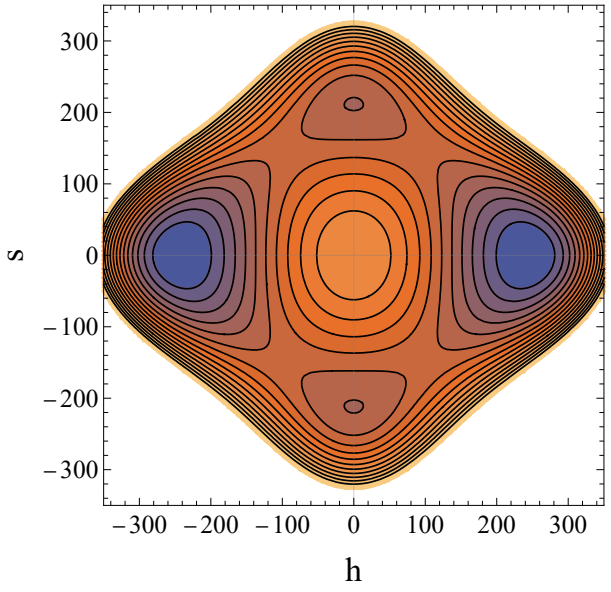

(d) $T = 50$ GeV.

Figure 10: Thermal history of the xSM model showing the symmetric state (a), followed by the formation of the scalar VEV (b), the critical temperature (c), and finally the broken Higgs state (d).

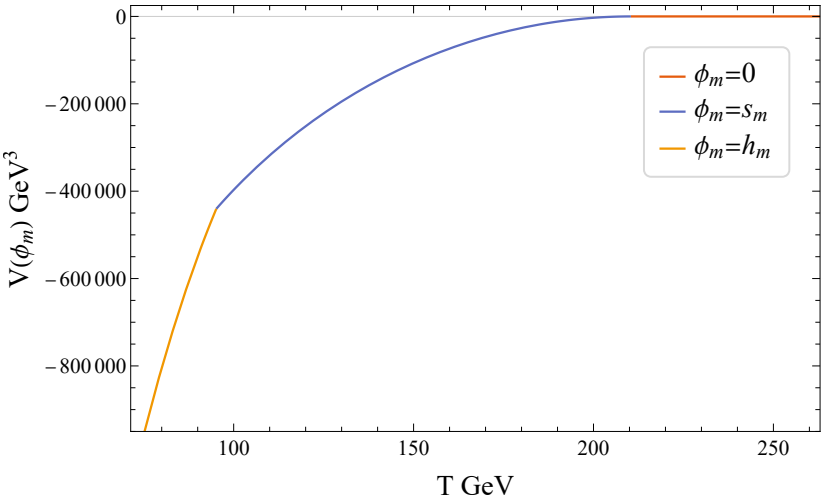

Figure 11: Evolution of the xSM minimum, assuming the EWSB transition occurs at $T = T_c$.

7.3.1 Critical Temperature

Using (7.2.4), the critical temperature occurs at the point $m_{h,3}^4\lambda_{s,3} = m_{s,3}^4\lambda_{h,3}$. This defines the following quadratic equation for T_c^2:

$$(-m_h^2 + \alpha_h T_c^2)^2(\xi_s T_c) = (-m_s^2 + \alpha_s T_c^2)^2(\xi_h T_c). \tag{7.3.1}$$

Which has the following solution:

$$T_c^2 = \frac{m_h^2\alpha_h^2\xi_s - m_s^2\alpha_s^2\xi_h - \sqrt{\xi_s\xi_h(m_s^4\alpha_h^2 - 2m_s^2m_h^2\alpha_s\alpha_h + m_h^4\alpha_h^2)}}{\alpha_h^2\xi_s - \alpha_s^2\xi_h}. \tag{7.3.2}$$

I then use this to find the critical temperature at each point in the parameter space. As α is RG dependent, T_c depends on μ_3 so I determine results for $\mu_3 = 0.5\pi T$ and $\mu_3 = 2\pi T$. In Figure 12 I show the variation of T_c with both μ_3 and the parameters m_s and λ_{hs} independently. We see slight but observable differences in the critical temperature as μ_3 is varied. Whilst small, as the critical temperature is a directly observable physical quantity, any dependence on μ_3 constitutes non-physical behaviour. Given higher loop orders of the potential have been shown to decrease the variation with μ_3, it's likely such dependence is lessened by going to higher orders in the effective potential. In the proceeding results we will set $\mu_3 = \pi T$.

The critical temperature in the xSM model is known in the 4d framework both numerically [50] and analytically [68]. The latter approach closely follows the methods I have adopted here, in that it uses resummation of thermal masses $m(T)^2 = -m^2 + cT^2$ to solve for the critical temperature. Since the T dependence in λ cancels in the above expression these approaches yield the same expression for the critical temperature. They depart however because the thermal mass approach takes the values of λ from the 4d Lagrangian, whilst in this method the 3d λ change from their 4d values in constructing the 3d EFT[11]. To leading order the thermal masses are the same in both methods, although I have opted to include beyond leading order corrections in these calculations.

In Figure 13a I have compared my results for the critical temperature across the parameter space to equivalent results calculated using the approach of [68], given in Figure 13b. The two theories yield nearly identical results across the entire parameter space. This qualitative similarity is expected from the similar approaches

[11] E.g., $\lambda_{hs} = 0.5$ and $\lambda_{hs,3}/T \approx 0.5234$, showing the deviation.

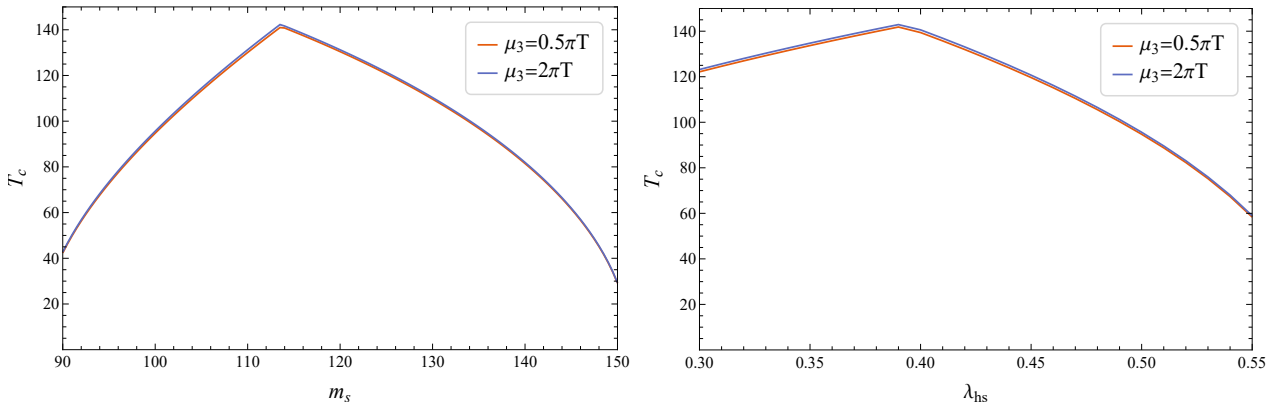

(a) (b)

Figure 12: Left (a): The evolution of the critical temperature with m_s, and Right (b): the evolution with λ_{hs}. Both sets of results have been calculated for two choices of the renormalisation scale: $\mu_3 = 0.5\pi T$ and $\mu_3 = 2\pi T$.

employed. Small quantitative differences exist between the two frameworks, with the 3d approach yielding higher on average critical temperatures across the parameter space. Indeed, the peak critical temperature is 6.31 GeV higher (4.40%), the mean is 4.04 GeV (16.62%), and the median is 4.67 Gev (4.55%).

Given our calculations have gone beyond leading-order in evaluating the thermal parameters m_3, λ_3, etc. I anticipate our results to be more accurate. Further accuracy can be achieved by going beyond leading order in the calculation of the effective potential. Naively this would require a numerical approach, however we could adopt an x-expansion and incorporate only the 1-loop gauge boson contributions allowing analytic solutions to be derived. Unfortunately, it is unclear how to handle multiple gauge couplings g in this approach, so this is left as an avenue for further work.

7.3.2 Order Parameter

A good indication of the strength of a FOPT is the value of ϕ_c/T_c. This quantity is gauge dependent and should not be taken as a rigorous indication of transition strength. Regardless, this specifies the discontinuity in the potential at the critical point, and can thus be considered as an indication of how 'strongly first-order' the transition is [69]. Such a transition satisfies the Sahkarov conditions and is thus a candidate for baryogenesis [14]. A typical value of a strongly first-order transition is $\phi_c/T_c \gtrsim 1$.

In the 3d theory, we note that:

$$\frac{\phi_4}{T} = \frac{\phi_3\sqrt{T}}{T} = \frac{\phi_3}{\sqrt{T}}, \tag{7.3.3}$$

such that we calculate $\phi_c/\sqrt{T_c}$. As both the location of the minima and the critical temperature are known analytically, these results are once again fully analytic. The results of this calculation are given in Figure 14a. We see that this model exhibits a strongly first-order phase transition across much of the parameter space, as expected [68].

7.3.3 Latent Heat

The final variable we calculate is the latent heat. This is defined in terms of the pressure p via $L = T\Delta p'$, where the prime indicates a temperature derivative [70]. This can be recast in terms of the potential

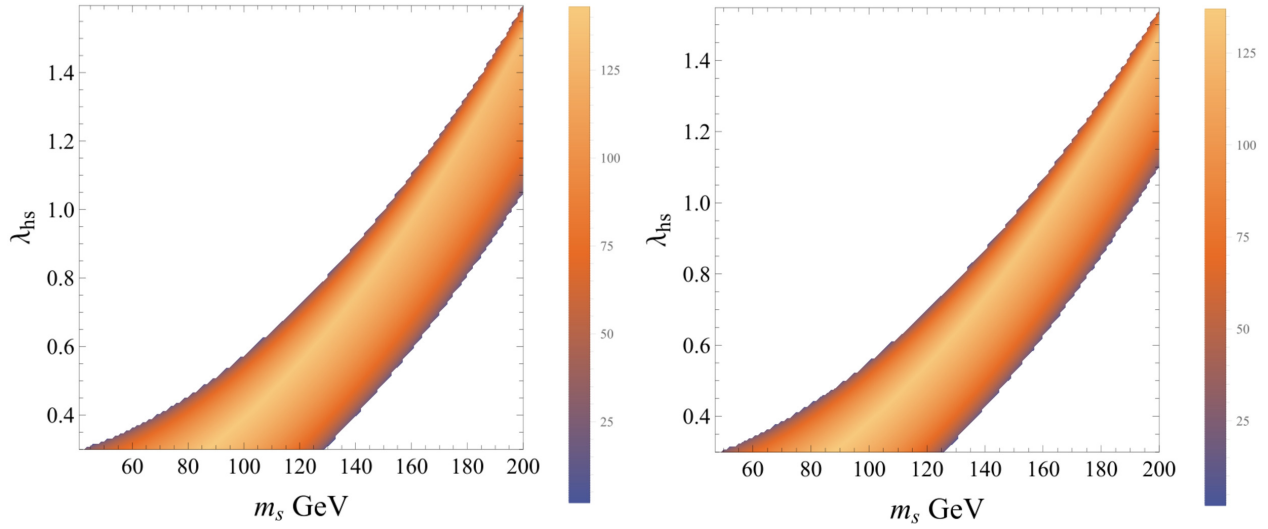

(a) (b)

Figure 13: Left (a): Calculation of the critical temperature for the EWSB phase transition within the scalar singlet extension using the thermal effective field theory approach; calculated across the parameter space that admits a first-order symmetry breaking transition. Right (b): Equivalent calculation performed using resummation of thermal masses (c.f. to Figure 1 of [68]).

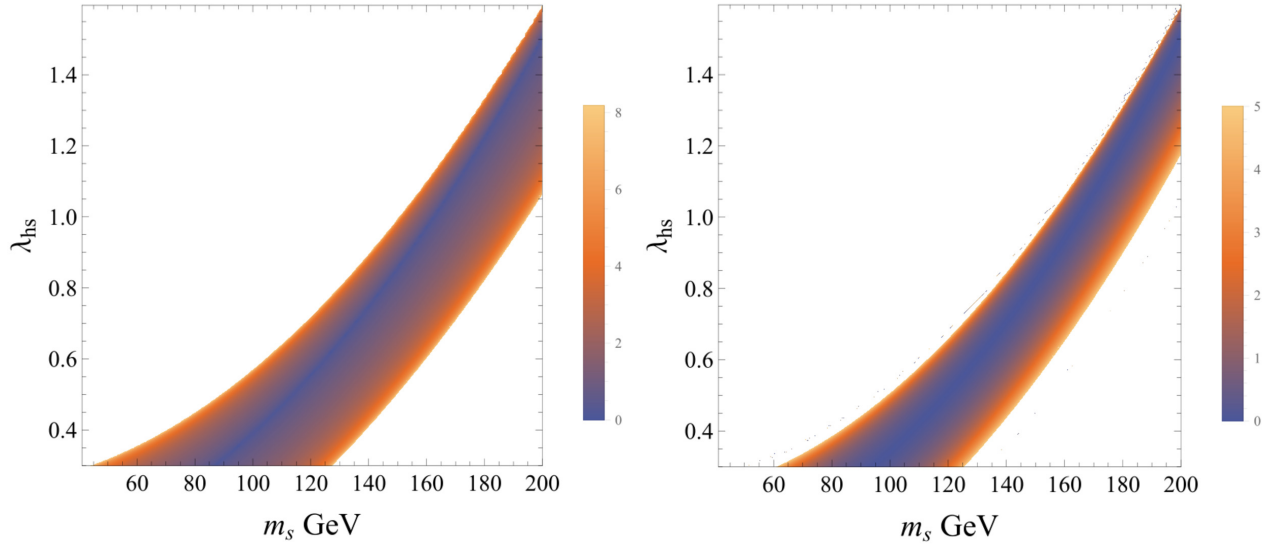

(a) (b)

Figure 14: Calculation of the order parameter (a) and latent heat (b) for the EWSB phase transition within the scalar singlet extension across the parameter space that admits a first-order symmetry breaking transition.

according to:

$$L = T\Delta\frac{dV_4}{dT} = T^2\Delta\frac{dV_3}{dT}. \tag{7.3.4}$$

Since the only temperature dependence of our potential comes from the couplings themselves, the derivative of the potential is evaluated as:

$$L = T^2\Delta\left(\frac{m'_{h,3}(T)^2}{2}h_3^2 + \frac{m'_{s,3}(T)^2}{2}s_3^2 + \frac{\lambda'_{hs,3}(T)}{4}h_3^2s_3^2 + \frac{\lambda'_{h,3}(T)}{4}h_3^4 + \frac{\lambda'_{s,3}(T)}{4}s_3^4\right), \tag{7.3.5}$$

where the primes again indicate temperature derivatives. I thus evaluate this expression for $T = T_c$, taking the fields at $(h_3,\ s_3) = (h_m,\ 0)$ and $(0,\ s_m)$. The thermodynamic significance of deriving the latent heat extends beyond a simple measure of transition strength. The energy released in the cosmological phase transition enters into the plasma of true minima. It thus contributes directly to the gravitational wave amplitude.

In Figure 14b I calculate the latent heat normalised by the critical temperature following the convention in [70]. Alternatively, we could normalise by the energy density of the radiation bath $\rho = g_*(T)\pi^2T^4/30$ [4], where g_* is the relativistic degrees of freedom [22]:

$$g_*(T) = \sum_{\text{bosons}} g_i\left(\frac{T_i}{T}\right)^4 + \frac{7}{8}\sum_{\text{fermions}} g_i\left(\frac{T_i}{T}\right)^4 \tag{7.3.6}$$

These prescriptions only differ by a numerical factor so I have not provided both results.

7.3.4 Prospects for the Bounce Action

I have thus far demonstrated that to leading order in the potential, we can replicate almost exactly the qualitative behaviour of phase transition dynamics, with only slight quantitative differences. This is an immensely exciting result. Most analysis in the field of cosmological phase transitions employs numerical methods, due to the complexity of beyond leading order contributions. Within this framework, the ability to perform meaningful analysis at leading order naturally begs the question of how much further the analysis can be performed analytically.

That is, whilst we can find basic thermodynamics such as the critical temperature or latent heat, much of the more complicated thermodynamics, such as the decay rate of the false vacuum, is locked behind evaluation of the bounce action. This the Lagrangian integrated over the $O(n)$ path in field space that the field takes in the decay to the true vacuum. This path is described by the bounce equations, which are a system of non-linear ODEs given by [71]:

$$\frac{d^2\phi_i}{d\rho^2} + \frac{n}{\rho}\frac{d\phi_i}{d\rho} = \frac{\partial V}{\partial\phi_i}, \tag{7.3.7}$$

where the field profile is $\phi_i(\rho)$. Naturally, any potential that is beyond quadratic in the fields will have non-linear terms arising on the right hand side. Adopting the methodology of [72], the linear equation is analytically solvable via an application of an n-dimensional spherical Hankel transformation: $\psi(s) = T_H\{\phi(\rho)\}$ [73]. This yields an algebraic equation for ψ, which can be used to find ϕ via inverting the transformation. The presence of terms like ϕ^n, $n > 2$ in the potential results in some difficulty for this approach. A quadratic term ϕ^2 in $F(\phi)$ can be handled via the convolution theorem: $T_H\{\phi^2\} = T_H\{\phi\} * T_H\{\phi\} = \int\psi(t)\psi(s-t)dt$, however this results in a non-linear integral equation ψ.

For example, consider the concrete example of $V(\phi) = m^2\phi^2/2 + g\phi^3/3$. Applying the Hankel transformation to the bounce equation gives the following:

$$s^2\psi(s) = m^2\psi(s) + g\int_0^\infty dt\ \psi(t)\psi(s-t), \tag{7.3.8}$$

where:

$$\psi(s) = \frac{2\pi}{s^m} \int_0^\infty d\rho \; \phi(\rho) J_m(2\pi s\rho) \rho^{m+1} \tag{7.3.9}$$

for Bessel functions $J_\nu(z)$ and $m = n/2 - 1$. This has just traded a difficult non-linear differential equation for a difficult non-linear integral equation, with the added challenge of needing to invert 7.3.9 once one obtains $\psi(s)$. There is some hope that this may solveable, for example via a Laplace transformation, but this avenue was not explored further. Despite this hurdle in the bounce action, recent developments in determining the nucleation rate within the effective field framework (side-stepping the bounce formalism) show promise [67, 74], and will be explored in further work.

7.4 Beyond Leading Order

I now also investigate the impact of going beyond leading order in the calculation of the critical temperature. NLO and NNLO potentials obtained from DRalgo are expressed in terms of eigenstates of the mass matrix. Fortunately, DRalgo can provide the NLO and NNLO potentials implicitly in terms of the eigenstates without one needed to find the eigenstates first, akin to how the potential is presented in equation (6.3.1). It the falls upon the user to diagonalise the mass matrix themselves. This problem was addressed in this project, and in Appendix G I provide the analytic diagonalisation of the mass matrices for three systems: xSM [68], cxSM [75], and 2HDM [76] with the intention that these can be implemented in further studies.

For now, I consider the NLO correction to the critical temperature. As expected, this is the point where I concede defeat to analytics and proceed numerically. Here I do not attempt to determine the NLO contributions across the entire parameter space, instead I will briefly investigate their effects at my benchmark point. To study the entire parameter space would require an integration of the DRalgo potentials into a more optimised phase tracing program, such as PhaseTracer, as the numerical efficiency of the native Mathematica is poor[12]

Firstly, I investigate the effects of NLO corrections to the phase structure. In Figure 15a, I have traced both the Higgs and scalar VEVs from $T = 350$ GeV to $T = 50$ GeV. The NLO corrections to the Higgs minima are small changing neither the temperature where the minima forms nor the qualitative behaviour of the potential to any large extent. However, the same cannot be said for the scalar minimum which is shifted drastically by the higher corrections. This asymmetry can be explained by the fact that the gauge boson corrections to the potential do not treat the two fields equally, as only the Higgs field appears in these diagrams, due to a lack of vector-scalar couplings for s.

In Figure 15b, I plot the value of the potential at the minimum for both LO and NLO cases. Here we identify something curious. Despite the scalar VEV forming much earlier in the NLO case, the critical temperature is not changed significantly due to the LO and NLO contributions converging together at lower temperatures. This gives us some hope that the unexpected behaviour in the scalar direction may not significantly alter the thermodynamics of the phase transition. To test this, I can derive the critical temperature numerically at NLO, which evaluates to $T_c = 93.9017$ GeV, compared at $T_c = 93.6367$ GeV at LO[13]. As suspected, this indicates that beyond leading order effects do not significantly alter the critical temperature. I avoid jumping to conclusions across the entire parameter space, however given the nature of this calculation it is reasonable to assume this tendency holds at other points, provided they are perturbative at zero temperature.

[12] That is, the efficiency of my ability to code in Mathematica is poor.

[13] To simplify the numerics in this derivation, we have taken the masses to leading order so as to avoid μ_3 dependence.

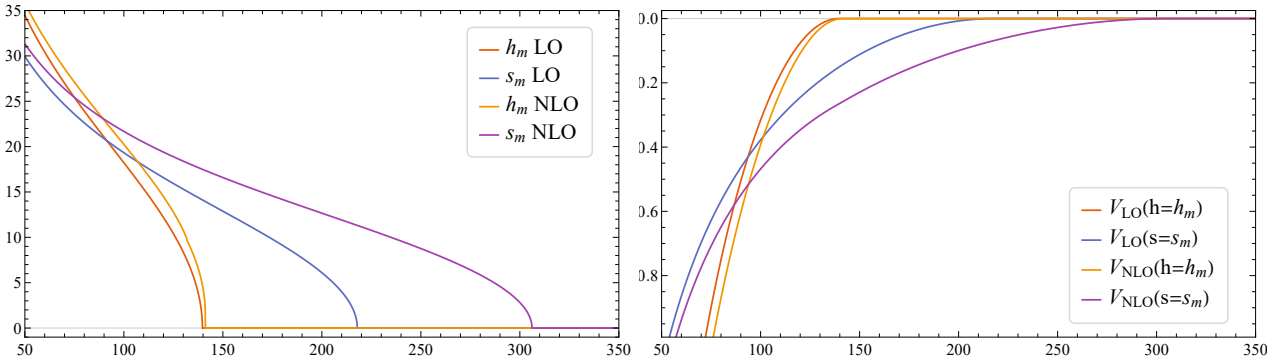

(a) (b)

Figure 15: Left (a): The evolution of LO and NLO phases with temperature. Right (b): The evolution of the minimum with temperature for both LO and NLO.

7.5 Final Remarks

To summarise this section, I have demonstrated the following:

- The leading order potential in the effective field theory framework captures much of the essential detail of more complicated models in the thermal resummation approach.
- The simplicity of leading order potentials allows these thermodynamics to be derived fully analytically, leading to efficient and accurate calculations.
- These thermodynamics are plagued by small but non-negligible renormalisation scale dependence.
- The simplicity of the LO potential suggests some positive prospects for solving the bounce equation.
- Beyond leading order corrections provide only a small contribution to the critical temperature at our benchmark point in the parameter space.

8 Conclusion

This thesis has provided an introduction to the theoretical basis underpinning the use of thermal effective field theories to study cosmological phase transitions. I have introduced the path integral formulation as the foundation of both zero and finite temperature quantum field theory. This framework has then been used to derive both the 4d thermal ressummation approach to finite temperature quantum field theory, as well as the 3d effective field theory approach. I have then demonstrated the applicability of the effective field theory framework using the Abelian Higgs model. Finally, I show the viability of the effective field theory approach for determining thermodynamics of a first-order phase transition within a Standard Model extension.

I have demonstrated that at leading order, the effective field theory approach is capable of replicating the results of the thermal ressummation approach to within an excellent agreement, with my results being derived analytically without the need to utilise numerical techniques. Additionally, my approach has been simple and versatile, lending itself to an application in other models. I have shown that beyond leading order corrections provide small alterations to these quantities, however these calculations introduce further complications such as divergences in the effective potential. I have demonstrated that these calculations are sensitive to the both the prescription for the renormalisation parameter, as well as the scale this parameter is set too. Fortunately, I have demonstrated this sensitivity is small, and diminishes with higher order

corrections to the effective potential. Finally, I have provided the diagonalisation for mass matrices of three Standard Model extensions, which can be used for further work in this field.

A fundamental issue with this framework I have discussed is that this theory is inherently high temperature. Consequently I cannot probe low temperatures using this approach, which has both practical issues for phase tracing and conceptual issues in the context of vacuum stability. A further limitation of this work is that I have focused only on the Abelian Higgs and xSM models. Much of the behaviour inferred from these models is however general enough to be applied to the wider study of thermal effective field theory thermodynamics. As well as this, limited by numerical capacity, I have performed these calculations at leading order in the effective potential. This limits the degree of accuracy I can obtain, and precision calculations should aim to extend beyond this first order approximation.

I conclude this project with several avenues for further work. Firstly, this approach can be easily applied to other extensions of the Standard Model, such as cxSM, 2HDM, or multi-field extensions. Potentials with $\mathbb{Z}_2$ symmetry can be treated easily in this framework at leading order, allow for derivation of basic thermodynamics as I have done here. Another alternative is to improve on these calculations by implementing the beyond leading order potentials into software such as PhaseTracer, which I intend to explore following this work. Finally, the accuracy in the leading order approach for replicating the results of using thermal resummation encourages us to continue using the leading order potential to explore analytic derivations for more complicated thermodynamic quantities, such as the false vacuum decay rate. The ultimate goal of this avenue would be a quasi-analytic calculation of a gravitational wave spectrum beginning at the level of a Lagrangian for a quantum field theory.

References

[1] W. de Boer, "Grand unified theories and supersymmetry in particle physics and cosmology," *Progress in Particle and Nuclear Physics*, vol. 33, p. 201–301, Jan. 1994. arXiv:hep-ph/9402266.

[2] S. Mukhi, "String theory: a perspective over the last 25 years," *Classical and Quantum Gravity*, vol. 28, p. 153001, Aug. 2011. arXiv:1110.2569 [gr-qc, physics:hep-ph, physics:hep-th, physics:physics].

[3] A. Mazumdar and G. White, "Cosmic phase transitions: their applications and experimental signatures," *Reports on Progress in Physics*, vol. 82, p. 076901, July 2019. arXiv:1811.01948 [hep-ph].

[4] C. Caprini, M. Hindmarsh, S. Huber, T. Konstandin, J. Kozaczuk, G. Nardini, J. M. No, A. Petiteau, P. Schwaller, G. Servant, and D. J. Weir, "Science with the space-based interferometer elisa. ii: Gravitational waves from cosmological phase transitions," *Journal of Cosmology and Astroparticle Physics*, vol. 2016, p. 001–001, Apr. 2016. arXiv:1512.06239 [astro-ph, physics:gr-qc, physics:hep-ph].

[5] D. J. Weir, "Gravitational waves from a first-order electroweak phase transition: a brief review," *Philosophical Transactions of the Royal Society A: Mathematical, Physical and Engineering Sciences*, vol. 376, p. 20170126, Mar. 2018.

[6] P. Amaro-Seoana and et al, "Laser interferometer space antenna," 2017.

[7] A. H. Guth, "Inflationary universe: A possible solution to the horizon and flatness problems," *Physical Review D*, vol. 23, p. 347–356, Jan. 1981.

[8] A. D. Linde, "A new inflationary universe scenario: A possible solution of the horizon, flatness, homogeneity, isotropy, and primordial monopole problems," *PHYSICS LETTERS*, vol. 108, no. 6, 1982.

[9] N. Turok, *Phase Transitions as the Origin of Large Scale Structure in the Universe*, p. 267–309. Berlin, Heidelberg: Springer Berlin Heidelberg, 1989.

[10] T. Vachaspati, "Lectures on cosmic topological defects," Feb. 2001. arXiv:hep-ph/0101270.

[11] R. L. Davis, "Texture: A cosmological topological defect," *Physical Review D*, vol. 35, p. 3705–3708, June 1987.

[12] A. Gangui, "Topological defects in cosmology," Oct. 2001. arXiv:astro-ph/0110285.

[13] R. H. Brandenberger, "Topological Defects and Structure Formation," *International Journal of Modern Physics A*, vol. 09, pp. 2117–2189, may 1994.

[14] A. D. Sakharov, "Violation of cp invariance, c asymmetry, and baryon asymmetry of the universe," 1991.

[15] G. A. White, *A pedagogical introduction to electroweak baryogenesis*. IOP concise physics, San Rafael, CA: Morgan & Claypool Publishers, version: 20161101 ed., 2016.

[16] P. Athron, C. Balázs, A. Fowlie, L. Morris, and L. Wu, "Cosmological phase transitions: from perturbative particle physics to gravitational waves," May 2023. arXiv:2305.02357 [astro-ph, physics:hep-ph].

[17] P. Ginsparg, "First and second order phase transitions in gauge theories at finite temperature," *Nuclear Physics B*, vol. 170, p. 388–408, Dec. 1980.

[18] T. Appelquist and R. D. Pisarski, "High-temperature yang-mills theories and three-dimensional quantum chromodynamics," *Physical Review D*, vol. 23, p. 2305–2317, May 1981.

[19] A. Ekstedt, P. Schicho, and T. V. I. Tenkanen, "Athrongo: a package for effective field theory approach for thermal phase transitions," *Computer Physics Communications*, vol. 288, p. 108725, July 2023. arXiv:2205.08815 [hep-ph].

[20] D. Croon, O. Gould, P. Schicho, T. V. I. Tenkanen, and G. White, "Theoretical uncertainties for cosmological first-order phase transitions," *Journal of High Energy Physics*, vol. 2021, p. 55, Apr. 2021.

[21] A. Linde, "Infrared problem in the thermodynamics of the yang-mills gas," *Physics Letters B*, vol. 96, p. 289–292, Nov. 1980.

[22] P. Peter and J.-P. Uzan, *Primordial Cosmology*. Oxford University Press, 2009.

[23] E. J. Copeland and T. W. B. Kibble, "Cosmic strings and superstrings," *Proceedings of the Royal Society A: Mathematical, Physical and Engineering Sciences*, vol. 466, pp. 623–657, jan 2010.

[24] S. Dawson, "Introduction to electroweak symmetry breaking," 1999.

[25] M. S. Turner, E. J. Weinberg, and L. M. Widrow, "Bubble nucleation in first-order inflation and other cosmological phase transitions," *Physical Review D*, vol. 46, p. 2384–2403, Sept. 1992.

[26] A. Mégevand and S. Ramírez, "Bubble nucleation and growth in very strong cosmological phase transitions," *Nuclear Physics B*, vol. 919, p. 74–109, June 2017.

[27] V. K. Shante and S. Kirkpatrick, "An introduction to percolation theory," *Advances in Physics*, vol. 20, p. 325–357, May 1971.

[28] S. Coleman, "Fate of the false vacuum: Semiclassical theory," *Physical Review D*, vol. 15, p. 2929–2936, May 1977.

[29] C. G. Callan and S. Coleman, "Fate of the false vacuum. ii. first quantum corrections," *Physical Review D*, vol. 16, p. 1762–1768, Sept. 1977.

[30] A. Linde, "Fate of the false vacuum at finite temperature: Theory and applications," *Physics Letters B*, vol. 100, p. 37–40, Mar. 1981.

[31] A. D. Linde, "Decay of the False Vacuum at Finite Temperature," *Nucl. Phys. B*, vol. 216, p. 421, 1983. [Erratum: Nucl.Phys.B 223, 544 (1983)].

[32] C. Caprini, R. Durrer, and G. Servant, "Gravitational wave generation from bubble collisions in first-order phase transitions: an analytic approach," *Physical Review D*, vol. 77, p. 124015, June 2008. arXiv:0711.2593 [astro-ph, physics:gr-qc, physics:hep-ph].

[33] S. J. Huber and T. Konstandin, "Gravitational wave production by collisions: More bubbles," *Journal of Cosmology and Astroparticle Physics*, vol. 2008, p. 022, Sept. 2008. arXiv:0806.1828 [astro-ph, physics:hep-ph].

[34] M. Hindmarsh, S. J. Huber, K. Rummukainen, and D. J. Weir, "Numerical simulations of acoustically generated gravitational waves at a first order phase transition," *Physical Review D*, vol. 92, p. 123009, Dec. 2015. arXiv:1504.03291 [astro-ph, physics:hep-ph].

[35] C. Caprini, R. Durrer, and G. Servant, "The stochastic gravitational wave background from turbulence and magnetic fields generated by a first-order phase transition," *Journal of Cosmology and Astroparticle Physics*, vol. 2009, p. 024–024, Dec. 2009. arXiv:0909.0622 [astro-ph, physics:gr-qc, physics:hep-ph].

[36] M. Schwartz, *Quantum Field Theory and the Standard Model*. Cambridge University Press, 1 ed., 2014.

[37] M. Laine and A. Vuorinen, *Basics of Thermal Field Theory*, vol. 925 of *Lecture Notes in Physics*. Springer, 1 ed., 2016.

[38] T. Matsubara, "A new approach to quantum-statistical mechanics," *Progress of Theoretical Physics*, vol. 14, p. 351–378, Oct. 1955.

[39] M. Peskin and D. Schroeder, *An Introduction to Quantum Field Theory*. The Advanced Book Program, CRC Press, 1 ed., 1995.

[40] M. Quiros, "Finite temperature field theory and phase transitions," Jan. 1999. arXiv:hep-ph/9901312.

[41] R. Jackiw, "Functional evaluation of the effective potential," *Physical Review D*, vol. 9, p. 1686–1701, Mar. 1974.

[42] G. 'T Hooft, "Dimensional regularization and the renormalization group," *Nuclear Physics B*, vol. 61, p. 455–468, Sept. 1973.

[43] S. Weinberg, "New approach to the renormalization group," *Physical Review D*, vol. 8, p. 3497–3509, Nov. 1973.

[44] N. Nielsen, "On the gauge dependence of spontaneous symmetry breaking in gauge theories," *Nuclear Physics B*, vol. 101, p. 173–188, Dec. 1975.

[45] I. J. R. Aitchison and C. M. Fraser, "Gauge invariance and the effective potential," *Annals of Physics*, vol. 156, no. 1, 1984.

[46] H. H. Patel and M. J. Ramsey-Musolf, "Baryon washout, electroweak phase transition, and perturbation theory," *Journal of High Energy Physics*, vol. 2011, p. 29, July 2011.

[47] L. Dolan and R. Jackiw, "Symmetry behavior at finite temperature," *Physical Review D*, vol. 9, p. 3320–3341, June 1974.

[48] J. M. Cline and P.-A. Lemieux, "Electroweak phase transition in two higgs doublet models," *Physical Review D*, vol. 55, p. 3873–3881, Mar. 1997. arXiv:hep-ph/9609240.

[49] C. L. Wainwright, "Cosmotransitions: Computing cosmological phase transition temperatures and bubble profiles with multiple fields," *Computer Physics Communications*, vol. 183, p. 2006–2013, Sept. 2012. arXiv:1109.4189 [astro-ph, physics:hep-ph].

[50] P. Athron, C. Balázs, A. Fowlie, and Y. Zhang, "Phasetracer: tracing cosmological phases and calculating transition properties," *The European Physical Journal C*, vol. 80, p. 567, June 2020.

[51] D. Kirzhnits and A. Linde, "Symmetry behavior in gauge theories," *Annals of Physics*, vol. 101, p. 195–238, Sept. 1976.

[52] S. Weinberg, "Gauge and global symmetries at high temperature," *Physical Review D*, vol. 9, p. 3357–3378, June 1974.

[53] P. Fendley, "The effective potential and the coupling constant at high temperature," *Physics Letters B*, vol. 196, p. 175–180, Oct. 1987.

[54] J. Espinosa, M. Quirós, and F. Zwirner, "On the phase transition in the scalar theory," *Physics Letters B*, vol. 291, p. 115–124, Sept. 1992.

[55] R. R. Parwani, "Resummation in a hot scalar field theory," *Physical Review D*, vol. 45, p. 4695–4705, June 1992.

[56] P. Arnold and O. Espinosa, "The effective potential and first-order phase transitions: Beyond leading order," *Physical Review D*, vol. 50, p. 6662–6662, Nov. 1994. arXiv:hep-ph/9212235.

[57] J. Kapusta and C. Gale, *Finite Temperature Field Theory Principles and Applications*. Cambridge Monographs on Mathematical Physics, Cambridge University Press, 2 ed., 2006.

[58] K. Farakos, K. Kajantie, K. Rummukainen, and M. Shaposhnikov, "3d physics and the electroweak phase transition: Perturbation theory," *Nuclear Physics B*, vol. 425, p. 67–109, Aug. 1994. arXiv:hep-ph/9404201.

[59] K. Kajantie, M. Laine, K. Rummukainen, and M. Shaposhnikov, "Generic rules for high temperature dimensional reduction and their application to the standard model," *Nuclear Physics B*, vol. 458, p. 90–136, Jan. 1996. arXiv:hep-ph/9508379.

[60] E. Braaten and A. Nieto, "Effective field theory approach to high-temperature thermodynamics," *Physical Review D*, vol. 51, p. 6990–7006, June 1995. arXiv:hep-ph/9501375.

[61] S. Dawson, "Tasi 2016 lectures: Electroweak symmetry breaking and effective field theory," Jan. 2018. arXiv:1712.07232 [hep-ph].

[62] A. Hebecker, "Finite temperature effective potential for the abelian higgs model to the order e^4, λ^2," *Zeitschrift for Physik C Particles and Fields*, vol. 60, p. 271–276, June 1993. arXiv:hep-ph/9307268.

[63] C. Balázs, Y. Xiao, J. M. Yang, and Y. Zhang, "New vacuum stability limit from cosmological history," Jan. 2023. arXiv:2301.09283 [astro-ph, physics:hep-ph].

[64] P. Athron, C. Balazs, A. Fowlie, L. Morris, G. White, and Y. Zhang, "How arbitrary are perturbative calculations of the electroweak phase transition?," *Journal of High Energy Physics*, vol. 2023, p. 50, Jan. 2023.

[65] A. Ekstedt, O. Gould, and J. Löfgren, "Radiative first-order phase transitions to next-to-next-to-leading order," *Physical Review D*, vol. 106, p. 036012, Aug. 2022.

[66] O. Gould and T. V. I. Tenkanen, "Perturbative effective field theory expansions for cosmological phase transitions," Sept. 2023. arXiv:2309.01672 [astro-ph, physics:hep-ph, physics:hep-th].

[67] J. Hirvonen, J. Löfgren, M. J. Ramsey-Musolf, P. Schicho, and T. V. I. Tenkanen, "Computing the gauge-invariant bubble nucleation rate in finite temperature effective field theory," *Journal of High Energy Physics*, vol. 2022, p. 135, July 2022.

[68] V. Vaskonen, "Electroweak baryogenesis and gravitational waves from a real scalar singlet," *Physical Review D*, vol. 95, p. 123515, June 2017. arXiv:1611.02073 [astro-ph, physics:hep-ph].

[69] A. Ahriche, "What is the criterion for a strong first order electroweak phase transition in singlet models?," *Physical Review D*, vol. 75, p. 083522, Apr. 2007. arXiv:hep-ph/0701192.

[70] P. Schicho, T. V. I. Tenkanen, and G. White, "Combining thermal resummation and gauge invariance for electroweak phase transition," *Journal of High Energy Physics*, vol. 2022, p. 47, Nov. 2022. arXiv:2203.04284 [hep-ph].

[71] P. Athron, C. Balázs, M. Bardsley, A. Fowlie, D. Harries, and G. White, "Bubbleprofiler: Finding the field profile and action for cosmological phase transitions," *Computer Physics Communications*, vol. 244, p. 448–468, Nov. 2019.

[72] R. V. Churchill, "Integral transforms and boundary value problems," *The American Mathematical Monthly*, vol. 59, no. 3, p. 149–155, 1952.

[73] C. J. Sheppard, S. S. Kou, and J. Lin, *The Hankel Transform in n-dimensions and Its Applications in Optical Propagation and Imaging*, vol. 188, p. 135–184. Elsevier, 2015.

[74] O. Gould and J. Hirvonen, "Effective field theory approach to thermal bubble nucleation," *Physical Review D*, vol. 104, p. 096015, Nov. 2021.

[75] V. Barger, P. Langacker, M. McCaskey, M. Ramsey-Musolf, and G. Shaughnessy, "Complex singlet extension of the standard model," *Physical Review D*, vol. 79, p. 015018, Jan. 2009. arXiv:0811.0393 [hep-ex, physics:hep-ph].

[76] G. C. Branco, P. M. Ferreira, L. Lavoura, M. N. Rebelo, M. Sher, and J. P. Silva, "Theory and phenomenology of two-higgs-doublet models," *Physics Reports*, vol. 516, p. 1–102, July 2012. arXiv:1106.0034 [hep-ph].

[77] D. S. Bernstein, *Scalar, Vector, and Matrix Mathematics*. Princeton University Press, Feb. 2018.

Appendix

A Loop Expansion of the Effective Potential

Here we derive the loop expansion of the effective potential, which is taken from [40]. Consider the following expansion of the effective action for a general (not necessarily translation invariant) theory:

$$\Gamma[\phi_{\text{cl}}] = \sum_{n=0}^{\infty} \frac{1}{n!} \int dx_1 \dots dx_n \; G_n^{\text{1PI}}(x_1, \dots, x_n) \phi_{\text{cl}}(x_1) \dots \phi_{\text{cl}}(x_n) \tag{A.1}$$

We take the Fourier transform of each Green's function as:

$$G_n^{\text{1PI}}(x_1, \dots, x_n) = \int \prod_{i=1}^{n} \left(\frac{d^4 p_i}{(2\pi)^4} e^{i p_i x_i} \right) (2\pi)^4 \delta^4(\Sigma p_i) \tilde{G}_n^{\text{1PI}}(p_1, p_2, \dots, p_n). \tag{A.2}$$

Inserting this into the effective action yields:

$$\begin{aligned}
\Gamma[\phi_{\text{cl}}] &= \sum_{n=0}^{\infty} \frac{1}{n!} \int \prod_{i=1}^{n} \left(d^4 x_i \frac{d^4 p_i}{(2\pi)^4} e^{i p_i x_i} \right) (2\pi)^4 \delta^4(\Sigma p_i) \phi_c(x_1) \phi_c(x_2) \dots \phi_c(x_n) \tilde{G}_n^{\text{1PI}}(p_1, p_2, \dots, p_n) \\
&= \sum_{n=0}^{\infty} \frac{1}{n!} \int \prod_{i=1}^{n} \left(d^4 x_i \frac{d^4 p_i}{(2\pi)^4} \phi_c(x_i) e^{i p_i x_i} \right) (2\pi)^4 \delta^4(\Sigma p_i) \tilde{G}_n^{\text{1PI}}(p_1, p_2, \dots, p_n) \\
&= \sum_{n=0}^{\infty} \frac{1}{n!} \int \prod_{i=1}^{n} \left(\frac{d^4 p_i}{(2\pi)^4} \tilde{\phi}_c(-p_i) \right) (2\pi)^4 \delta^4(\Sigma p_i) \tilde{G}_n^{\text{1PI}}(p_1, p_2, \dots, p_n).
\end{aligned} \tag{A.3}$$

Where we have used the definition of the Fourier transform of our field:

$$\tilde{\phi}_c(-p_i) = \int d^4 x_i \phi_c(x_i) e^{i p_i x_i} = \phi_c \int d^4 x_i e^{i p_i x_i} = \phi_c (2\pi)^4 \delta^4(p_i). \tag{A.4}$$

In the second equality we have assumed a spacetime invariant theory $\phi_c(x_i) \equiv \phi_c$. Inserting this into our expansion, we obtain:

$$\begin{aligned}
\Gamma[\phi_{\text{cl}}] &= \sum_{n=0}^{\infty} \frac{\phi_c^n}{n!} \int \prod_{i=1}^{n} \left(d^4 p_i \; \delta^4(p_i) \right) (2\pi)^4 \delta^4(\Sigma p_i) \tilde{G}_n^{\text{1PI}}(p_1, p_2, \dots, p_n) \\
&= \sum_{n=0}^{\infty} \frac{\phi_c^n}{n!} \left((2\pi)^4 \delta^4(0) \right) \tilde{G}_n^{\text{1PI}}(p_1, p_2, \dots, p_n) \\
&= \sum_{n=0}^{\infty} \frac{\phi_c^n}{n!} \tilde{G}_n^{\text{1PI}}(p_i = 0) \int d^4 x,
\end{aligned} \tag{A.5}$$

where we have exchanged $\delta^4(0)$ for an overall spacetime volume via a Fourier transformation. Then, we compare to the definition of the effective potential (4.2.3) to arrive at the formal loop expansion:

$$V_{\text{eff}} = -\sum_{n=0}^{\infty} \frac{\phi_c^n}{n!} \tilde{G}_n^{\text{1PI}}(p_i = 0). \tag{A.6}$$

B Feynman Rules for Phi Fourth Theory

Here we provide the Feynman rules for ϕ^4 theory at both zero temperature and finite temperature.

B.1 Zero Temperature

At zero temperature, a vertex with j external legs is associated with a factor of $-i\lambda/j!$ (the $1/j!$ factor accounts for symmetry under permutation of the j external legs), whilst external lines contribute the factor ϕ^2. For each internal line we have the propagator:

$$\frac{i}{p^2 - m^2 + i\epsilon}, \tag{B.1.1}$$

whilst each loop is associated with the integral:

$$\frac{d^4p}{(2\pi)^4}. \tag{B.1.2}$$

Hence, the amplitude for an n-point one loop diagram (without symmetry factors) is:

$$\mathcal{A} = \int \frac{d^4p}{(2\pi)^4} \left(\frac{i}{p^2 - m^2 + i\epsilon}\right)^n \left(-\frac{i\lambda}{2}\right)^n \phi^{2n}, \tag{B.1.3}$$

where $j = 2$.

B.2 Finite Temperature

At finite temperature, within the imaginary time formalism we replace our temporal momentum with Matsubara frequencies: $p^0 = i\omega_n$, and hence integration over this momentum is replaced by a discrete sum over n. Thus, whilst our vertex factors and external line factors remain the same, the propagator is now:

$$\frac{i}{p^2 - m^2} = -\frac{i}{\omega_n^2 + \omega^2}, \tag{B.2.1}$$

for $\omega_n = 2n\pi\beta^{-1}$ and $\omega^2 = \mathbf{p}^2 + m^2$. Furthermore, loop integrals are replaced with:

$$\frac{i}{\beta} \sum_{n=-\infty}^{\infty} \int \frac{d^3\mathbf{p}}{(2\pi)^3}. \tag{B.2.2}$$

Hence, the amplitude for an n-point one loop diagram (without symmetry factors) is:

$$\mathcal{A} = \frac{i}{\beta} \sum_{k=-\infty}^{\infty} \int \frac{d^3\mathbf{p}}{(2\pi)^3} \left(\frac{-i}{\omega_k^2 + \omega^2}\right)^n \left(-\frac{i\lambda}{2}\right)^n \phi^{2n}, \tag{B.2.3}$$

where again $j = 2$.

C Dimensional Regularisation of 1-Loop Scalar Corrections

Here we regularise the ultraviolet divergent integral (4.3.6). First, we introduce the regularisation constant μ with positive mass dimension of one and scale our integral to d dimensions:

$$V_1(\phi) = (\mu^2)^{2-d/2} \frac{1}{2} \int \frac{d^dp}{(2\pi)^d} \log\left(p^2 + m^2(\phi)\right). \tag{C.1}$$

Then, we differentiate with respect to m^2 to obtain the regularisable integral:

$$V_1(\phi) = \int dm^2 \left\{ \frac{(\mu^2)^{2-d/2}}{2} \int \frac{d^dp}{(2\pi)^d} \frac{1}{p^2+m^2} \right\}. \tag{C.2}$$

The momentum integral is then performed using the following formula [39]:

$$\int \frac{d^dp}{(2\pi)^d} \frac{1}{(p^2+\Delta)^n} = \frac{1}{(4\pi)^{d/2}} \frac{\Gamma(n-d/2)}{\Gamma(n)} \left(\frac{1}{\Delta}\right)^{n-d/2}. \tag{C.3}$$

Applying this to our result, we obtain:

$$\begin{aligned} V_1(\phi) &= \int dm^2 \left\{ \frac{(\mu^2)^{2-d/2}}{2} \left(\frac{1}{m^2}\right)^{1-d/2} \frac{1}{(4\pi)^{d/2}} \frac{\Gamma(1-d/2)}{\Gamma(1)} \right\} \\ &= \frac{(\mu^2)^{2-d/2}}{2} \left(\frac{1}{m^2}\right)^{-d/2} \frac{1}{(4\pi)^{d/2}} \Gamma(2-d/2) \frac{1}{\frac{d}{2}(1-\frac{d}{2})} \\ &= -\frac{m^4}{2} \frac{1}{\frac{d}{2}(\frac{d}{2}-1)} \frac{1}{(4\pi)^{d/2}} \left(\frac{\mu^2}{m^2}\right)^{2-d/2} \Gamma(2-d/2). \end{aligned} \tag{C.4}$$

In taking the limit $d \to 4$, we have the expansion:

$$\frac{1}{(4\pi)^{d/2}} \left(\frac{1}{\Delta}\right)^{2-d/2} \Gamma\left(2-\frac{d}{2}\right) \to \frac{1}{(4\pi)^2} \left(\frac{2}{4-d} - \log(\Delta) - \gamma_E + \log(4\pi)\right), \tag{C.5}$$

where γ_E is the Euler-Mascheroni constant, and the divergent term can be subtracted via the addition of counter terms to our Lagrangian. We apply this to our potential to obtain:

$$V_1(\phi) = \frac{m^4}{64\pi^2} \left(\log\left(\frac{m^2}{\mu^2}\right) - \log(e^{\gamma_E}) + \log(4\pi) - \frac{3}{2} \right). \tag{C.6}$$

Then, in the modified minimal subtraction scheme, we re-scale our constant and introduce $\overline{\mu}^2 = \mu^2 e^{\gamma_E}/4\pi$, which removes the additional constant terms (alternatively, one can view this as us subtracting these terms when we initially removed the divergent $1/(4-d)$ term). This leaves us with the regularised, one-loop correction to the effective potential for ϕ^4 theory of:

$$V_1(\phi) = \frac{m^4}{64\pi^2} \left(\log\left(\frac{m^2}{\overline{\mu}^2}\right) - \frac{3}{2} \right). \tag{C.7}$$

D Gauge Fixing and Faddeev-Popov Ghosts

Here we pedagogically demonstrate the inconsistencies with gauge theories in the path integral formalism, following [39]. Consider the $U(1)$ gauge theory described by the Lagrangian:

$$\mathcal{L} = -\frac{1}{4}F^2, \tag{D.1}$$

where $F_{\mu\nu} = \partial_\mu A_\nu - \partial_\nu A_\mu$. The associated action can be written

$$\begin{aligned} S[A] &= \int d^4x \left(-\frac{1}{4}F^2\right) \\ &= -\frac{1}{2}\int d^4x \left[(A_\mu \partial_\nu)(\partial^\mu A^\nu) - (\partial_\mu A_\nu)(\partial^\nu A^\mu)\right] \\ &= \frac{1}{2}\int d^4x \left[A_\nu \partial^2 A^\nu - A_\nu \partial^\mu \partial^\nu A^\mu\right] \\ &= \frac{1}{2}\int d^4x A_\mu(x)(\partial^2 g^{\mu\nu} - \partial^\mu\partial^\nu) A_\nu(x), \end{aligned} \tag{D.2}$$

where we have integrated by parts between the second and third lines. Now, we note that the operator $\partial^2 g_{\mu\nu} - \partial^\mu \partial^\nu$ has the momentum space eigenvector $k_\nu \alpha(k)$, for any scalar function $\alpha(k)$, which is associated with the null eigenvalue 0. Thus, this operator is singular, which has two consequences. Firstly, it implies that the Green's function equation for this differential operator has no solution, such that the Feynman propagator is formally ill-defined. Secondly, it implies the following functional integral diverges:

$$I = \int \mathcal{D}A e^{iS[A]}. \tag{D.3}$$

The reason for this problem is because of the gauge invariance of the $U(1)$ Lagrangian. Indeed, the troublesome modes are those that are equivalent to $A_\mu(x) = 0$ under the transformation

$$A_\mu(x) \to A_\mu + \frac{1}{e}\partial_\mu \alpha(x). \tag{D.4}$$

Thus, the functional integral above is taken over an infinity of redundant gauge equivalent field configurations, causing the divergence. The solution is to introduce a gauge-fixing condition which counts each physically unique field configuration once and only once. We establish this using the method derived by Faddeev and Popov.

To begin, we consider a general (not necessarily $U(1)$) pure gauge theory and consider the functional integral

$$I = \int \mathcal{D}A \exp\left[i \int d^4x \left(-\frac{1}{4} (F^a_{\mu\nu})^2 \right) \right] \tag{D.5}$$

where the integral is taken over each gauge field, indexed by a: $A^a_\mu(x)$. We constrain our gauge by introducing the gauge condition $G(A) = 0$[14]. We include this in our integral by multiplying by unity in the following form:

$$1 = \int \mathcal{D}A \delta(G(A^\alpha)) \det\left(\frac{\delta G(A^\alpha)}{\delta \alpha} \right), \tag{D.6}$$

where A^α is the gauge-fixed field

$$(A^\alpha)^a_\mu = A^a_\mu + \frac{1}{g}\partial_\mu \alpha^a + f^{abc} A^b_\mu \alpha^c \equiv A^a_\mu + \frac{1}{g} D^{ab}_\mu \alpha^c. \tag{D.7}$$

The structure constants f^{abc} define the structure of the gauge Lie algebra according to $[t^a,\ t^b] = i f^{abc} t^c$. Making this substitution the functional integral becomes:

$$I = \left(\int \mathcal{D}\alpha \right) \int \mathcal{D}A e^{iS[A]} \delta(G(A)) \det\left(\frac{\delta G(A^\alpha}{\delta \alpha} \right). \tag{D.8}$$

Note that we have obscured some detail in making this substitution. In particular, upon making the substitution we have shifted the integration variable in the original expression from A to A^α, which leaves both the integration measure (as it is a simple shift) and the action (as it is gauge invariant) unchanged. Then, we have relabelled the new dummy variable A^α back to A.

Ignoring the functional determinant that appears in our expression for the time being, we want to specify a specific gauge condition. We pick for this the set of generalised Lorenz conditions specified by the scalar field $\omega(x)$:

$$G(A) = \partial^\mu A_\mu(x) - \omega(x). \tag{D.9}$$

[14] For example, the Lorenz gauge is specified by $G(A) = \partial_\mu A^\mu$.

Focusing only on the relevant part of functional integral[15], we obtain:

$$\int \mathcal{D}A e^{iS[A]} \delta(\partial^\mu A_\mu - \omega(x)). \tag{D.10}$$

This holds for any weighting function $\omega(x)$, and thus any normalised linear combination of such function. Thus, we introduce the integral over all such functions with a Gaussian weighting function centred on $\omega(x) = 0$. Incorporating this, the above expression is equivalent to:

$$\begin{aligned} N(\xi) \int \mathcal{D}\omega \mathcal{D}A \exp\left[-i \int d^4x \frac{\omega^2}{2\xi}\right] e^{iS[A]} \delta(\partial^\mu A_\mu - \omega(a)) \\ = N(\xi) \int \mathcal{D}A e^{iS[A]} \exp\left[-i \int d^4x \frac{(\partial^\mu A_\mu)^2}{2\xi}\right]. \end{aligned} \tag{D.11}$$

Hence, we have had the effect of fixing the gauge by introducing the following term to our Lagrangian:

$$\mathcal{L}_{\text{GF}} = -\frac{(\partial^\mu A_\mu)^2}{2\xi}. \tag{D.12}$$

The choice of ξ specifies the gauge, with two particular examples being the Landau gauge with $\xi = 0$ and the Feynman gauge with $\xi = 1$. Upon initial inspection, it would seem we have added a term for free into our Lagrangian — however this is not the case. The effect of the gauge fixing term above is mitigated within the physics of our theory by the presence of the functional determinant in our integral, just as this functional determinant allows us to insert the gauge condition in the first place. Returning to this term in more detail, we have

$$\begin{aligned} \frac{\delta G(A^\alpha)}{\delta \alpha} &= \frac{\delta}{\delta \alpha}\left[\partial^\mu\left(A^a_\mu + \frac{1}{g} D_\mu \alpha^a\right) - \omega(x)\right] \\ &= \frac{1}{g}\partial^\mu D_\mu \\ &= \frac{1}{g}\left(\partial^2 + g\partial^\mu f^{abc} A^b_\mu\right). \end{aligned} \tag{D.13}$$

This functional determinant can be represented as a Gaussian integral over two Grassmann-valued fields, $\bar{c}(x)$ and $c(x)$. That is, we have:

$$\det\left(\frac{1}{g}\partial^\mu D_\mu\right) = \int \mathcal{D}c\mathcal{D}\bar{c} \exp\left[i \int d^4x \bar{c}(-\partial^\mu D_\mu)c\right]. \tag{D.14}$$

We have absorbed the factor of $1/g$ into the new fields. Note these fields are required to be Lorentz scalars, and yet they are anti-commuting. This violation of spin statistics leads to quantum excitations of these fields being nonphysical particles known as Faddeev-Popov ghosts. As with the gauge-fixing term, we see the functional determinant has had the effect of adding an additional term to the Lagrangian, written in full it becomes:

$$\mathcal{L}_{\text{ghost}} = \bar{c}^a\left(-\partial^2\delta^{ac} - g\partial^\mu f^{abc} A^b_\mu\right) c^c. \tag{D.15}$$

Thus, the full Lagrangian, including the gauge-fixing term and ghost fields, becomes:

$$\begin{aligned} \mathcal{L} &= \mathcal{L}_{\text{G}} + \mathcal{L}_{\text{GF}} + \mathcal{L}_{\text{ghost}} \\ &= -\frac{1}{4}(F^a_{\mu\nu})^2 - \frac{(\partial^\mu A^a_\mu)^2}{2\xi} + \bar{c}^a\left(-\partial^2\delta^{ac} - g\partial^\mu f^{abc} A^b_\mu\right) c^c. \end{aligned} \tag{D.16}$$

[15] That is, momentarily disregarding the normalisation factor $\int \mathcal{D}\alpha$ and the determinant.

E Thermal Sum for Scalar Field Free Energy

In 5.2, we derived the following thermal sum for the logarithm of a non-interacting real scalar field partition function:

$$\ln(Z) = -\frac{1}{2}\sum_n \sum_{\mathbf{p}} \ln\left(\beta^2(\omega_n^2 + \omega^2)\right). \tag{E.1}$$

We now want to relate this expression to the 1-loop corrections of the effective potential. This derivation is due to [57]. Firstly, we notice that the logarithm can be written as follows:

$$\ln\left(\beta(\omega^2 + \omega_n^2)\right) = \int_1^{(\beta\omega)^2} \frac{d\theta^2}{\theta^2 + \omega_n^2} + \ln\left(1 + (2\pi n)^2\right), \tag{E.2}$$

where this second constant term can be neglected. We are thus left with the task of evaluating the following thermal sum:

$$\sum_n \frac{1}{\theta^2 + \omega_n^2}. \tag{E.3}$$

We do this by using the Residue theorem. Firstly, we consider the following function of some imaginary variable z:

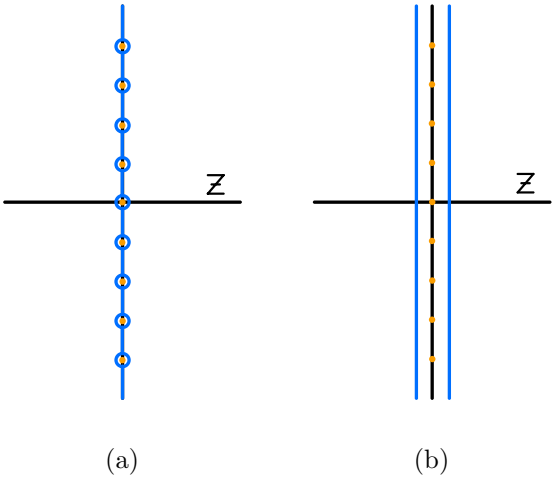

(a) (b)

Figure 16: Left (a): Contour used in the evaluation of the contour integral (E.6). Right (b): Deformed contour used in the rearranged expression (E.7).

$$f(z) = \frac{1}{\theta^2 - z^2}, \tag{E.4}$$

such that the sum becomes

$$\sum_n \frac{1}{\theta^2 + \omega_n^2} = \sum_n f(z = i\omega_n). \tag{E.5}$$

Then, notice that the function $\frac{1}{2}\beta\coth(\frac{1}{2}\beta z)$ has poles along the imaginary z axis at values $z = 2n\pi T i = \omega_n i$. Hence, we write this sum as the contour integral:

$$\frac{1}{2\pi i}\oint_\Gamma dz f(z)\frac{\beta}{2}\coth\left(\frac{\beta z}{2}\right). \tag{E.6}$$

The contour Γ is given in Figure 16a. Now, we can then deform this contour into that seen in Figure 16b, such that this contour integral can instead be written as (rearranging the hyperbolic cotangent):

$$\frac{\beta}{2\pi i}\int_{i\infty-\epsilon}^{-i\infty-\epsilon} dz f(z)\left(-\frac{1}{2} - \frac{1}{e^{-\beta z} - 1}\right) + \frac{\beta}{2\pi i}\int_{-i\infty+\epsilon}^{i\infty+\epsilon} dz f(z)\left(\frac{1}{2} + \frac{1}{e^{\beta z} - 1}\right). \tag{E.7}$$

The final trick is to replace $z \to -z$ in the first integral to give:

$$\frac{\beta}{2\pi i}\int_{-i\infty}^{i\infty} dz\frac{1}{2}\left(f(z) + f(-z)\right) + \frac{\beta}{2\pi i}\int_{-i\infty+\epsilon}^{i\infty+\epsilon} dz\frac{1}{2}\left(f(z) + f(-z)\right)\frac{1}{e^{\beta z} - 1}. \tag{E.8}$$

From here, we simply need to calculate these expressions for $f(z) + f(-z) = 2/(\theta^2 - z^2)$. This can again be done using contour integration, in which we close the contour for the first integral in the positive z plane picking up the pole at $z = \theta$, such that:

$$\int_{-i\infty}^{i\infty}\frac{dz}{\theta^2 - z^2} = -2\pi i\ \text{Res}\left\{\frac{1}{\theta^2 - z^2},\ z = \theta\right\} = \frac{i\pi}{\theta}. \tag{E.9}$$

Likewise, for the second integral we close the contour in the negative plane picking up the pole at $z = -\theta$:

$$\int_{-i\infty+\epsilon}^{i\infty+\epsilon} \frac{dz}{\theta^2 - z^2} \frac{1}{e^{\beta z} - 1} = 2\pi i \ \text{Res}\left\{ \frac{1}{\theta^2 - z^2} \frac{1}{e^{\beta z} - 1},\ z = \theta \right\} = \frac{2i\pi}{\theta} \frac{1}{e^{\theta} - 1}. \tag{E.10}$$

Thus, the thermal sum (E.3) evaluates to:

$$\sum_n \frac{1}{\theta^2 + \omega_n^2} = \frac{1}{2\theta} \left(1 + \frac{2}{e^{\theta} - 1} \right), \tag{E.11}$$

and likewise our expression for $\ln(Z)$ becomes:

$$\ln(Z) = -\frac{1}{4} \sum_{\mathbf{p}} \int_1^{(\beta\omega)^2} d\theta^2 \frac{1}{\theta} \left(1 + \frac{2}{e^{\theta} - 1} \right) = -\sum_{\mathbf{p}} \int_1^{\beta\omega} d\theta \left(\frac{1}{2} + \frac{1}{e^{\theta} - 1} \right). \tag{E.12}$$

We then perform the θ integration neglecting any temperature independent terms to obtain:

$$\ln(Z) = -\sum_{\mathbf{p}} \left(\frac{\beta\omega}{2} + \ln(1 - e^{-\beta\omega}) \right). \tag{E.13}$$

Lastly, replacing the momentum sum with an integration gives the required result:

$$\ln(Z) = -V \int \frac{d^3p}{(2\pi)^3} \left(\frac{\beta\omega}{2} + \ln(1 - e^{-\beta\omega}) \right). \tag{E.14}$$

F Matching Relations for 3d EFTs

In this appendix we provide expressions for the 3d parameters for both the Abelian Higgs and xSM models seen above. Note we make use of

$$L_b = \ln\left(\frac{\mu^2}{T^2} \right) + 2\gamma_E - 2\ln(4\pi), \quad L_f = L_b + 4\ln(2). \tag{F.0.1}$$

F.1 Abelian Higgs

Here we detail the 3d Lagrangian parameters for the Abelian Higgs model, and how they relate to the 4d parameters (m, λ, g). Note the 3d mass is given at LO for the sake of brevity. Finally, the hypercharge for the Higgs field, Y_ϕ, is equal to one and has been omitted from these expressions.

F.1.1 Soft Scale Parameters

At the soft scale, our Lagrangian parameters are:

$$\begin{aligned} \lambda_3 &= T \frac{g^4(2 - 3L_b) + 6g^2 L_b \lambda + 2\lambda(8\pi^2 - 5L_b\lambda)}{16\pi^2} \\ g_3^2 &= -g^2 T - T \frac{g^2 L_b}{48\pi^2} \\ m_3^2 &= m^2 + T^2 \frac{3g^2 + 4\lambda}{12} \end{aligned} \tag{F.1.1}$$

The temporal scalar couplings for the $A_0^2\phi^2$ and A_0^4 vertices, λVL_1 and λVLL_1 respectively, are given by:

$$\begin{aligned}\lambda VL_1 &= T\frac{g^2(48\pi^2 - g^2(-4 + L_b) + 24\lambda)}{24\pi^2} \\ \lambda VLL_1 &= T\frac{g^4}{\pi^2}.\end{aligned} \tag{F.1.2}$$

Finally, the Debye mass for the $U(1)$ boson, $\mu_{U(1)}^2$, is given by:

$$\mu_{U(1)}^2 = T^2\frac{g^2}{2} \tag{F.1.3}$$

F.1.2 Ultrasoft Scale Parameters

At the ultrasoft scale, our couplings and masses gain the following corrections:

$$\begin{aligned}\lambda_{3,US} &= \lambda_{3,S} - \frac{\lambda VL_1^2}{32\pi\mu_{U(1)}} \\ g_{3,US}^2 &= g_{3,S}^2 \\ m_{3,US}^2 &= m_{3,S}^2 + \frac{\mu_{U(1)}\ \lambda VL_1}{8\pi}\end{aligned} \tag{F.1.4}$$

F.2 xSM

Here we detail the 3d Lagrangian parameters for the Abelian Higgs model, and how they relate to the 4d parameters $(\mu_h, \mu_s, \lambda_h, \lambda_s, \lambda_{hs}, g_1, g_2, g_3)$. Note the 3d masses are given at LO for the sake of brevity. As well as the Lagrangian parameters, we also have the following hypercharge values:

$$Y_q = \frac{1}{3};\ Y_u = \frac{4}{3};\ Y_d = -\frac{2}{3};\ Y_l = -1;\ Y_e = -2;\ Y_\phi = 1. \tag{F.2.1}$$

which correspond to the left-handed quarks, right-handed up quark, right-handed down quark, left-handed leptons, right-handed leptons, and the Higgs boson respectively. The only quark given a Yukawa coupling to the Higgs boson is the top quark, $y_t = 1$. Also, we have three fermion families $n_F = 3$.

F.2.1 Soft Scale Parameters

At the soft scale, our gauge couplings are:

$$g_{1,3}^2 = g_1^2 T + T\frac{g_1^2(18L_f y_t^2(Y_q - Y_u)^2 + (-L_f(18y_t^2 + g_1^2 n_F(3Y_d^2 + Y_e^2 + 2Y_l^2 + 6Y_q^2 + 3Y_u^2))Y_\phi^2 - g_1^2 L_b Y_\phi^4)}{96\pi^2 Y_\phi^2}$$

$$g_{2,3}^3 = g_2^2 T + T\frac{g_2^2(4 + 43L_b - 8L_f n_F)}{96\pi^2}$$

$$g_{3,3}^2 = g_3^2 T + T\frac{g_3^2(3 + 33L_b - 4L_f n_F)}{48\pi^2}$$

The 3d couplings and masses are given by:

$$\begin{aligned}
\lambda_{h,3} &= \lambda_h T + \frac{T}{256\pi^2}(48L_f y_t^4 + (2-3L_b)(3g_2^4 + 2g_1^2 g_3^2 Y_\phi^2 + g_1^4 Y_\phi^4) \\
&\quad + 24(3g_2^2 L_b - 4L_f y_t^2 + g_1^2 L_b Y_\phi^2)\lambda_h - 4L_b(48\lambda_h^2 + \lambda_{hs}^2)) \\
\lambda_{hs,3} &= \lambda_{hs} T + T\frac{\lambda_{hs}(9g_2^2 L_b - 12L_f y_t^2 + 3g_1^2 L_b Y_\phi^2 - 4L_b(6\lambda_h + 2\lambda_{hs} + 3\lambda_s))}{64\pi^2} \\
\lambda_{s,3} &= \lambda_s T - T\frac{L_b(\lambda_{hs}^2 + 9\lambda_s^2)}{16\pi^2} \\
\mu_{h,3}^2 &= \mu_h^2 + T^2\frac{9g_2^1 + 12y_t^2 + 3g_1^2 Y_\phi^2 + 24\lambda_h + 2\lambda_{hs}}{48} \\
\mu_{s,3}^2 &= \mu_s^2 + T^2\frac{2\lambda_{hs} + 3\lambda_s}{12}
\end{aligned} \tag{F.2.2}$$

The temporal scalar couplings for the V^2S^2 vertices, λVL, are given by:

$$\begin{aligned}
\lambda VL_1 &= -T\frac{g_3^2 y_t^2}{4\pi^2} \\
\lambda VL_2 &= T\frac{g_2^2(g_2^2(51 + 43L_b + 8n_F - 8L_f n_F + 96\pi^2 - 36y_t^2 + 3g_1^2 Y_\phi^2 + 72\lambda_h)}{192\pi^2} \\
\lambda VL_3 &= -T\frac{g_1 g_2}{384}\Bigg(192Y_\phi + \frac{1}{\pi^2}(36(2-L_f)Y_q y_t^2 + 36L_f y_t^2(Y_u - Y_\phi) - g_2^2(12 - 43L_b - 8n_F)Y_\phi \\
&\quad + 6g_1^2(1-L_f)n_F Y_q^2 Y_\phi - L_f n_F(8g_2^2 + g_1^2(3Y_d^2 + Y_e^2 + 2Y_l^2 + 3Y_u^2))Y_\phi \\
&\quad + g_1^2 Y_\phi(n_F 3Y_d^2 + Y_e^2 + 2Y_l^2 + 3Y_u^2) + (4-L_b)Y_\phi^2) + 48Y_\phi\lambda_h)\Bigg) \\
\lambda VL_4 &= \frac{1}{192\pi^2}g_1^2 T\Bigg(96Y_\phi^2 - 36L_f Y_q y_t^2 Y_u - 18y_t^2((2-L_f)Y_u^2 + L_f Y_\phi^2) \\
&\quad - 6Y_q^2(3(2-L_f)y_t^2 - g_1^2(1-L_f)n_F Y_\phi^2) + Y_\phi^2(9g_2^2 \\
&\quad + g_1^2((n_F(1-L_f)(3Y_d^2 + Y_e^2 + 2Y_l^2 + 3Y_u^2) + (1-L_b)Y_\phi^2) + 72\lambda_h))\Bigg) \\
\lambda VL_5 &= T\frac{g_1^2\lambda_{hs}}{8\pi^2} \\
\lambda VL_6 &= T\frac{g_1^2 Y_\phi^2\lambda_{hs}}{8\pi^2}
\end{aligned} \tag{F.2.3}$$

The Debye masses for our gauge bosons are given by:

$$\begin{aligned}
\mu_{SU(3)}^2 &= T^2\frac{g_3^2(3+n_F)}{3} \\
\mu_{SU(2)}^2 &= T^2\frac{g_2^2(5+2n_F)}{6} \\
\mu_{U(1)}^2 &= T^2\frac{g_1^2(n_F(3y_d^2 + Y_e^2 + 2Y_l^2 + 6Y_q^2 + 3Y_u^2) + 4Y_\phi^2)}{24}
\end{aligned} \tag{F.2.4}$$

F.2.2 Ultrasoft Scale Parameters

At the ultrasoft scale, our gauge couplings are given by:

$$\begin{aligned} g_{1,US}^2 &= g_{1,S}^2 \\ g_{2,US}^2 &= g_{2,S}^2 - \frac{g_{2,S}^4}{24\pi\mu_{SU(2)}} \\ g_{3,US}^2 &= g_{3,S}^2 - \frac{g_{3,S}^4}{16\pi\mu_{SU(3)}} \end{aligned} \tag{F.2.5}$$

The ultrasoft masses and couplings are then given by:

$$\begin{aligned} \lambda_{h,US} &= \lambda_{h,S} - \frac{1}{32\pi}\left(\frac{8\lambda V L_1^2}{\mu_{SU(3)}} + \frac{3\lambda V L_2^2}{\mu_{SU(2)}} + \frac{4\lambda V L_3^2}{\mu_{SU(2)}+\mu_{U(1)}} + \frac{4\lambda V L_4^2}{\mu_{U(1)}}\right) \\ \lambda_{hs,US} &= \lambda_{hs,S} - \frac{1}{192\pi}\left(\frac{36\lambda V L_2 \lambda V L_5}{\mu_{SU(2)}}\right) \\ \lambda_{s,US} &= \lambda_{s,S} - \frac{1}{96\pi}\left(\frac{9\lambda V L_5^2}{\mu_{SU(2)}}\right) \\ \mu_{h,US}^2 &= \mu_{h,S}^2 - \frac{1}{8\pi}\left(\mu_{SU(3)}\lambda V L_1 + 3\mu_{SU(2)}\lambda V L_2 + \mu_{U(1)}\lambda V L_4\right) \\ \mu_{s,US}^2 &= \mu_{s,S}^2 - \frac{1}{16\pi}\left(6\mu_{SU(2)}\lambda V L_5\right) \end{aligned} \tag{F.2.6}$$

G Mass Matrix Diagonalisation

Going beyond leading order in the effective potential requires one to diagonalise the mass matrix. For extensions of the standard model, the mass matrix is of dimension $4 + n_S$, where n_S gives the number of additional scalar degrees of freedom. For the xSM model, this corresponds to a 5×5 matrix, for cxSM this is a 6×6 matrix, whilst for 2HDM this is 8×8. Naturally, these can be tedious to diagonalise. In this section I provide the diagonalisation of the mass matrices for these systems analytically. The motivation for such a diagonalisation is simple: these matrices are functions of both our various scalar fields ϕ_i, as well as temperature T. Consequently numerical diagonalisation would be an extremely time consuming task, as not only do these need to be diagonalised numerically for all points in the parameter space, but also all points in the corresponding field space and at every temperature considered — leading to a very long computation time for even an efficient numerical process. Doing the process analytically circumvents this by replacing this with a single expression for the diagonalised mass matrix that is known for all points in the parameter, field, and temperature spaces.

G.1 xSM

Consider the xSM model. The mass matrix for this system is given by:

$$M = \begin{pmatrix} a & 0 & 0 & 0 & c \\ 0 & \mu_3 & 0 & 0 & 0 \\ 0 & 0 & \mu_3 & 0 & 0 \\ 0 & 0 & 0 & \mu_3 & 0 \\ c & 0 & 0 & 0 & b \end{pmatrix}. \tag{G.1.1}$$

Here μ_3 is an eigenvalue of M with algebraic multiplicity 3. M can thus be written as the direct sum:

$$M = \begin{pmatrix} a & c \\ c & b \end{pmatrix} \oplus \mu_3 I_3 = A \oplus \mu_3 I_3, \tag{G.1.2}$$

where I_3 is the 3×3 identity matrix. Thus, diagonalising M requires the matrix $R \in SO(2)$ that diagonalises A. Firstly, we solve the characteristic equation for A to obtain the additional two eigenvalues of M:

$$c(\lambda) = \det(A - \lambda I_2) = (a-\lambda)(b-\lambda) - c^2 = \lambda^2 - (a+b)\lambda + ab - c^2 = 0. \tag{G.1.3}$$

Which gives the following eigenvalues:

$$\mu_{1,2} = \frac{a+b\pm\Delta}{2}, \tag{G.1.4}$$

for $\Delta = \sqrt{(a-b)^2+4c^2}$. Then, to find the diagonalisation matrix R, we solve:

$$R^T M R = \mathrm{diag}(\mu_1, \mu_2). \tag{G.1.5}$$

R can be most easily found by parameterising it as:

$$R = \frac{1}{\sqrt{2}}\begin{pmatrix} \sqrt{1+\xi} & -\sqrt{1-\xi} \\ \sqrt{1-\xi} & \sqrt{1+\xi} \end{pmatrix}. \tag{G.1.6}$$

Inserting this into our equation, we find:

$$\xi = \frac{a-b}{\Delta}. \tag{G.1.7}$$

These expressions can then be used in both the NLO and NNLO potentials. That is, we have the mass eigenstates as functions of our fields and temperature, given by μ_i, as well as the full diagonalisation matrix, which is given by $R \oplus I_3$, where I_3 acts on the diagonal component of M.

G.2 cxSM

Consider the cxSM model. The mass matrix for this system is given by:

$$M = \begin{pmatrix} a & 0 & 0 & 0 & d & 0 \\ 0 & \mu_4 & 0 & 0 & 0 & 0 \\ 0 & 0 & \mu_4 & 0 & 0 & 0 \\ 0 & 0 & 0 & \mu_4 & 0 & 0 \\ d & 0 & 0 & 0 & b & e \\ 0 & 0 & 0 & 0 & e & c \end{pmatrix}. \tag{G.2.1}$$

So, as before we are required to diagonalise the 3×3 matrix defined by:

$$M = \begin{pmatrix} a & d & 0 \\ d & b & e \\ 0 & e & c \end{pmatrix} \oplus \mu_4 I_3 = A \oplus \mu_4 I_3. \tag{G.2.2}$$

This is a harder task than the xSM case, and requires the matrix $R \in SO(3)$ that diagonalises A. We leave obtaining the eigenvalues μ_i for $i \in \{1,2,3\}$ as a task for the reader. The characteristic equation is cubic in the eigenvalues and as such an analytic solution can be obtained using the cubic equation. To obtain R we can in theory solve $R^T A R = \mathrm{diag}(\mu_1, \mu_2, \mu_3)$. However, an easier task is to find the eigenvectors of A, $\mathbf{v}_i$, in terms of μ_i. To achieve this, we need to solve

$$A\mathbf{v}_i = \mu_i A. \tag{G.2.3}$$

If $\mathbf{v}_i = (v_1, v_2, v_3)^T$, this defines the following system of equations:

$$0 = (a-\mu_i)v_1 + dv_2 \tag{G.2.4}$$

$$0 = dv_1 + (b-\mu_i)v_2 + ev_3 \tag{G.2.5}$$

$$0 = ev_2 + (c-\mu_i)v_3 \tag{G.2.6}$$

We solve for v_1 and v_3 to obtain:

$$v_1 = \frac{d}{\mu_i - a} v_2; \quad v_3 = \frac{e}{\mu_i - c} v_2. \tag{G.2.7}$$

Upon substituting these into the third equation, we yield an expression of the form $c(\mu_i)v_2 = 0$, where $c(\lambda)$ is the characteristic polynomial, ensuring this vanishes for all v_2. Hence, $\mathbf{v}_i$ is given by:

$$\mathbf{v}_i = \begin{pmatrix} \frac{d}{\mu_i - a} & 1 & \frac{e}{\mu_i - c} \end{pmatrix}^T. \tag{G.2.8}$$

Thus, once we obtain μ_i by solving the characteristic polynomial $c(\lambda)$, we can obtain each eigenvector of A. We can then normalise each eigenvector and use them to construct the rotation matrix R to act on A, whilst the full matrix that acts on M is given by $R \oplus I_3$. This solution is somewhat inelegant, due to the complicated structure of the eigenvalues μ_i. We suggest the user investigate more delicate alternatives.

G.3 2HDM

Finally, we consider the 2HDM model. This has a mass matrix given by:

$$M = \begin{pmatrix} \alpha_1 & 0 & 0 & 0 & \beta & 0 & -\gamma & 0 \\ 0 & \alpha_2 & 0 & 0 & 0 & \delta & 0 & -\gamma \\ 0 & 0 & \alpha_3 & 0 & \gamma & 0 & \epsilon & 0 \\ 0 & 0 & 0 & \alpha_4 & 0 & \gamma & 0 & \delta \\ \beta & 0 & \gamma & 0 & \alpha_5 & 0 & 0 & 0 \\ 0 & \delta & 0 & \gamma & 0 & \alpha_6 & 0 & 0 \\ -\gamma & 0 & \epsilon & 0 & 0 & 0 & \alpha_7 & 0 \\ 0 & -\gamma & 0 & \delta & 0 & 0 & 0 & \alpha_8 \end{pmatrix}. \tag{G.3.1}$$

We can write M in the following partitioned form:

$$M = \begin{pmatrix} D_1 & A \\ B & D_2 \end{pmatrix}, \tag{G.3.2}$$

where D_1 and D_2 are diagonal. A and B are not diagonal, however we can write A as $A = S + N$, where S is diagonal and N is skew-symmetric $N^T = -N$. In this form, A and B are related by $A = S + N$ and $B = S - N$. This relation will imply that M can be diagonalised by an orthogonal transformation $R \in SO(8)$. To do this diagonalisation, we use the fact that for any 2×2 partitioned matrix [77]:

$$\begin{pmatrix} A & B \\ C & D \end{pmatrix} = \begin{pmatrix} I & BD^{-1} \\ 0 & I \end{pmatrix} \begin{pmatrix} A - BD^{-1}C & 0 \\ 0 & D \end{pmatrix} \begin{pmatrix} I & 0 \\ D^{-1}C & I \end{pmatrix}, \tag{G.3.3}$$

which implies:

$$\begin{pmatrix} D_1 & A \\ B & D_2 \end{pmatrix} = \begin{pmatrix} I & AD_2^{-1} \\ 0 & I \end{pmatrix} \begin{pmatrix} D_1 - AD_2^{-1}B & 0 \\ 0 & D_2 \end{pmatrix} \begin{pmatrix} I & 0 \\ D_2^{-1}B & I \end{pmatrix}. \tag{G.3.4}$$

Now, we notice:

$$\begin{aligned} \begin{pmatrix} I & AD_2^{-1} \\ 0 & I \end{pmatrix}^T &= \begin{pmatrix} I & (S+N)D_2^{-1} \\ 0 & I \end{pmatrix}^T \\ &= \begin{pmatrix} I & 0 \\ D_2^{-1}(S+N)^T & I \end{pmatrix} \\ &= \begin{pmatrix} I & 0 \\ D_2^{-1}(S-N) & I \end{pmatrix} \\ &= \begin{pmatrix} I & 0 \\ D_2^{-1}B & I \end{pmatrix} \end{aligned}. \tag{G.3.5}$$

Furthermore, we can show this transformation is orthogonal. Hence, (G.3.4)is an expression of the form $M = R^T N R$ for $R \in SO(8)$. Since D_2 is diagonal, we are left needing diagonalise $D_1 - AD_2^{-1}B$. This is a 4×4 matrix which can be written in 2×2 partitioned form, hence we simply need to apply this algorithm again. For brevity we don't repeat the process here, instead we quote the result, namely the eigenvalues of M that can be read off the diagonalised matrix are:

$$\begin{aligned}
\mu_1 &= \frac{(\alpha_1\alpha_2 - \beta^2 - \gamma^2)(-\alpha_1\alpha_5 + \gamma^2 + \epsilon^2) + \gamma^2(\beta - \epsilon)^2}{\alpha_5(-\alpha_1\alpha_5 + \gamma^2 + \epsilon^2)} \\
\mu_2 &= \frac{-(\gamma^2 + \delta^2)^2 + \alpha_2(-\alpha_4\alpha_6\alpha_8 + \alpha_8\gamma^2 + \alpha_6\delta^2) + \alpha_4(\alpha_6\gamma^2 + \alpha_8\delta^2)}{-\alpha_4\alpha_6\alpha_8 + \alpha_8\gamma^2 + \alpha_6\delta^2} \\
\mu_3 &= \frac{\alpha_1\alpha_5 + \gamma^2 + \epsilon^2}{\alpha_5} \\
\mu_4 &= \alpha_4 - \frac{\gamma^2}{\alpha_6} - \frac{\delta^2}{\alpha_8} \\
\mu_i &= \alpha_i, \ 5 \leq i \leq 8.
\end{aligned} \tag{G.3.6}$$

Likewise, the rotation matrix R is of the form:

$$R = \begin{pmatrix} R_1 & 0 \\ R_2 & I_4 \end{pmatrix}, \tag{G.3.7}$$

where

$$R_1 = \begin{pmatrix} 1 & 0 & 0 & 0 \\ 0 & 1 & 0 & 0 \\ \frac{\gamma(\beta-\epsilon)}{\alpha_1\alpha_5 - \gamma^2 - \epsilon^2} & 0 & 1 & 0 \\ 0 & \frac{\alpha_8 - \alpha_6)\gamma\delta}{\alpha_4\alpha_6\alpha_8 + \alpha_8\gamma^2 + \alpha_6\delta^6} & 0 & 1 \end{pmatrix}, \tag{G.3.8}$$

and

$$R_2 = \begin{pmatrix} \frac{\beta(\alpha_1\alpha_5 - \gamma^2 - \epsilon^2) + \gamma^2(\beta-\epsilon)}{-\alpha_5(\alpha_1\alpha_5 - \gamma^2 - \epsilon^2)} & 0 & -\frac{\gamma}{\alpha_5} & 0 \\ 0 & -\frac{\delta(\alpha_4\alpha_8 - \gamma^2 - \delta^2)}{\alpha_4\alpha_6\alpha_8 - \alpha_8\gamma^2 - \alpha_6\delta^6} & 0 & -\frac{\gamma}{\alpha_6} \\ \frac{\gamma(\alpha_1\alpha_5 - \gamma^2 - \epsilon^2) - \epsilon\gamma(\beta-\epsilon)}{\alpha_5(\alpha_1\alpha_5 - \gamma^2 - \epsilon^2)} & 0 & -\frac{\epsilon}{\alpha_5} & 0 \\ 0 & \frac{\gamma(\alpha_4\alpha_6 - \gamma^2 + \delta^2)}{\alpha_4\alpha_6\alpha_8 + \alpha_8\gamma^2 - \alpha_6\delta^2} & 0 & -\frac{\delta}{\alpha_8} \end{pmatrix}. \tag{G.3.9}$$

Finally, we remark that this method can be used to diagonalise any extension where the mass matrix can be partitioned into a 2×2 block matrix. This includes models with n Higgs doublets, or extensions with symmetry in the mass matrix, such as an extension with 2 complex scalar fields.